Titre: Title:	Encapsulation of nanoparticles by polymerization compounding in a gas/solid fluidized bed reactor
Auteur: Author:	Babak Esmaeili Pour Farsangi
Date:	2008
Type:	Mémoire ou thèse / Dissertation or Thesis
Référence: Citation:	Esmaeili Pour Farsangi, B. (2008). Encapsulation of nanoparticles by polymerization compounding in a gas/solid fluidized bed reactor [Thèse de doctorat, École Polytechnique de Montréal]. PolyPublie. https://publications.polymtl.ca/8133/

UNIVERSITÉ DE MONTRÉAL

ENCAPSULATION OF NANOPARTICLES BY POLYMERIZATION COMPOUNDING IN A GAS/SOLID FLUIDIZED BED REACTOR

BABAK ESMAEILI POUR FARSANGI

DÉPARTEMENT DE GÉNIE CHIMIQUE

ÉCOLE POLYTECHNIQUE DE MONTRÉAL

THÈSE PRÉSENTÉE EN VUE DE L'OBTENTION

DE DIPLÔME DE PHILOSOPHIAE DOCTOR

(GÉNIE CHIMIQUE)

AVRIL 2008

Your file Votre référence
ISBN: 978-0-494-41747-8
Our file Notre référence
ISBN: 978-0-494-41747-8

UNIVERSITÉ DE MONTRÉAL

ÉCOLE POLYTECHNIQUE DE MONTRÉAL

Cette thèse intitulée:

ENCAPSULATION OF NANOPARTICLES BY POLYMERIZATION COMPOUNDING IN A GAS/SOLID FLUIDIZED BED REACTOR

présentée par: ESMAEILI POUR FARSANGI Babak

en vue de l'obtention du diplôme de : Philosophiae Doctor

a été dûment acceptée par le jury d'examen constitué de :

M. PATIENCE Gregory-S., Ph.D., président

M. CHAOUKI Jamal, Ph.D., membre et directeur de recherche

M. DUBOIS Charles, Ph.D., membre et codirecteur de recherche

M. LAFLEUR Pierre, Ph.D., membre

M. ARASTOOPOUR Hamid, Ph.D., membre

ACKNOWLEDGEMENTS

I would like to express my sincere gratitude to those who helped me in the completion of this work. First of all, I am indebted to my supervisors, *Prof. Jamal Chaouki* and *Prof. Charles Dubois* for their kind guidance, helpful suggestions, encouragement and confidence in me.

I would like to extent my thanks to the technicians of chemical engineering department, *Jean Huard*, *Daniel Dumas*, *Robert Delisle*, *Carol Painchaud*, *Gino Robin*, *Martine Lamarche* and *Jacque Beausoleil* that without their helps, this project could not go through.

I would like to thank *Dr. Jitka Kirchnerova, Suzie Poulin, Phillipe Plamondon, Phillipe Beaulieu, Marie-Hélène Bernier*, and *Laurent Mouden* for helping me in characterization methods and analysis.

I also thank *Prof. Gregory Kennedy* and *Mr. Jean St-Pierre* for activating the tracer.

I wish also to thank my friends, who their helps, discussions and encouragements were so valuable for me to accomplish the work: *Rouzbeh, Antoine, Ramin, Youcef, Rachid, Jean-Philippe, Mahmoud, Gaetan, Shant, Nick, Jocelyn, Ebrahim, Omid, Lionel, Ali, Sepehr, Shahram, Amin, Gang, Zhenyu.*

I would like to thank the entire staff of the chemical engineering department in Ecole Polytechnique de Montreal.

I finally would like to appreciate my parents and family for all their support and encouragements.

RÉSUMÉ

'Polymerization compounding', appelé également polymérisation par greffage, est une technique bien connue dans le domaine de la préparation et l'encapsulation des nano composites. Dans cette méthode, le substrat est impliqué dans la réaction de polymérisation de manière à améliorer les propriétés interfaciales entre la surface d'origine et la couche de polymère. Ceci permet de produire des particules modifiées ayant les propriétés requises pour être utilisées comme matériaux composites de haute performance. Toutefois, pratiquement toutes les méthodes traitant de ce sujet ont été effectuées en phase liquide où de nombreuses difficultés interviennent lors de la purification du solvant et des impuretés, mais également lors du séchage des particules. Ainsi, l'objectif de ce travail est de développer un nouveau procédé permettant d'enrober les nanoparticules par 'Polymerization compounding' dans un réacteur à lit fluidisé qui permet d'éviter l'utilisation de solvant et donc d'éviter les inconvénients reliés au procédé en phase liquide.

La première partie consistait à tester la faisabilité de la polymérisation de l'éthylène sur de la poudre de zirconium à l'aide d'un catalyseur de Ziegler-Natta, ceci permettant d'obtenir des nanoparticules de zirconium ayant une couche de quelques nanomètres de polyéthylène déposée uniformément sur leurs surfaces. L'avantage du système catalytique de Ziegler-Natta vient du fait qu'il permet de modérer les conditions d'opérations de la polymérisation de l'éthylène. Les résultats de l'analyse de

thermogravimétrie a confirmé la présence de polyéthylène à haut poids moléculaire à la surface des particules de zirconium. La spectroscopie de photoélectron à rayons X a permis de montrer la présence du catalyseur Ziegler-Natta à l'interface entre la surface des particules et le polymère, prouvant ainsi que la réaction de polymérisation débutait à la surface du substrat. L'encapsulation des nanoparticules de zirconium par le polyéthylène par l'approche de 'Polymerization compounding' est faisable en utilisant un système catalytique de type Ziegler-Natta. La microscopie électronique montre une très fine couche de polymère d'environ 6 nm enrobant les nanoparticules de manière uniforme. Bien que les résultats confirment que les nanoparticules soient individuellement enrobées de polyéthylène, quelques images montrent que l'encapsulation d'agglomérats de particules est également possible. D'un autre côté, ces observations peuvent être le résultat d'une agglomération de particules déjà enrobées individuellement.

Dans la seconde partie de cette recherche, la fluidisation des nanoparticules de zirconium et d'aluminium a été étudiée de manière à évaluer leur comportement dans un lit fluidisé. L'objectif était de déterminer dans quelles conditions expérimentales la fluidisation de ces nanoparticules est uniforme. À première vue la fluidisation des nanoparticules de zirconium et d'aluminium entraîne une expansion du lit limitée et une ascension rapide des bulles à travers le lit. Elle consiste également en une distribution non uniforme des agglomérats dans le lit ; les plus petits apparaissant à la surface fluidisée dans la partie supérieure du lit et les plus gros tombant graduellement dans la

partie inférieure du lit. L'expansion du lit fluidisé pour les particules de zirconium est plus limitée comparativement à celui des particules d'aluminium. De plus, la distribution de taille des agglomérats pour le zirconium est plus large que pour l'aluminium. Que ce soit pour les particules de zirconium ou d'aluminium les résultats de la densimétrie radioactive et des fibres optiques montrent que la concentration de solide est uniforme sur une section donnée pour différentes vitesses de gaz et différentes hauteurs de lit. Dans le cas du zirconium, le taux moyen de rétention de solide à travers une section est pratiquement indépendant de la hauteur du lit et la réduction de la rétention est faible lorsque la vitesse augmente. Au contraire, pour l'alumine, le taux de rétention de solide dans le lit fluidisé varie selon la hauteur du lit.

La concentration globale de solide obtenue par densimétrie radioactive est en accord avec les mesures de l'expansion du lit. Toutefois, le taux de rétention calculé à partir de la méthode des fibres optiques conduit à des résultats surestimés pour les vitesses de gaz les plus élevées.

Dans la dernière partie, la méthode de 'Polymerization compouding' a été appliquée à l'encapsulation des nanoparticules de zirconium et d'aluminium dans un réacteur à lit fluidisé. Le défi majeur à surmonter lors de cette partie a été de déposer de manière homogène le catalyseur à la surface des nanoparticules. En effet, seule une très faible quantité de catalyseur est requise pour une très grande surface de particules (environ 1 $\mu l/m^2$). Lorsque l'encapsulation a lieu en suspension liquide, cette étape ne pose pas de problème, parce que les particules sont dispersées dans un solvant organique dans lequel

le catalyseur est injecté et dissout. Ainsi, les particules dispersées dans le solvant sont uniformément exposées au catalyseur dissout. D'un autre côté, lorsque l'encapsulation a lieu en phase gazeuse, tel qu'en lit fluidisé, aucun média liquide ne peut être utilisé pour dissoudre le catalyseur. La procédure choisie pour déposer le catalyseur sur les nanoparticules consiste en l'évaporation du catalyseur avant l'entrée dans le lit fluidisé suivi par sa condensation sous forme solide à la surface des particules.

Comme les résultats le montrent, les nanoparticules sont enrobées par du polyéthylène à haut poids moléculaire. De plus, la présence de catalyseur à l'interface entre les particules et le polymère, visible au XPS, confirme que la réaction de polymérisation a été initiée à partir du substrat. Une analyse au TGA de différents échantillons provenant de la même expérience a permis de montrer que la quantité de polymère de chacun était similaire, ce qui prouve que l'encapsulation se produit de manière uniforme dans le réacteur. Les résultats montrent que la température ainsi que la pression ont une influence importante sur la réaction de polymérisation. Les images prises au microscope illustrent l'encapsulation uniforme des nanoparticules d'aluminium par le film de polymère. Cependant, pour les particules de zirconium, l'uniformité de l'enrobage de polymère n'a pas pu être observée. De plus, les particules de zirconium ont tendance à être enrobé sous forme agglomérée contrairement aux particules d'aluminium.

ABSTRACT

Polymerization compounding, often referred to as "graft polymerization", is a well-known technique in the field of nanocomposites preparation and nanoparticles encapsulation. In this method, the substrate is involved in the polymerization reaction in order to improve interfacial properties between the polymer and the original surface, thus producing modified nanoparticles with the improved properties required to obtain high performance composite materials. However, nearly all the research dealing with encapsulation of nanoparticles via polymerization compounding has been carried out in the liquid phase where difficulties arise with respect to separating the organic solvent and impurities from the encapsulated particles, and drying those without agglomeration. Accordingly, the target in this work is to develop a new process to coat nanoparticles by a solvent-free process using the polymerization compounding approach in a fluidized bed reactor, and consequently to eliminating drawbacks due to performing the process in liquid phase.

The first part of project was devoted to encapsulating nanoparticles in a slurry phase reactor to investigate the feasibility of ethylene polymerization on zirconia powder via a Ziegler-Natta catalyst system to obtain zirconia nanoparticles whose surface is uniformly modified by a layer of polyethylene, a few nanometers in thickness. The advantage of Ziegler-Natta catalyst system is to allow the ethylene polymerization reaction under very moderate operational conditions. The thermogravimetry analysis results confirmed the presence of high molecular weight polyethylene on the surface of

zirconia nanoparticles. It was shown by X-ray photoelectron spectroscopy that the Ziegler-Natta catalyst is effectively found at the interface between the nanoparticle surface and the polymer. It can therefore be concluded that the polymerization reaction starts at the surface of the substrate. Therefore, the encapsulation of zirconia nanoparticles by polyethylene via polymerization compounding approach is feasible using a simple Ziegler-Natta catalyst. The electron microscopy results demonstrated a thin polymer coat, about 6 nm in thickness, uniformly applied around the nanoparticles. Although the results confirmed that nanoparticles were individually coated by polyethylene, some images also revealed that coating agglomerates of particles agglomerate may also occur. However, the same images could also be interpreted as the result of the late agglomeration of individually coated particles.

In the second part of the research, efforts were focused on the fluidization of zirconia and aluminum nanoparticles. The objective was to understand under what experimental conditions the fluidization of these nanoparticles is uniformly achieved. At first glance, the fluidization of zirconia and aluminum nanoparticles involved limited bed expansion and bubbles rising up quickly through the bed. It also consisted of the non-uniform distribution of agglomerates in the bed where the small agglomerates appear to be fluidized in the upper part while the larger agglomerates move gradually to the bottom of the bed. The fluidized bed expansion was much more limited in the case of zirconia particles than with aluminum powder. In addition, the agglomerates size distribution for zirconia was wider than that in aluminum. The radioactive densitometry and fiber optic results showed that the solid concentration was uniform over the cross section of

zirconia and aluminum fluidized bed for a wide range of gas velocity at different heights of bed. In the case of zirconia, it was found that the average solid hold-up over the cross section was almost independent of bed height and the solid hold-up reduction was very small when increasing the gas velocity. However, the average solid hold-up in the fluidized bed of aluminum varied at different bed heights.

The overall solid concentration obtained by the radioactive densitometry technique was in a good agreement with the global measurement obtained by bed expansion data. On the contrary, the overall solid hold-up calculated by fiber optic method was overestimated for higher gas velocities.

In the last part, the polymerization compounding method was applied to encapsulate zirconia and aluminum nanoparticles in a fluidized bed reactor. The main challenge in this part was to graft the catalyst on the surface of nanoparticles, since a only very small amount of catalyst must be fixed on relatively large surface of particles (about 1 $\mu l/m^2$). When performing the encapsulation process in slurry phase, there is no obstacle to do so since the particles are dispersed in an organic solvent where the catalyst is itself injected and dissolved. Therefore, the particles dispersed in the solvent are uniformly exposed to the catalyst. On the other hand, when encapsulating particles in a gas phase reactor, such as a fluidized bed, there is no liquid media where the catalyst can be dissolved. The procedure applied in this research to deposit the catalyst on nanoparticles consisted of evaporating of Ziegler- Natta catalyst before entering fluidized bed reactor, which was followed by condensing the catalyst vapor on particles surface in the reactor.

As results showed, the nanoparticles were coated by high molecular weight polyethylene. In addition, the presence of the catalyst in the interface of particles and polymer coat, proved by XPS, confirmed that the polymerization reaction was initiated from the substrate. It was also confirmed that the encapsulation occurred uniformly on the particles within the reactor, since the polymer content determined by TGA was similar for different tested samples in the same batch. The results showed that both temperature and pressure have a great effect on the reaction of polymerization. The microscope images illustrated that aluminum nanoparticles were uniformly coated by polymer film. However, for zirconia nanoparticles, the uniformity of polymer coat around the particles was not observed in the images. Moreover, it was found that zirconia particles tended to be more often coated as agglomerates in comparison to reaction conducted on aluminum particles.

CONDENSÉ EN FRANÇAIS

L'encapsulation des nano particules par des polymères est recherchée dans de nombreuses applications afin d'améliorer leur stabilité chimique, de réduire leur toxicité, et de faciliter leurs stockage, transport et manipulation. Afin de donner aux particules modifiées les propriétés requises pour obtenir un matériel composite de haute performance, les propriétés inter faciales entre la surface des particules et la couche de polymère doivent être améliorées. 'Polymerization compounding' (PC) est une approche qui consiste à forcer la formation du polymère à partir de la surface du solide en utilisant des sites catalytiques liés de manière covalente aux particules. Ainsi un contact très spécifique entre la surface de la particule et le polymère est créé entraînant de meilleures propriétés inter faciales, et par conséquence l'amélioration des propriétés du nano composite. En accord avec le fait que la 'Polymerization compounding', aussi connu sous le nom de polymérisation de greffe, est une technique très connue dans le domaine de la préparation des composites et nano composites, de nombreuses études ont été effectuées concernant cette approche. Cependant, pratiquement la totalité des recherches traitant de l'encapsulation des nano particules via la 'Polymerization compounding' ont été réalisées en phase liquide, ce qui génère de nombreuses contraintes telles que retirer le solvant organique, les impuretés et sécher les particules encapsulées. De ce fait l'objectif principal de cette recherche est de développer un nouveau procédé permettant d'enrober les nano particules en utilisant la technique de la 'Polymerization

compounding' dans un réacteur en phase gaz, plus spécifiquement un réacteur à lit fluidisé, ce qui permettrait de travailler sans solvant. Par conséquent, tous les inconvénients reliés à la réalisation en phase liquide sont éliminés.

Dans cette recherche est tout d'abord présenté, dans la première partie de la revue de la littérature, un bref résumé concernant les derniers développements sur la 'Polymerization compounding' pour enrober les nano particules. La seconde partie de la revue de la littérature traite de la fluidisation des nano particules, incluant sa caractéristique particulière la fluidisation agglomérante, et des méthodes pour favoriser la qualité de la fluidisation des nano particules. Ensuite les résultats expérimentaux réalisés dans un lit fluidisé en phase gaz pour préparer l'encapsulation des nano particules via la méthode de la 'Polymerization compounding' sont présentés sous forme de trois articles scientifiques. Dans la première partie, est traité l'encapsulation des nano particules dans un réacteur slurry afin d'étudier la possibilité d'appliquer la 'Polymerization compounding' en utilisant un catalyseur de type Ziegler-Natta. La seconde partie consiste en l'étude de la fluidisation des nano particules de manière à comprendre leur comportement, et plus spécialement la distribution de concentration des particules dans le lit. Enfin, la dernière étape, réalisé en combinant les résultats précédents, est la réalisation de notre objectif principal, l'encapsulation des nano particules dans un réacteur à lit fluidisé en utilisant la 'Polymerization compounding'.
L'objectif de cette première partie était de tester la faisabilité de la polymérisation de l'éthylène sur de la poudre de zirconium à l'aide d'un catalyseur de Ziegler-Natta, ceci

permettant d'obtenir des nano particules de zirconium ayant une couche de quelques nanomètres de polyéthylène déposé uniformément sur leurs surfaces. L'éthylène a été choisi comme monomère pour deux raisons principales. Tout d'abord parce que l'objectif principal de cette recherche était d'encapsuler les particules dans un lit fluidisé, ce qui nécessite l'utilisation d'un monomère gazeux qui possède également de bonnes propriétés de gaz fluidisant. De plus, puisque l'éthylène possède des propriétés de dégradation thermale très intéressantes, permettant ainsi la libération des particules comme désiré dans les diverses applications possibles de l'encapsulation. L'avantage du système catalytique de Ziegler-Natta vient du fait qu'il permet de modérer les conditions d'opérations de la polymérisation de l'éthylène. Avant de réaliser la polymérisation, nous avons quantifié les groupes hydroxyl présents à la surface des nano particules afin de pouvoir évaluer la masse de catalyseur requis pour couvrir la totalité de leurs surfaces par le polymère. Les résultats de l'analyse thermogravimétrique ont confirmé la présence de polyéthylène à haut poids moléculaire à la surface des nano particules de zirconium. Le catalyseur Ziegler-Natta a été observé à l'interface entre la surface des nano particules et le polymère par une analyse de spectroscopie de photoélectron à rayons X, ce qui prouve que la réaction de polymérisation débute bien à la surface du substrat. Ainsi l'encapsulation des nano particules de zirconium par le polyéthylène par l'approche de 'Polymerization compounding' est faisable en utilisant un système catalytique de type Ziegler-Natta. Nous avons également mené les mêmes expériences pour l'encapsulation de particules d'alumine, les résultats correspondant n'ont pas été inclus dans l'article traitant de ce sujet. La microscopie électronique montre une très fine

couche de polymère d'environ 6 nm enrobant les nano particules de manière uniforme. Bien que les résultats confirment que les nano particules sont individuellement enrobés de polyéthylène, quelques images montrent que l'encapsulation d'agglomérats de particules est également possible. D'un autre côté, ces observations peuvent être le résultat d'une agglomération de particules déjà enrobées individuellement.

Dans la seconde partie de cette recherche, la fluidisation des nano particules de zirconium et d'alumine a été étudiée de manière à évaluer leur comportement dans un lit fluidisé. L'objectif était de déterminer dans quelles conditions expérimentales la fluidisation de ces nano particules est uniforme. De nombreuses études ont montré que la fluidisation des nano particules se déroule sous forme agglomérée, mais il était important de savoir si la fluidisation de ces particules avait lieu de manière homogène en terme de concentrations des phases solide et gazeuses à l'intérieur du lit. Dans le cas contraire, l'encapsulation par le polymère ne pourrait pas se produire uniformément sur la surface des particules ultra fines. Donc l'évaluation de la distribution des concentrations de chacune des phases dans le lit fluidisé a été étudiée grâce à un densimètre radioactif et à la fibre optique. À première vue la fluidisation des nano particule de zirconium et d'alumine entraîne une expansion du lit limitée et une ascension rapide des bulles à travers le lit. Elle consiste également en une distribution non uniforme des agglomérats dans le lit ; les plus petits apparaissant à la surface fluidisent dans la partie supérieure du lit et les plus gros tombant graduellement dans la partie inférieure du lit. L'expansion du lit fluidisé pour les particules de zirconium est

plus limitée comparativement à celui des particules d'alumine. Ceci s'explique par l'écart de densité apparente entre les deux types de nano particules. Que ce soit pour les particules de zirconium ou d'alumine les résultats de la densimétrie radioactive et des fibres optiques montrent que la concentration de solide est uniforme sur une section donnée pour différentes vitesses de gaz et différentes hauteurs de lit. Dans le cas du zirconium, le taux moyen de rétention de solide à travers une section est pratiquement indépendant de la hauteur du lit et la réduction de la rétention est faible lorsque la vitesse augmente au-delà de 6.64 m/s de 20% à 17%. Au contraire, pour l'alumine, le taux de rétention de solide dans le lit fluidisé varie selon la hauteur du lit.

La concentration globale de solide obtenue par densimétrie radioactive est en accord avec les mesures de l'expansion du lit. Toutefois, le taux de rétention calculé à partir de la méthode des fibres optiques conduit à des résultats surestimés pour les vitesses de gaz les plus élevées.

Pour étudier l'effet de la densité apparente sur la fluidisation des nano particules, la fluidisation des oxydes de silice et titane ayant une très faible densité apparente a également été testée. Il a été compris que la densité apparente est un facteur clé dans la fluidisation des nano particules comme mentionné dans la littérature. Dans ce sens, les nano particules ayant une densité apparente inférieure à 100 kg/m^3, tel que la silice dans notre étude, produisent 'Agglomerate Particulate Fluidization' (APF) comprenant une expansion importante du lit, une distribution uniforme des agglomérats dans le lit, et aucune bulle. De l'autre côté, les nano particules ayant une densité apparente supérieure

à 100 kg/m^3, tel que le zirconium, l'alumine et le titane dans notre cas, montre 'Agglomerate Bubbling Fluidization' (ABF), une limite d'expansion du lit et une distribution non uniforme des agglomérats dans le lit.

La présence d'humidité lors de la fluidisation des nano particules a également été étudiée. Les résultats prouvent que l'humidité a un effet important sur la fluidisation notamment sur les APF, en effet une augmentation de l'humidité au sein du gaz de fluidisation entraîne un changement de régime de fluidisation passant d'un état de APF à un régime de bulles.

Dans la dernière partie, la méthode de 'Polymerization compouding' a été appliquée à l'encapsulation des nano particules de zirconium et d'aluminium dans un réacteur à lit fluidisé. Le défi majeur à surmonter lors de cette partie a été de déposer de manière homogène le catalyseur à la surface des nano particules. En effet, seule une très faible quantité de catalyseur est requise pour une surface très grande de particules (environ 1 µl/m^2). Lorsque l'encapsulation a lieu en phase slurry, cette étape ne pose pas de problème, parce que les particules sont dispersées dans un solvant organique dans lequel le catalyseur est injecté et dissout. Ainsi, les particules dispersées dans le solvant sont uniformément exposées au catalyseur dissout. D'un autre côté, quand l'encapsulation a lieu en phase gaz, tel qu'en lit fluidisé, aucun média liquide ne peut être utilisé pour dissoudre le catalyseur. La procédure choisie pour déposer le catalyseur sur les nano particules consiste en l'évaporation du catalyseur avant l'entrée dans le lit fluidisé suivi

par sa condensation sous forme solide à la surface des particules. Étant donné qu'il n'y a pas de gradient de température dans le réacteur et que par conséquence toutes les particules sont à la même température, la vapeur du catalyseur peut se déposer uniformément à la surface des particules.

Comme les résultats le prouvent, les nano particules sont enrobés par du polyéthylène à haut poids moléculaire. De plus, la présence de catalyseur à l'interface entre les particules et le polymère, visible au XPS, confirme que la réaction de polymérisation a été initiée à partir du substrat. Une analyse au TGA de différents échantillons provenant de la même expérience a permis de montrer que la quantité de polymère de chacun était similaire, ce qui prouve que l'encapsulation se produit de manière uniforme dans le réacteur. Les résultats montrent que la température ainsi que la pression ont une influence importante sur la réaction de polymérisation. Par exemple, en augmentant la pression de 20 à 30 psi, la quantité de polymère enrobée sur les particules passent de 2 à 7 %. Les images prises au microscope illustrent l'encapsulation uniforme des nano particules d'aluminium par le film de polymère. Cependant, pour les particules de zirconium, l'uniformité de l'enrobage de polymère n'a pas pu être observée. De plus, les particules de zirconium ont tendance à être enrobé sous forme agglomérée contrairement aux particules d'aluminium.

TABLE OF CONTENTS

LIST OF FIGURES

LIST OF TABLES

LIST OF SYMBOLS

H	Bed height (cm)
H_o	Initial bed height (cm)
ΔP	Pressure drop across the bed (kPa)
r	Local position over the cross section in fiber optic test(cm)
R	Bed Radius (cm)
U	Superficial gas velocity (cm/s)
W	Weight of bed over bed cross section (kPa)
x	Linear position over the cross section in densitometry test(cm)

Greek letters

$\rho_{b\ loose}$	Loose bulk density (cm^3/gr)
$\rho_{b\ tapped}$	Tapped bulk density (cm^3/gr)

INTRODUCTION

One way to improve nanoparticles properties such as their chemical stability is to encapsulate them with polymer. Accordingly, it is necessary to improve interfacial properties between the original surface of particles and polymer coat in order to provide the modified particles with the properties required to obtain high performance composite materials. Polymerization compounding (PC) is an approach in which the polymer is forced to grow from the surface of the solid using catalyst sites covalently bonded to the particles. Therefore, a very intimate contact between the particle surface and polymer is established, bringing improved interfacial properties, and consequently enhanced properties of the nanocomposite. Polymerization compounding, also known as graft polymerization, is a well-known approach in the composite and nanocomposite preparation field and there are a number of studies concerning this approach. However, nearly all the researches dealing with encapsulation of nanoparticles via polymerization compounding have been carried out in the liquid phase where difficulties arise with respect to removing organic solvent and impurities and drying the encapsulated particles. Accordingly, the main objective in this research is to develop a new process to coat nanoparticles using polymerization compounding technique, in a gas-phase reactor, particularly a fluidized bed reactor, free from solvent and consequently, avoiding further drawbacks due to performing the process in liquid phase. To achieve the target, the following sections are presented in this work:

1- In the literature review, first, the polymerization compounding approach is introduced and the recent researches dealing with this method in order to improve the interfacial properties in nanocomposite preparation and nanoparticles encapsulation are presented. It is followed by a literature survey concerning nanoparticle fluidization and their particular characteristic such as agglomerate fluidization.

2- The first paper deals with nanoparticles encapsulation via polymerization compounding technique in slurry phase reactor. In this part, the feasibility of coating of zirconia nanoparticles by polyethylene using Ziegler-Natta catalyst is investigated.

3- The second paper objective is to study the nanoparticles behaviour in fluidized bed. In this paper, the fluidization behaviour of zirconia and aluminum nanoparticles is assessed by focusing on evaluation of phase concentration distribution in the bed.

4- The third paper deals with the final objective of the research, which is encapsulation of nanoparticles by polymerization compounding in fluidized bed reactor using Ziegler-Natta catalyst.

5- Finally, in the section of general discussion, a full review of the work is presented.

CHAPTER 1

LITERATURE REVIEW

1.1 Polymerization Compounding

Coating or encapsulating nanoparticles with polymers is desirable in many applications in order to improve their chemical stability, reduce their toxicity, and facilitate their storage, transport, and processing. In recent years, several methods and approaches have been investigated to carry out polymer coating on nanoparticles (Wang et al. 2004, Zhang et al. 2005, Gass et al. 2006, Avella et al. 2006). However, not all of them provide the modified particles with the properties required to obtain high performance composite materials. The mechanical properties of polymer composites greatly depend on the combined behavior of particles (filler), the polymer matrix, and, most importantly, the interface between them. The latter is readily affected by any change to the particle surface, such as a polymer coating of the same nature as the polymer matrix. Under such a configuration, the quality of the interactions between the particles and encapsulating polymer becomes an important factor favorably affecting the nanocomposites performance. If a catalyst supported on the surface of particles gets involved in a polymerization reaction, a very intimate contact between the particle surface and polymer will be established, bringing improved interfacial properties and, consequently, enhanced properties of the nanocomposite. Polymerization compounding

(PC), also known as graft polymerization, is an approach in which the solid becomes involved in the polymerization reaction so that the polymer is forced to grow from the surface of the solid providing good adhesion and interaction between the particles and the encapsulating polymer.

1.1.1 Polymerization compounding on fibers

The PC technique has been developed and extensively studied by Ait-Kadi and his coworkers for polyethylene and nylon coating applications on the surface of different types of fibers (Wang et al. 1992, Wang et al. 1993, Salehi-Mobarakeh et al. 1996, Salehi-Mobarakeh et al. 1997, Salehi-Mobarakeh et al. 1998). When incorporated in composite materials, they observed that the surface of fibers having received the grafted polymerization catalyst was completely covered, while ungrafted fibers, where no catalyst was grafted on, were only scattered by polymers after polymerization (Wang et al. 1993). Therefore, when the catalyst was chemically bonded to the fibers, the monomer was polymerized from the fiber's surface forming a polymer coating on each fiber, which ensured their dispersion in the polymer matrix and a good wetting of fiber surfaces by the polymer. Also, solvent extraction experiments confirmed the strong adhesion between the fiber surface and polymer obtained by the polymerization process (Wang et al. 1992). Moreover, SEM images of fractured composites revealed a smooth surface for fibers with no polymer on, while adhered polymer was clearly observed on the treated fiber surface (Salehi-Mobarakeh et al. 1997). More recently, Rajabian and Dubois (2006) applied the PC approach to make a HDPE coating on the Kevlar pulps to

be used as reinforcement in the polyethylene matrix. Composites with fiber content as high as 15% were successfully obtained, owing to the improved adhesion and dispersion of the treated fibers. All of the results mentioned above confirm that catalyst-grafted polymerization provides an excellent dispersion of solid in the polymer binder, an excellent wetting of the solid substrates by the polymer, and a good interaction between the solid substrate and encapsulating polymer, which are not always very satisfied by other and more conventional methods of composite preparation, such as melt mixing.

1.1.2 Polymerization Compounding on Nanoparticles

In the field of nanoparticle fillers and substrates, several investigations were devoted to apply the PC approach for nanocomposite preparation and fine particle encapsulation (Rovira-Bru et al. 2001, Shi et al. 2001, Kasseh et al. 2003, Roy et al. 2004, Ding et al. 2004, He et al. 2004, Wang et al. 2005, Dubois et al. 2006, Esmaeili et al. 2006, Che et al. 2007, Garcia et al. 2007). Kasseh et al. (2003) conducted free radical polymerization of styrene on the surface of ultrafine silica to prepare highly filled composite. They obtained highly loaded composites (77.9 %), which could not be otherwise achieved by techniques, such as mechanical mixing, solvent dispersion, and precipitation. Roy et al. (2004) carried out the in-situ synthesis of high density polyethylene on the surface of aluminum nanoparticles, using a Ziegler-Natta catalyst. They applied a thin polymer layer, in the order of a few nanometers, around particles in a process, which was flexible enough to control the amount of polyethylene grafted on powders up to 25% w/w, as shown in Figure 1.1.

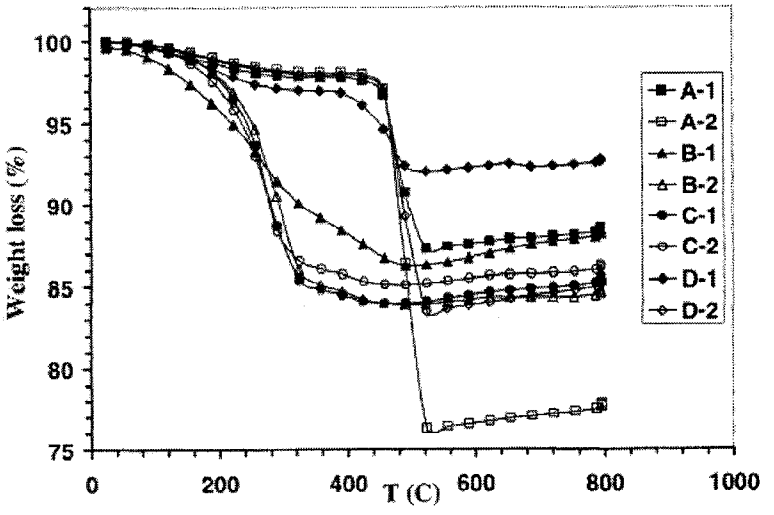

Fig. 1.1 TGA of samples of polyethylene coated aluminum (Roy et al. 2004).

He et al. (2004) deposited a thin layer of polyethylene film on zirconia nanoparticles by inductively coupled plasma polymerization and the covalent bond between the substrate and polymer was confirmed by XPS, as shown in Figure 1.2.

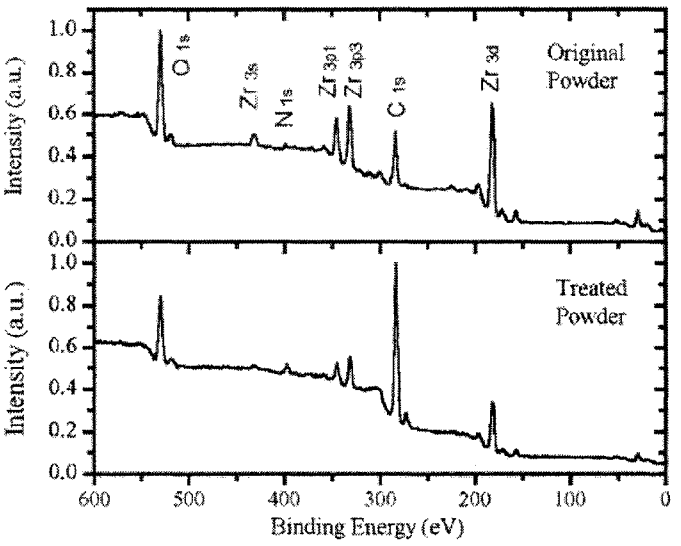

Fig. 1.2 Compared XPS results in survey binding energy scan between untreated and treated powders (He et al. 2004)

Rovira-Bru et al. (2001) treated zirconia nanoparticles to first modify the density of the hydroxyl group at the particle surface and then carry out vinylpyrolidone polymerization. The atomic force microscopy (AFM) confirms that the surface was fully covered by a well-dispersed polymer coating of about 20 nm in thickness, shown in Figure 1.3.

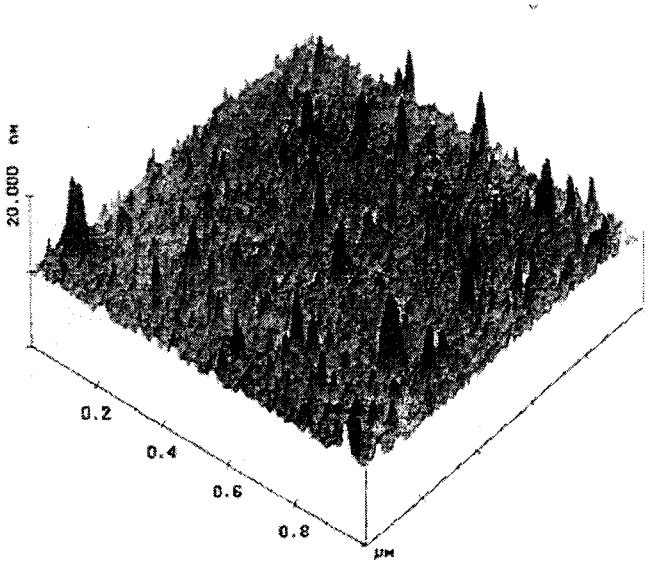

Fig. 1.3 AFM image of polymer –grafted silicon surface (Rovira-Bru et al. 2001).

Dubois et al. (2006) incorporated fumed silica ultrafine particles into polyurethane at concentrations as high as 25% via the PC approach. They explained that the enhancement in water absorption and thermorheological and mechanical properties was due to improved bonding between the solid substrate and the binder. Esmaeili et al. (2006) successfully applied this technique to encapsulate zirconia nanoparticles with a thin layer of polyethylene in the order of a few nanometers. In the TEM image of coated particles, shown in Figure 1.4, the light part represents the polymer coating in contrast to the dark one, which represents the original particles.

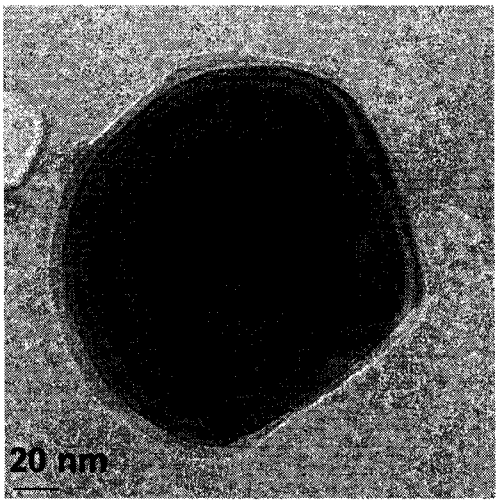

Fig. 1.4 TEM image of polymer coated zirconia (Esmaeili et al. 2006).

To improve the particles dispersion in a non-aqueous media, Che et al. (2007) applied PC to graft polyacetal onto the surface of SiC nanoparticles of 50 nm. TEM images and sedimentation experiments showed that an ideal dispersion state of the SiC nanoparticles in butanone medium was achieved after surface modification. With the aim of improving the dispersion of organic particles inside an organic matrix, Garcia et al. (2007) generated polystyrene brushes grown on the surface of iron oxide magnetic nanoparticles with an atom transfer radical polymerization. The density of grafted PS brushes was determined at 0.9 chains/nm^2.

As mentioned above, polymerization compounding is a well-known technique for nanoparticles encapsulation and nanocomposite preparation to achieve the appropriate interfacial properties between the substrate and polymer coat or matrix. Nevertheless, nearly all the works dealing with the encapsulation of nanoparticles via polymerization compounding have been carried out in the liquid phase where difficulties arise with respect to removing organic solvent and impurities and drying the encapsulated particles. Therefore, it is desirable to carry out the encapsulation process in a gas solid reactor where no solvent is needed. Consequently, coating the surface of nanoparticles, on the one hand using the polymerization compounding approach to obtain a composite with high interfacial properties and on the other hand in a gas-solid reactor would be the target of this research. For this purpose, it is believed that the fluidized bed reactor is the appropriate choice because not only the process of coating is carried out away from organic solvent and impurities, but also it is flexible for extending to the continuous process. In addition, the fluidized bed is widely used in powder processing applications because it enables continuous powder handling and good particles mixing. Besides, fluidization exhibits excellent advantages, e.g., high heat and mass-transfer rates, temperature homogeneity and high flowability of particulate materials. Therefore, it is required to understand the behavior of nanoparticles and when to be fluidized. Accordingly, in the next section, a complete review is presented about different aspects of nanoparticle fluidization, including nanoparticle fluidization features, nanoparticle agglomerate fluidization, agglomerate size prediction in fluidization, and the methods to improve nanoparticle fluidization quality.

1.2 Fluidization of Nanoparticles

Ultrafine particles belong to group C of Geldart classification, as shown in Figure 1.5. Since these particles are very cohesive, normal fluidization of such powders is extremely difficult. These particles lift as a plug in small diameter tubes or channels caused by extending the voids from distributor to bed surface. This problem arises where the interparticle forces are higher than those, which the fluidizing gas exerts on the particle, such as drag force. The interparticle forces are generally the consequence of very small particle size, the humidity, or strong electrostatic charges. Under these circumstances, particle mixing and, accordingly, heat and mass transfer in the bed are much poorer compared to the bed of other groups (Geldart, 1973). Therefore, ultrafine powders are rarely fluidized individually, but only as agglomerates. However, if the agglomerate structure and properties, particularly the interaction effects between agglomerates, can be artificially controlled, the fluidization of ultrafines is achievable. By applying some external forces, such as vibration and acoustic field, the fluidization quality of these cohesive powders can be improved.

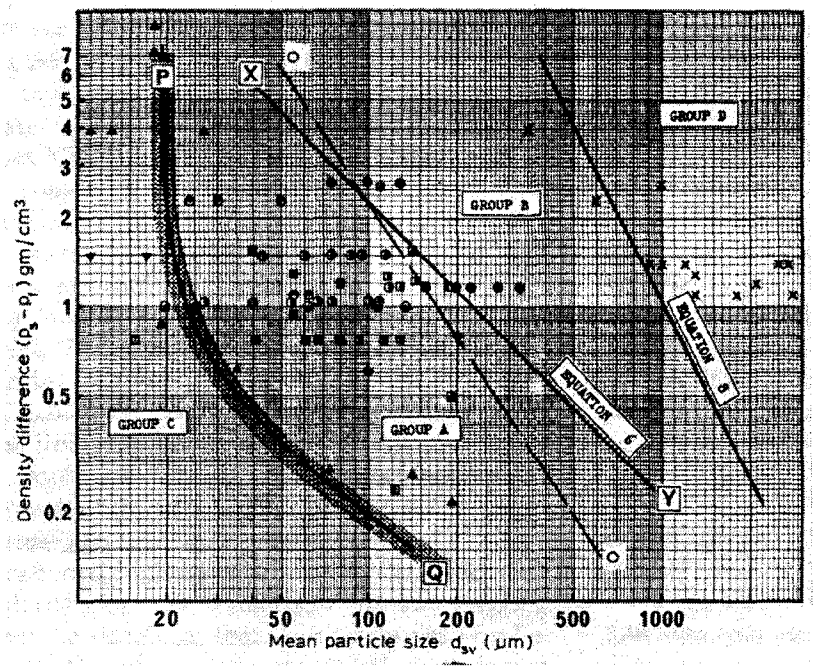

Fig. 1.5 Geldart classification of particle fluidization (Geldart, 1973).

1.2.1 Agglomerate Fluidization of Fine Particles

As shown in Figure 1.6, the fluidization of fine particles usually consists of channeling, slugging, disrupting, agglomeration, and their combination, depending on the particle characteristics (Wang et al. 1998, Li et al. 1999). The agglomerate formation is a common phenomenon in fine particle processing caused by the strong cohesive forces between primary particles. These forces are due to the high surface-to-volume ratio of particles and the short distance between them. Many properties of bulk powders, such as flowability and chemical reactivity, are strongly influenced by the formation of

agglomerates. The agglomerates, in comparison with fine particles, are more essential for many powder processes, since they flow more easily and more predictably.

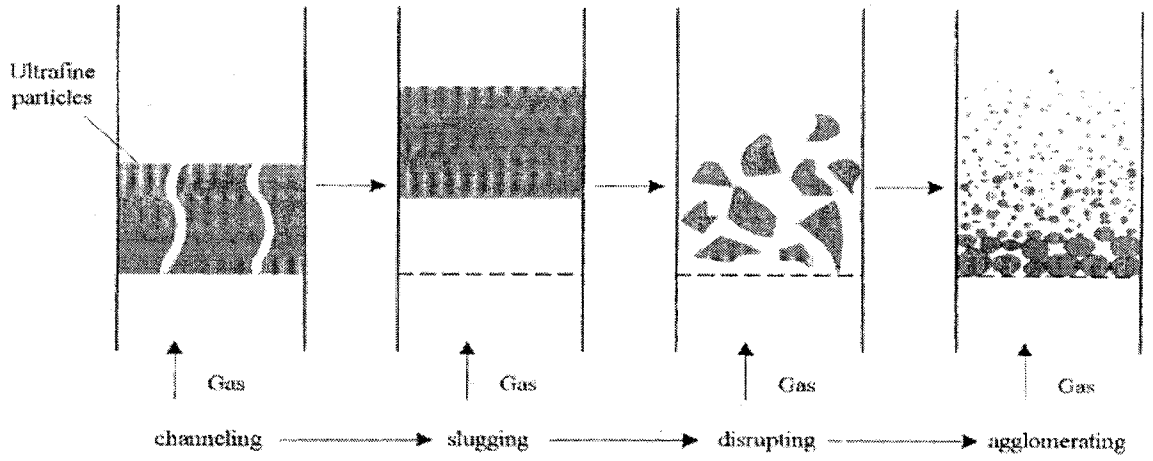

Fig.1.6 Process of fluidizing ultrafine particles (Wang et al. 1998, Li et al. 1999).

As shown in Figure 1.7, there are three regions in the fluidized bed of nanoparticles agglomerate, i.e., a fixed-bed region of large agglomerates at the bottom, a fluidized region of smaller agglomerates in the middle, and a diluted-phase region of even smaller agglomerates further up in the fluidized bed. The third part may include individual and unassociated particles. When the small agglomerates are taken out from the top of the bed and returned repeatedly at the bottom, such as what happens in circulating fluidized

beds, the nonuniform size of these agglomerates can generally reach a steady and relatively uniform value (Wang et al. 1998, Li et al. 1999).

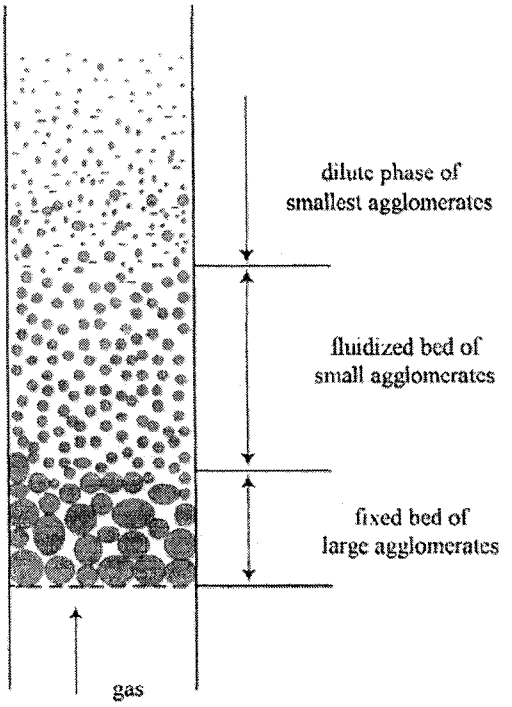

Fig. 1.7 Structure of agglomerate fluidized bed (Li et al, 1999).

In previous studies dealing with gas fluidization of nanoparticle agglomerates (Chaouki et al.1985, Yao et al. 2002), it has been shown that the minimum fluidization velocity u_{mf} is about several orders of magnitude greater than the minimum fluidization velocity of primary nanoparticles as calculated by using available correlations (Kunii and

Levenspiel, 1991). Chaouki et al. (1985) investigated the fluidization of Cu/Al_2O_3 aerogels having a very small particle diameter in the order of a few nanometers, and a very small bulk density (60 kg/m^3). They found that when air passed through a bed of aerogel, self-agglomeration happened and the bed of agglomerates fluidized smoothly at a velocity above 0.04 m/s, which is about 20000 times higher than the u_{mf} calculated for the primary particles. They observed at low gas velocities that preferential channeling usually occurred. However, with increasing the velocity, the original bed of particles reached an unstable state at about 0.04 m/s and rearranged itself into a new system consisting of agglomerates. Below that point, gas channeling was large enough to cause pressure drops to be very small, as shown in Figure 1.8. It was found that the size of the agglomerates was uniform throughout the bed with a diameter of the order of 1 mm, using a rough photographic analysis. They observed, except for a few local cavities, a texture for an expanded bed much closer to the smooth homogenous fluidized state than the aggregative bubbling regime.

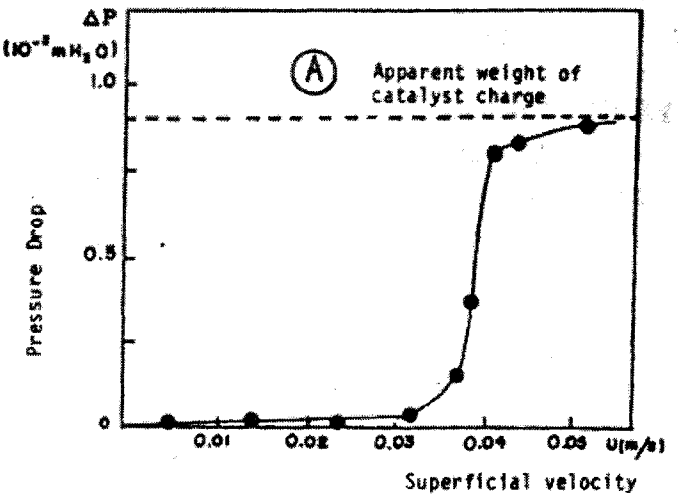

Fig. 1.8 Pressures drop of CuO/Al_2O_3 (Chaouki et al. 1985)

The mechanism illustrated in Figure 1.9 was proposed for the hydrodynamic of the bed based on the experimental results (Chaouki et al. 1985). The gas flows through the fixed bed of initial particles at low superficial velocities. By increasing the gas velocity, systems with negligible interparticle forces reach a bed loosening velocity corresponding to the minimum fluidization velocity of the individual particle. For very cohesive systems, primary particles can not loosen up at predictable minimum fluidization velocities and preferential spouting may occur. They found the behavior of aerogels to be between these two limiting cases. According to the model described above, they supposed the density of a cluster equals the bulk density of a fixed bed and, accordingly, they calculated an average cluster to be equivalent to a spherical diameter of 0.7 mm that was comparable to the size estimated from their photographic analysis.

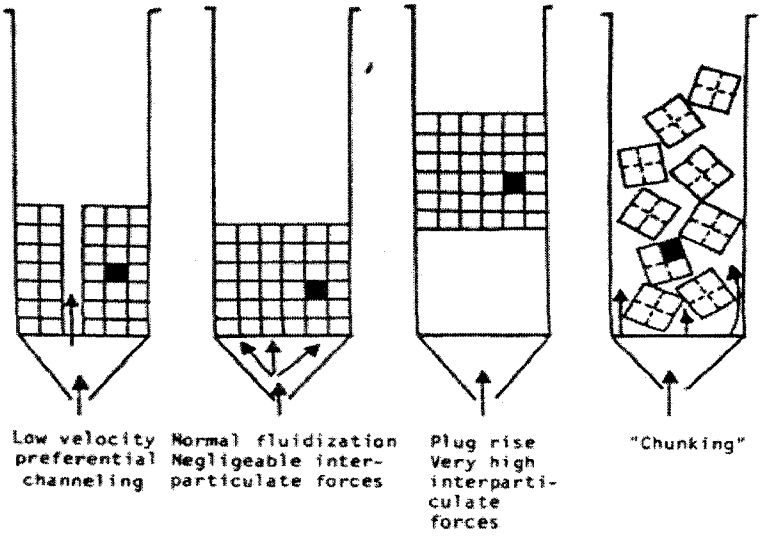

Fig. 1.9 Descriptive hydrodynamic behavior of fluidized aerogels (Chaouki et al. 1985).

Morooka et al. (1988) observed that submicron particles of Ni, Si_3N_4, SiC, Al_2O_3, and TiO_2 were smoothly fluidized when the gas velocity was high enough to disintegrate the particle structure and avoid the coalescence of agglomerates. The size of agglomerates in the bed was in the order of 70-700 μm, depending on the particle type and gas properties. As indicated in Figure 1.10, the bed expansion for some powders attained up to more than 200% of the fixed bed level, depending on the gas velocity. The minimum fluidization velocity of particles was obtained in the range of 1-8 cm/s using pressure drop measurement across the bed. It was found that the agglomerates of $CaCO_3$ and ZrO_2 were very cohesive and easily coalesced to form a homogeneous structure. Accordingly, the diameters of these powders were not determined. Therefore, the size of the primary particle is not a proper factor for the classification of fluidized particles.

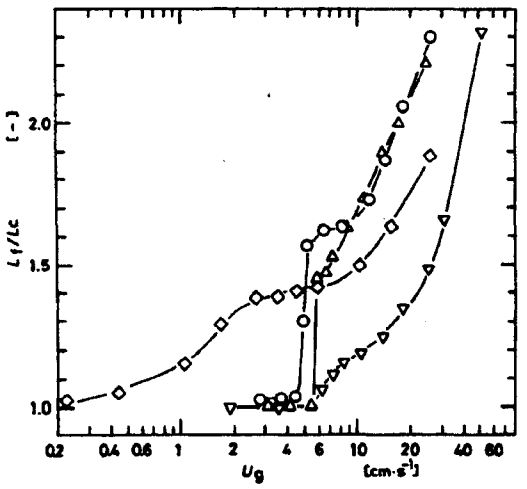

Fig. 1.10 Bed expansion across the bed (Morouka et al. 1988).

Yao et al. (2002) studied the fluidization of six kinds of SiO_2 powders with high void fractions and particle sizes from 7 to 16 nm. They observed that the agglomerate formation of SiO_2 aerogels occurred in several steps, called multi-stage agglomeration. Firstly, nonporous spheres of less than 20 nm aggregate into chain clusters. These chain clusters connect as tridimensional netlike structures to form an extremely porous skeleton with a very low bulk density. Subsequently, the tridimensional netlike structures aggregate into simple agglomerates, mostly with a diameter of 1–100 μm. Finally, the simple agglomerates further join into complex agglomerates during fluidization. They observed that these SiO_2 agglomerates smoothly fluidized with extremely high bed expansion and without any bubble, as indicated in Figure 1.11. They claimed that the relationship between gas velocity and the voidage around the fluidized agglomerates is consistent with the Richardson-Zaki equation (Richardson and Zaki,

1953). This type of nanoparticle agglomerate fluidization was termed *agglomerate particulate fluidization* (APF) (Yao et al. 2002).

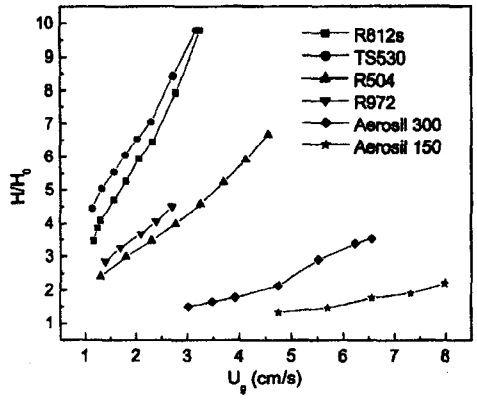

Fig. 1.11 Homogenous expansion of the fluidized bed (Yao et al. 2002).

On the contrary, fluidization of some nanoparticles showed a very limited bed expansion, large bubbles rising up very quickly through the bed, and agglomerates distributing non-uniformly within the bed. This type of fluidization was termed *agglomerate bubbling fluidization* (ABF). They believed that the difference between APF and ABF depends greatly on the bulk density and the primary particle size (Yao et al. 2002). The fluidization of relatively small nanoparticles (< 20 nm) with low bulk density (< 100 kg/m^3) is likely to behave as APF, whereas larger nanoparticles with higher bulk density appear to behave as ABF. Notable differences between APF and ABF are summarized in Table 1.1

Table 1.1 Comparison of the fluidization behavior of APF and ABF (Yao et al. 2002).

	APF	ABF
Primary particle size	Nano-particles	Micro-, submicro-, nanoparticles
Agglomerates	Porous, multi stage, light in weight	Compact, single-stage, heavy
Bulk density	Low (< 100 kg/m^3)	High (>100 kg/m^3)
Fluidization Characteristics	1. Bubbleless 2. High bed expansion 3. Agglomerates uniformly distributed in the bed 4. Homogeneous expansion of bed, decrease of bed density with u_g	1. With bubbles 2. Low bed expansion 3. Large agglomerates at the bottom of the bed, with small ones at the top 4. No change of bed expansion and emulsion phase density with u_g

In accordance with previous research, Zhu et al. (2005) investigated the fluidization of 11 different nanoparticle materials with two types of fluidization behavior, APF and ABF. They found, for both APF and ABF nanoparticle agglomerates, the pressure drop increased with increasing gas velocity reaching a plateau and became independent of gas velocity. For APF nanoparticles, it was observed that the bed fluidized and expanded uniformly without bubbles with a high bed expansion ratio, shown in Figure 1.12. Moreover, by increasing gas velocity, the bed expansion increased and agglomerates distributed uniformly in the bed. For ABF nanoparticles, the bed expanded very little, less than 50%, with increasing gas velocity (Fig. 1.12 b). They observed large bubbles rising up quickly through the bed and the agglomerates distributing non-uniformly within the bed.

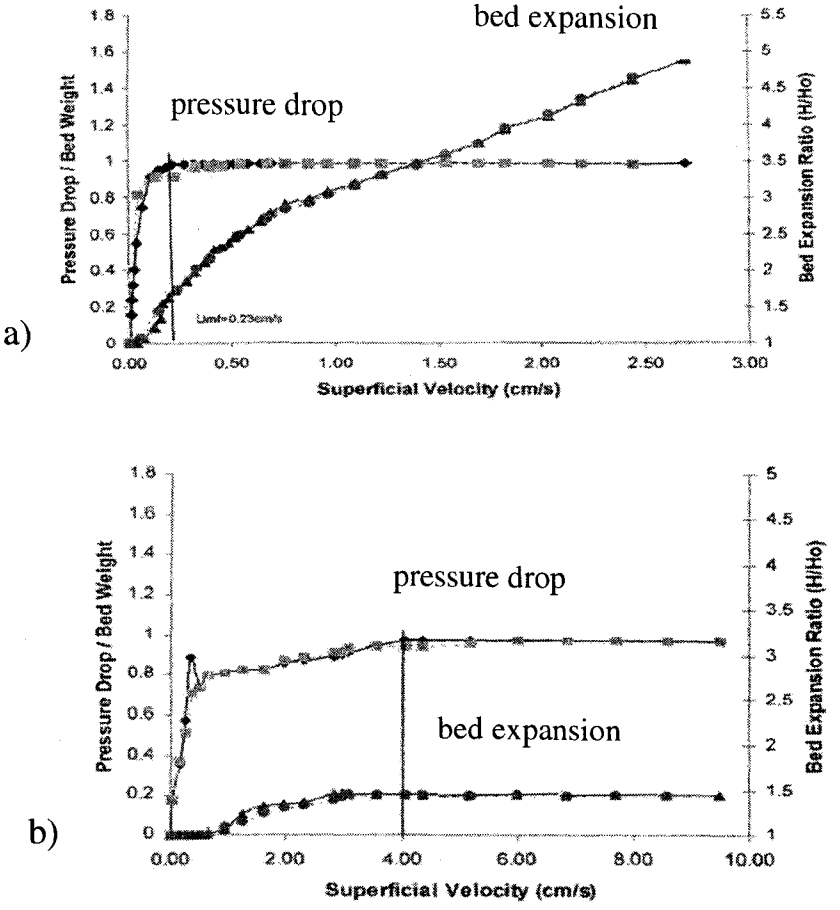

Fig. 1.12 Typical fluidization curves for a) APF and b) ABF nanoparticles (Zhu et al. 2005).

Jung and Gidaspow (2002) studied the fluidization of 10 nm diameter fumed silica and observed that the agglomerates of these nanoparticles with very low density were fluidized without bubbles. The minimum fluidization velocity was determined at 0.0115 m/s by means of a pressure drop measurement as a function of superficial gas velocity. The fluidized bed height at the minimum fluidization was around 2.8 times the static bed height and solid concentration at this condition was 0.0077. In this work, γ-ray

adsorption technique was applied for evaluating the time-averaged volume fractions of the particle phase at a designated location. Figure 1.13 shows the solid volume fraction as a function of bed height obtained using the γ-ray densitometry.

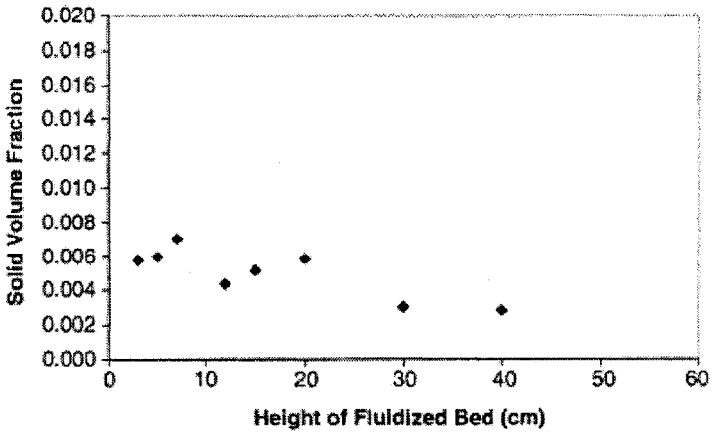

Fig. 1.13 Time-averaged solid volume fraction profile as a function of height of the fluidized bed (Jung and Gidaspow, 2002).

Esmaeili et al. (2008), also, applied the γ-ray densitometry technique as well as fiber optic measurements to evaluate phase dispersion distribution in the fluidized bed of zirconia and aluminum nanoparticles. The results showed that the distribution of solid hold-up across the bed cross section and along the bed height is uniform, although the fluidization of those nanoparticles was similar to ABF behavior, as it would be anticipated according to their quite high bulk density.

Recently, Quevedo et al. (2007) investigated the effect of the humidity level on conventional and assisted fluidization of hydrophilic nanoparticles. It was found that the

mass transfer between the gas and the nanopowder was larger in the case of fluidization under the influence of the assisting method in comparison with conventional fluidization.

1.2.2 Models for Agglomerate Size Prediction

To predict an equilibrium agglomerate size, several mathematical models were developed based on force/energy balance in agglomerate fluidization of ultrafine particles (Chaouki et al. 1985, Morooka et al. 1988, Iwadatw and Horio 1988, Zhou and Li 1999, Zhou and Li 2000, Matsuda et al. 2004, Guo et al. 2007). Chaouki et al. (1985) applied the force balance exerted on each agglomerate in a fluidized bed assuming the adhesion force works on a single contact point between two adjacent agglomerates. To evaluate the agglomerate size, they assumed that the drag force due to gas flow, which is approximately equal to gravity force acting on the agglomerate, is equal to the van der Waals force of attraction between primary particles. The model was in good agreement with the experimental results of light aerogel particles. Morooka et al. (1988) proposed a model for the formation and disintegration of agglomerates. They considered while the agglomerate formation occurs because of adhesive force, it can be disintegrated into smaller agglomerates by any body force or drag force, as shown in Figure 1.14. Consequently, the equilibrium size of agglomerates is determined when the collision energy does not exceed the energy required to break agglomerates.

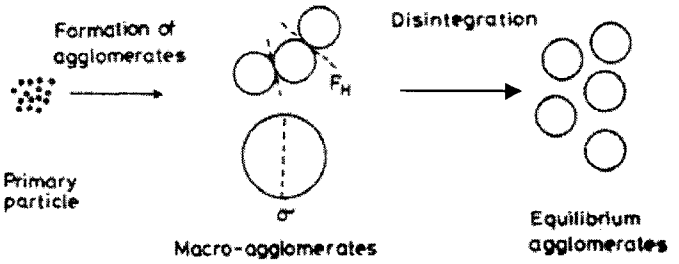

Fig. 1.14 Model for formation of equilibrium agglomerates (Morooka et al. 1988)

Iwadat and Horio (1998) predicted agglomerate size in an agglomerating bubbling fluidized bed of Geldart group C particles. In their model, the agglomerate size was obtained using the balance of bed expansion force caused by bubbles and agglomerate-to-agglomerate cohesive rupture force. The agglomerate-to-agglomerate interaction force was approximated by van der Waals force. The model was fairly consistent with previous experimental data and additional data in that work. Zhou and Li (1999) developed a model of force balance for the collision between two agglomerates of different sizes. They mentioned that after a collision between two agglomerates, three scenarios may take place: a) separation; b) agglomeration; c) disintegration or breaking, shown in Figure 1.15.

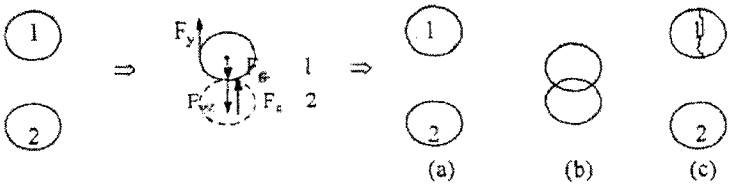

Fig. 1.15 A schematic of a proposed model of an agglomerate collision (Zhou and Li 1999).

They considered that four forces were acting when two agglomerates collided with each other; drag force, collision force, gravity force, and the cohesion force between two agglomerates. In another work, Zhou and Li (2000) proposed an agglomeration criterion as a function of the above mentioned forces where separation or coalescence happens after the collision of agglomerates. Matsuda et al. (2004) represented a comprehensive model based on the energy balance model respecting energy consumption for the disintegration of agglomerates. They applied the method of Morooka et al. (1998) taking into consideration that the energy required to break the agglomerate decreases due to disintegration. The number of agglomerates, however, increases, leading to an increase in the total disintegration energy required per unit weight of agglomerates. The model was validated by experimental results in the fluidization of TiO_2 particles (7nm). Recently, Guo et al. (2007) developed a mathematical model to predict the agglomerate size in nanoparticle fluidization with sound assistance. The model was developed based on the energy balance between the agglomerate collision energy, the energy arising from the sound wave, and cohesive energy. The experimental results showed that agglomerate size decreased with increasing sound frequency up to a critical value, whereas it was thought that the agglomerate size tended to grow by an increase in sound frequency.

1.2.3 Methods for Improving the Fluidization of Ultrafine Particles

A number of studies have dealt with improving the fluidization of ultrafine particles using different methods. As mentioned before, there is a wide distribution of agglomerate sizes along the height of bed in the fluidization of ultrafine particles (Wang

et al. 1998, Li et al. 1999). Accordingly, there is a fixed-bed region of large agglomerates at the bottom of the bed. Deiva Vanketash et al. (1996) and Li and Tong (2004) applied a conical bed to improve the fluidization quality of the above powders. Since the gas velocity decreased when increasing the bed height, it prevented the elutriation of smaller agglomerates at the top of the bed, while fluidizing larger agglomerates at the bottom of the bed.

In some research, the fluidization of nanoparticles has been developed in a rotating or centrifugal fluidized bed where the centrifugal force acting on the agglomerates is much higher than gravity (Noda et al. 1998, Matsuda et al. 2001, Watano et al. 2003). The large agglomerates formed in fluidization under normal G were not monitored in centrifugal fluidization and agglomerate size decreased as G increased.

Many researchers improved the fluidization quality of ultrafine particles by introducing external force excitations to the bed, such as vibration (Wank et al. 2001, Matsuda et al. 2004, Nam et al. 2004, Quevedo et al. 2007) and sound waves (Russo et al.1995, Herrera et al. 2001, Zhu et al. 2004, Liu et al., 2007)). It was found that the minimum fluidization velocity for a bed of ultrafine particles decreased considerably. Therefore, with a much lower fluidizing gas velocity, nanoparticle elutriation was significantly reduced.

CHAPTER 2

METHODOLOGY

2.1 Originality of the Work

As mentioned in the literature survey, polymerization compounding is a well-known approach in the domain of nanocomposite preparation and nanoparticles encapsulation. Accordingly, many studies have been carried out to encapsulate nanoparticles with a thin polymer layer using this approach. However, the majority of these researches took place in the liquid phase where difficulties arise with respect to removing organic solvent and impurities and drying the encapsulated particles. Although some attempts at polymerization compounding on the surface of nanoparticles in the gas phase have been made, they consisted of the plasma techniques which bring additional cost and complexity to the process. Therefore, encapsulating nanoparticles, on the one hand using the polymerization compounding approach to obtain a composite with the appropriate interfacial properties and on the other hand in a gas-solid reactor free of an organic solvent, would be the final solution for all obstacles cited above and in the previous section. For this purpose, it is believed that a fluidized bed reactor is the appropriate choice, since it possesses the excellent advantages of high heat and mass transfer rate, temperature homogeneity, and high flowability of particulate materials, which are not all

achievable when applying other competing gas-solid reactors. In addition, the process of nanoparticle coating would be flexible enough to extend to the continuous process.

2.2 Objective

The objective of present work is to encapsulate zirconia and aluminum nanoparticles via a polymerization compounding approach in a gas/solid fluidized bed reactor.

To achieve the above mentioned objective, the following specific aims are defined:

i) To investigate the feasibility of performing the polymerization compounding technique for encapsulating zirconia and aluminum nanoparticles in a slurry-phase reactor

ii) To study the fluidization behavior of zirconia and aluminum nanoparticles in a fluidized bed

iii) To encapsulate zirconia and aluminum nanoparticles by polymer in a fluidized bed reactor using the polymerization compounding method by combining the results obtained in two previous steps

2.3 Methodology

2.3.1 Materials

Zirconia powder prepared by Sigma-Aldrich and aluminum powder manufactured by TEKNA were used for all polymerization and fluidization experiments. Ethylene gas with a purity of 99.5%, supplied by Canadian Liquid Air, was used as a monomer in the

encapsulation process. For fluidization experiments, air was used as a fluidizing gas in most cases; however, to assess the effect of humidity on fluidization, dry nitrogen was used in some experiments. The same Ziegler-Natta catalyst system, consisting of titanium tetrachloride ($TiCl_4$), manufactured by Acros, as a catalyst, and triethylaluminum ($AlEt_3$) obtained from Sigma-Aldrich, as a co-catalyst, was used for all polymerization experiments. The component of the catalytic system were stored and handled in a glove box in order to protect them from moisture and oxygen.

2.3.2 Processes

2.3.2.1 Nanoparticle Encapsulation in the Slurry Phase

Encapsulation of nanoparticles in the slurry phase was carried out in a 1 liter pressurized glass vessel BUCHI reactor (BUCHI laboratory autoclave BEP 280) as shown in Figure 2.1. The jacketed reactor was heated to 65 ^{o}C by an external oil bath circulator and mixing was provided by a top mounted magnetic drive impeller. The pressure in the reactor was measured by a pressure gauge located on the top of unit. In a typical polymerization process, the previously oven-dried particles were dispersed in dried hexane by mechanical agitation at the reaction temperature. The dried nitrogen with a low flow rate was purged to remove oxygen and any trace of water. An ultrasonic processor mounted on the top of the reactor was periodically activated to facilitate the dispersion of nanoparticles in the hexane during degassing. After an hour, the desired quantity of catalyst $TiCl_4$ was injected through a septum feeding port, and a few minutes later, co-catalyst $AlCl_4$ was injected through the same port. The reaction of polymerization starts once nitrogen is replaced by the ethylene monomer and continues

under a moderate overpressure of 30 kPA for the desired reaction time duration before being stopped by an injection of ethanol.

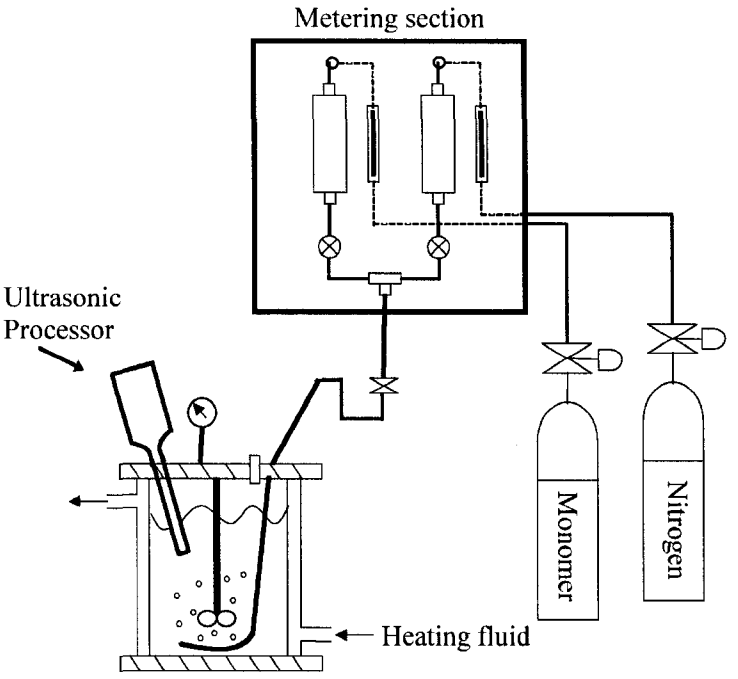

Figure 2.1 Schematic of the reactor setup

2.3.2.2 Nanoparticles Fluidization

A cylindrical column was used as a fluidized bed for fluidization experiments. As demonstrated in Figure 2.2, air, after passing through a rotameter, enters the wind box. The wind box contains small glass beads, which distribute the gas flow very well before being introduced into the bed. Gas then enters the column homogenously through a porous plate with pores 20 microns in size. The Plexiglas column consists of three

transparent parts: bed, freeboard, and disengagement zone. The internal diameter and total height of the bed and freeboard are 5 cm and 60 cm, respectively. There are a number of small ports at different heights of the bed and the freeboard provided for the fiber optic probe, as well as sampling. The disengagement zone has a diameter about 6 times higher than the bed diameter that provides a significant decrease in gas velocity to permit elutriated particles to return to the bed. After the column, a bag filter is available to remove the entrained nanoparticles in the gas.

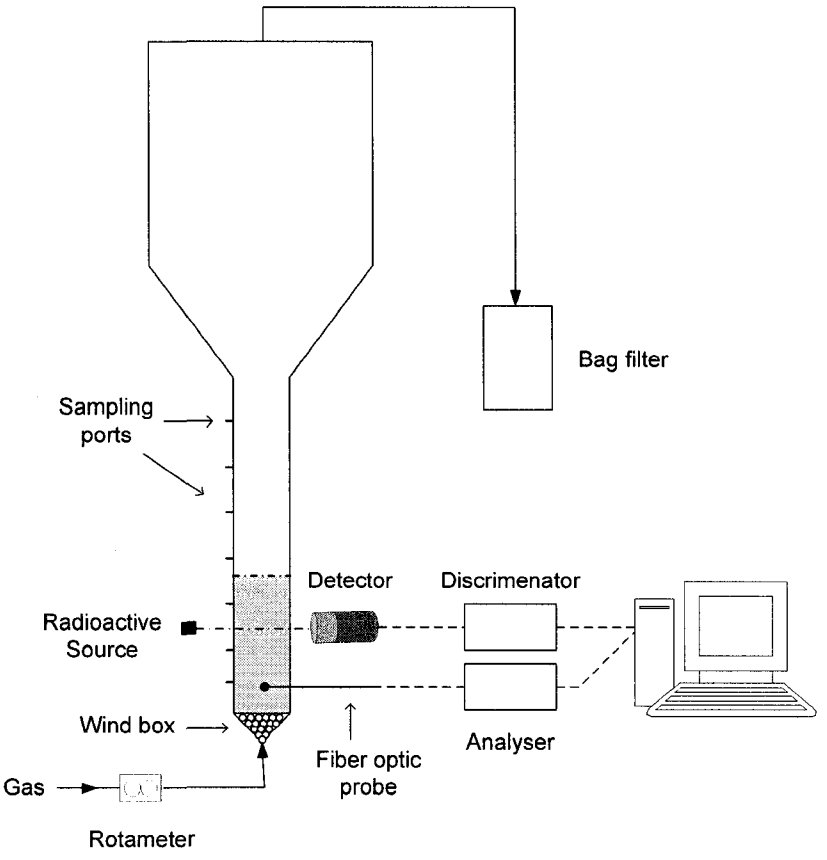

Figure 2.2 Schematic of a fluidized bed and its accessories

2.3.2.3 Nanoparticles Encapsulation in Fluidized Bed

Figure 2.3 illustrates the encapsulation of nanoparticles in a fluidized bed reactor, which is a cylinder made of stainless steel, 2 cm in diameter and 3 cm in height. A porous plate with a 5 μm pore size is provided as a distributor to introduce gas to fluidize particles homogenously in the bed. First, nitrogen, by passing through an electrical heater, provides sufficient energy to heat the entire system so that the injection point attains a higher temperature than the boiling temperature of the catalyst. A second electrical heater was also located around the fluidized bed to adjust the reactor temperature at the desired reaction temperature. Then, the catalyst and, after a few minutes, the co-catalyst are injected into the system. Since the temperature at the injection point is higher than the boiling temperature of $TiCl_4$ and $AlEt_3$, the catalyst and co-catalyst evaporate and enter the reactor in the gas phase. Subsequently, the catalyst and co-catalyst vapors uniformly sublime on nanoparticles in the reactor where the temperature is lower than the catalyst and co-catalyst boiling points. Afterward, the polymerization reaction starts by switching nitrogen to ethylene. After a certain desired time, the ethylene flow rate stops and the system is flashed by nitrogen.

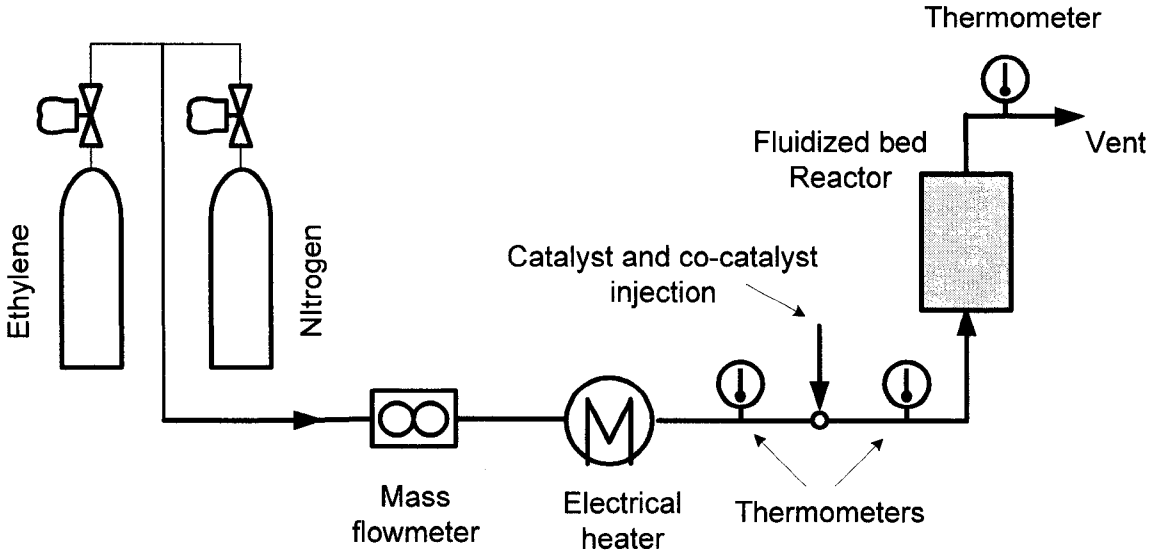

Fig. 2.3 Encapsulation of nanoparticles in a fluidized bed reactor

2.3.3 Analysis and Characterization

2.3.3.1 Coated Particles Characterization

Quantity of polymer coating

The amount of polymer coated on the particles was measured by TGA experiments. The experiments were conducted over a 25- 800 °C temperature range at a 10 °C/min heating rate under a flow of argon. Since it is known that the degradation of polyethylene occurs at 450 to 500 °C, the weight loss in this range of temperatures refers to the amount of polyethylene.

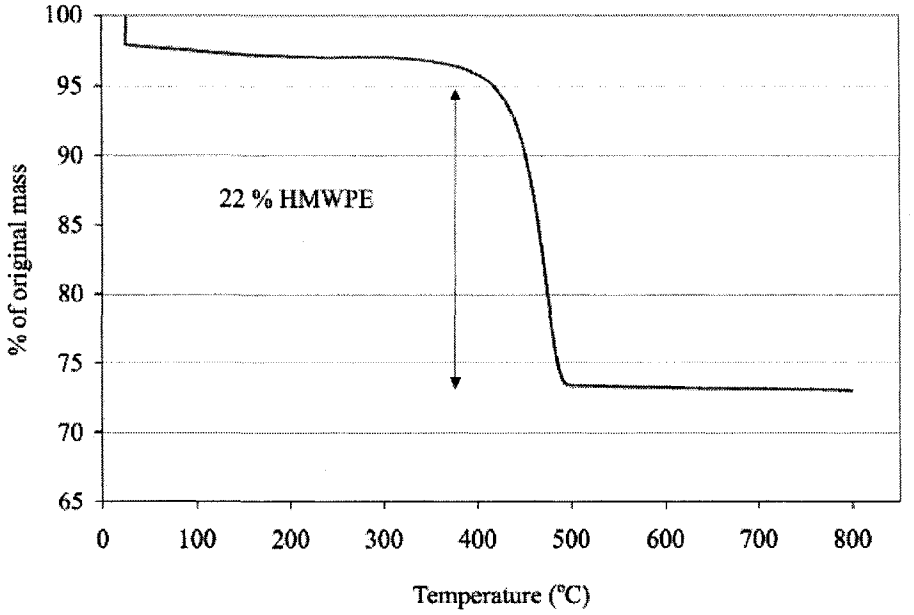

Fig. 2.4 TGA graph of polyethylene-coated zirconia nanoparticles.

Figure 2.4 shows a TGA graph of polyethylene-coated zirconia nanoparticles. The nanoparticles were coated by polymerization of ethylene using a Ziegler-Natta catalyst in the slurry phase. As can be seen, a 22 % weight loss occurs in the 450-500 °C range corresponding to the amount of polyethylene.

Thickness of polymer layer

The thickness of the polymer layer on the surface of nanoparticles was estimated from a picture using Transmission Electron Microscopy (TEM). In this technique, the image is formed by electrons passing through the sample. The principle of the transmission electron microscope operation is almost the same as that of an optical microscope, where glass lenses and photons are replaced by magnetic lenses and electrons, respectively. A

beam of electrons emitted by an electron gun is focused into a small spot (~ 2-3 μm) on the sample and after passing through the sample is focused to project the magnified image onto the screen. While passing through a sample, the flux of the electron loses part of its intensity because of scattering. This lost part is greater for a thicker region or regions with a higher atomic number species. Therefore, the thicker region or regions with a higher atomic number appear dark and the image contrast is monitored. Figure 2.5 shows a TEM image of aluminum nanoparticles coated with a thin layer of polyethylene in the slurry phase. The light part surrounding the particle represents a thin polymer layer of about 6 nm, which uniformly coated the particles. It is seen that particles appear to be individually coated.

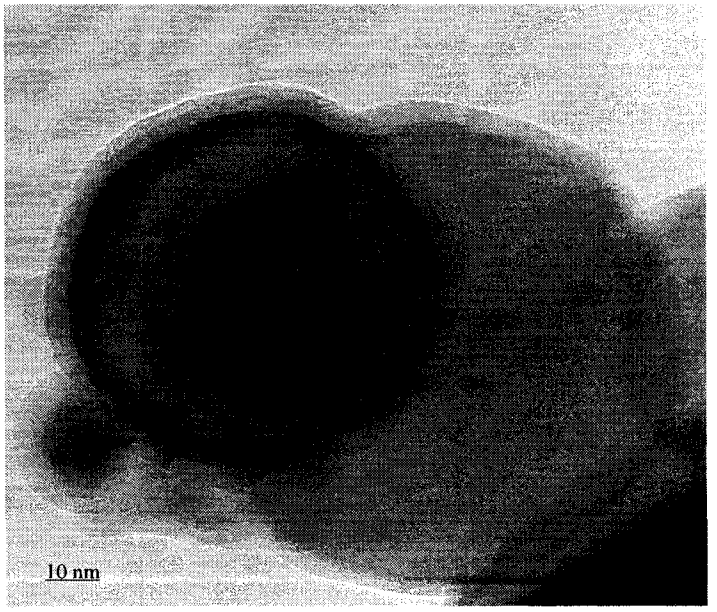

Fig. 2.5 A TEM image of polyethylene-coated aluminum nanoparticles.

Morphology observation

The morphology of coated particles was observed using the scanning electron microscope (SEM). In this technique, an electron beam with primary electron energy is focused into a spot 1-10 nm in diameter on the sample surface and scanned across the sample. Many low energy secondary electrons are generated and the intensity of these secondary electrons is governed by the surface topography of the sample. Therefore, an image of the sample surface is constructed by measuring secondary electron intensity as a function of the position of the scanning primary electron beam. Figure 2.6 shows the SEM images of aluminum nanoparticles coated by a polyethylene layer in the slurry phase. The three dimensional agglomerates of spherical nanoparticles can be observed. One can also observe the presence of some very thin bridges of polymer between particles. It could be because of too much polymer made during the reaction.

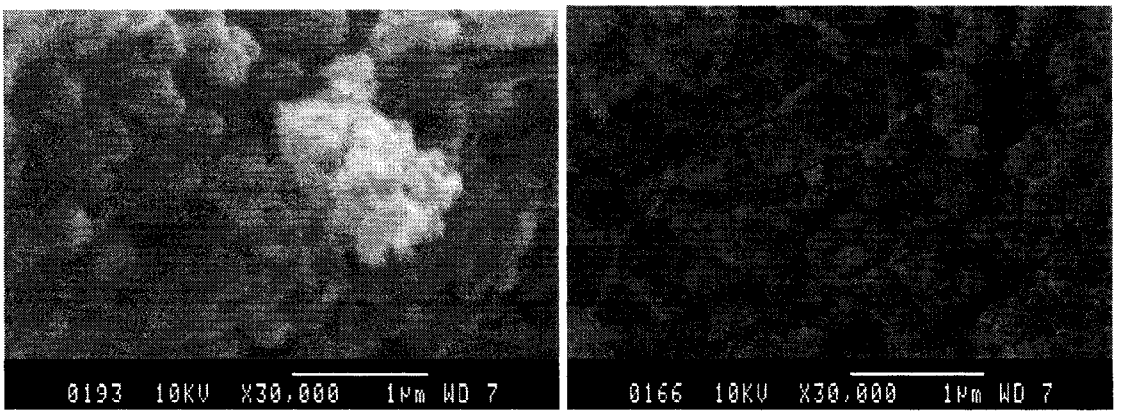

Fig 2.6 SEM images of polyethylene-coated aluminum nanoparticles.

Interfacial analysis

X-ray photoelectron spectroscopy will be used to study the quality of the interfacial link between the polymer coat and particle. Using this method, the existence of chemical bond between the polymer and the surface of particles can be confirmed. X-ray photoelectron spectroscopy (XPS) is accomplished by irradiating a sample with a monoenergetic soft x-ray and analyzing the energy of the emitted electron. The photons with limited penetration power in a solid (1-10 μm) interact with atoms in the surface region, causing electrons to be emitted by the photoelectric effect. Since the emitted electrons have measured kinetic energies, the binding energy of the atomic orbital from which the electron originates can be calculated. The spectrum is obtained as a plot of the detected electron numbers per energy interval versus their binding energy. Each element has a unique set of energies, therefore, XPS is able to identify and determine the concentration of the elements in the surface. Since the mean free path of electrons in a solid is very small, the emitted electrons only originate from the top few atomic layers and it makes XPS a unique surface-sensitive technique for chemical analysis. XPS has already been employed to reveal the quality of the interfacial link in nanocomposites. Figure 2.7 shows the XPS results of original and coated zirconia nanoparticles.

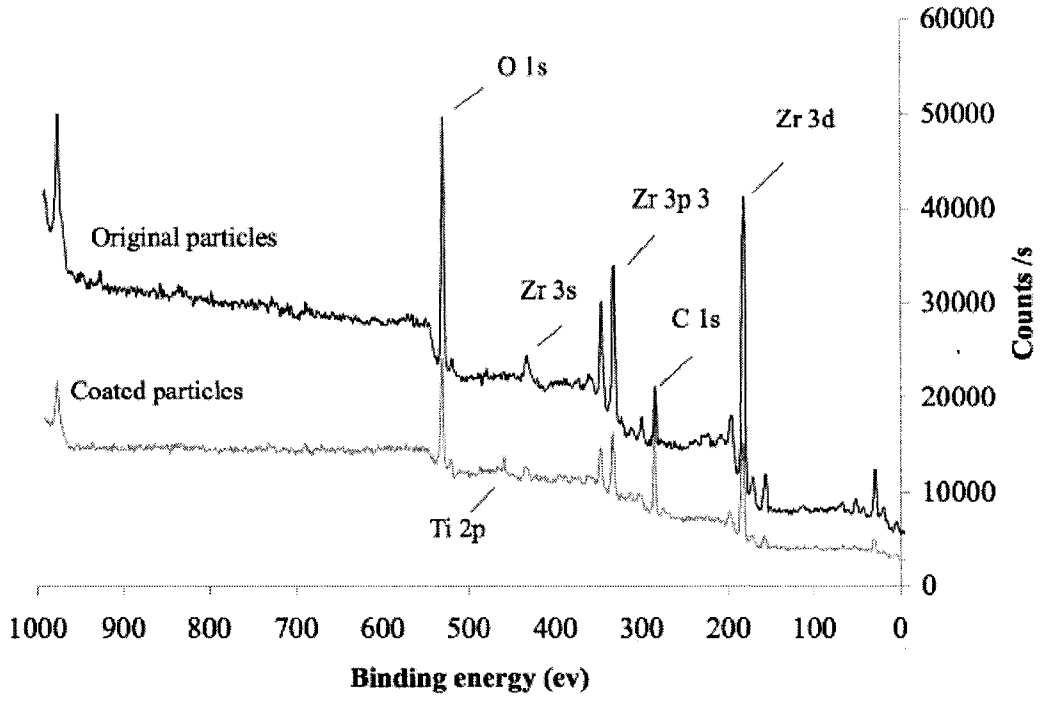

Fig. 2.7 XPS graphs of coated and original zirconia nanoparticles

2.3.3.2 Fluidization Characteristics

The conventional method of pressure drop variation as a function of superficial gas velocity was applied to evaluate minimum fluidization velocity. To investigate the solid concentration distribution in the bed, two different techniques, radioactive densitometry and fiber optic measurement, were utilized. The γ- ray densitometry used in this work consists of a radioactive source and a NaI scintillation detector located on opposite sides of the bed. The radioactive source is a Scandium element (Sc 46) with a half-life of 84 days and an intensity of about 10 μCu activated in the SLOWPOKE nuclear reactor at

École Polytechnique de Montréal. As shown in Figure 2.8, the source and the detector move along a path to scan the entire cross section of the bed. Therefore, a series of line average hold-ups and, consequently, an average hold-up over the cross section would be determined. For the fiber optic technique, a fiber optic probe consisting of one emitter in the middle and 2 receivers located on opposite sides were used. The sampling frequency was fixed at 1.953 kHz (0.512ms) and the sampling time was 16.77s. Using these two methods, the solid holdup distribution over the cross section as well as along the bed height were evaluated. Consequently, the fluidization quality of zirconia and aluminum nanoparticles was identified with respect to radial and axial solid dispersion in the bed.

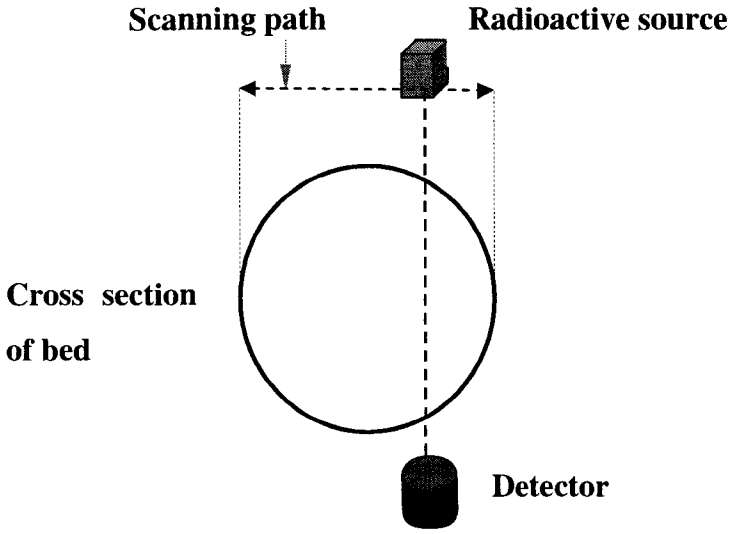

Figure 2.8 γ- ray densitometry

CHAPTER 3

ORGANIZATION OF ARTICLES AND THESIS STRUCTURE

Chapters 4 to 6 give the main results of the thesis and corresponding scientific findings. Each of these chapters consists of an individual article.

A brief description of the each chapter is presented as follows:

- Chapter 4 investigates the feasibility of applying the polymerization compounding approach to encapsulate zirconia in the slurry-phase.
- Chapter 5 studies the fluidization behavior of zirconia and aluminum nanoparticles.
- Chapter 6 investigates the encapsulation of zirconia and aluminum nanoparticles in a fluidized bed reactor using the polymerization compounding method.

Chapter 7 is a general discussion and summary of the results obtained in this work. Finally, a conclusion and recommendation for future work are presented.

CHAPTER 4

POLYMERIZATION COMPOUNDING ON THE SURFACE OF ZIRCONIA NANOPARTICLES*

4.1 Presentation of the article

The objective of the first article is to study the polymerization compounding technique to encapsulate zirconia nanoparticles in slurry-phase. In this article, we investigated the feasibility of ethylene polymerization on zirconia powder via a Ziegler-Natta catalyst system to obtain zirconia nanoparticles whose surface is uniformly modified by a layer of polyethylene in the scale of a few nanometers. It was found that the polymerization compounding is a capable technique to coat the surface of zirconia nanoparticle by polyethylene considering appropriate interfacial properties such as interaction between the polymer coatad substrate, surface wetting by polymer and dispersion of polymer on the surface of particles.

* *Macromolecular Symposia* 243, 268-276 (2006).

4.2 Polymerization Compounding on the Surface of Zirconia Nanoparticles

Babak Esmaeili, Jamal Chaouki, Charles Dubois*

E-mail : charles.dubois@polymtl.ca

Département de Génie Chimique, École Polytechnique de Montréal,

C.P. 6079, succ. Centre-ville, Montréal, Québec, H3C 3A7, Canada

4.2.1 Abstract

Zirconia nanoparticles were encapsulated by polyethylene via a polymerization compounding method using a Ziegler-Natta catalyst. The chemical reaction was carried out in an organic solvent under moderate pressure of ethylene monomer. Transmission electron microscopy (TEM) indicated the presence of a thin layer of polymer, about 6 nm, uniformly applied around the particles. However, the thickness of coating layer can be controlled as a function of time and operating conditions of the process. The morphology study using scanning electron microscopy (SEM) as well as TEM revealed that although the nanoparticles seem to be coated individually, some agglomerates, encapsulated by a polymer film, could be observed. The grafting of the catalyst to the original surface of particles was further confirmed by X-ray photoelectron spectroscopy (XPS).

4.2.2 Introduction

Coating or encapsulating nanoparticles by polymers is desirable in many applications in order to improve their chemical stability, to reduce their toxicity, and to facilitate their storage, transport, and processing. Over the recent years, several methods and approaches have been investigated to carry out polymer coating of nanoparticles. Among them, we note melt mixing, solvent dispersion and precipitation. [1-4] However, not all of these methods provide the modified particles with the properties required to obtain high performance composite materials. The mechanical properties of polymer composites greatly depend on the combined behavior of particles (filler), the polymer matrix, and, most importantly, the interface between them. The latter is readily affected by any change to the particles surface, such as a polymer coating of the same nature of the polymer matrix. Under such a configuration, the quality of the interactions between the particles and encapsulating polymer becomes an important factor favorably affecting the nanocomposite performance. If a catalyst supported on the surface of particles gets involved in a polymerization reaction, a very intimate contact between the particle surface and polymer will be established, bringing improved interfacial properties, and consequently enhanced properties of the nanocomposite. Polymerization compounding (PC) is an approach in which the polymer is forced to grow from the surface of the solid using catalyst sites covalently bonded to the particles.

The PC technique have been developed and extensively studied by Ait-Kadi and his coworkers for polyethylene and nylon coating applications on the surface of fibers[5-10]. When incorporated in composite materials, they observed that the surface of fibers having received the grafted polymerization catalyst were completely covered, while ungrafted fibers, where no catalyst was grafted on, were only scattered by polymer after polymerization.[7] Therefore, when the catalyst was chemically bonded to the fibers, the monomer was polymerized from the fibers surface forming a polymer coating of each fiber, which ensured their dispersion in the polymer matrix and good wetting of fibers surfaces by polymer. Also, solvent extraction experiments confirmed the strong adhesion between the fibers surface and polymer obtained by the polymerization process.[5] Moreover, SEM images of fractured composites revealed a smooth surface of fibers with no polymer on for untreated fibers, while adhered polymer was clearly observed on the treated fibers surface.[9] Recently, Rajabian and Dubois applied PC approach to make a HDPE coating on the Kevlar pulps to be used as reinforcement in polyethylene matrix.[11] Composites with fibers contents as high as 15 % were successfully obtained, owing to the improved adhesion and dispersion of the treated fibers. All of the results mentioned above confirmed that catalyst-grafted polymerization provides an excellent dispersion of solid in the polymer binder, wetting of solid substrate by polymer, and interaction between the solid substrate and encapsulating polymer, which are not always well satisfied by conventional methods of composite preparation such as melt mixing.

In the field of nanoparticle fillers and substrates, several recent investigations were devoted to applying the PC approach to nanocomposites preparation and fine particles encapsulation.[12-19] Kasseh et al conducted free radical polymerization of styrene on the surface of ultrafine silica to prepare highly filled composite.[12] They obtained highly loaded composites (77.9 %) which could not be otherwise achieved by techniques such as mechanical mixing, solvent dispersion and precipitation. Roy et al. (2004) carried out the in-situ synthesis of high density polyethylene on the surface of aluminum nanoparticles using Ziegler-Natta catalyst.[14] They applied a thin polymer layer, in the order of a few nanometer, around particles in a process which was flexible enough to control the amount of polyethylene grafted on powders up to 25% w/w. He et al deposited a thin layer of polyethylene film on zirconia nanoparticles by inductively coupled plasma polymerization and the covalent bond between the substrate and polymer was confirmed by XPS.[17] Rovira-Bru et al treated zirconia nanoparticles to first modify the density of hydroxyl group at the particle surface and then carry out vinylpyrolidone polymerization. [18] They claimed that the surface was fully covered by a well-dispersed polymer coating of about 20 nm in thickness. Recently, Dubois et al incorporated fumed silica ultrafine particles into polyurethane at concentrations as high as 25% via PC approach.[19] They explained that the enhancement in water absorption, thermorheological and mechanical properties was due to improved bonding between the solid substrate and the binder.

In this research, we apply the polymerization compounding process to encapsulate zirconia nanoparticles by polyethylene. The objective of the present work is to investigate the feasibility of ethylene polymerization on zirconia powder via a Ziegler-Natta catalyst system to obtain zirconia nanoparticles whose surface is uniformly modified by a layer of polyethylene in the scale of a few nanometers. As mentioned earlier, Ziegler-Natta catalysts were successfully used for encapsulation of aluminum nanoparticles and Kevlar pulps by high molecular weight polyethylene via PC approach.[11, 14] The polymerization reaction, based on coordination polymerization, starts from the surface of nanoparticles so that ethylene monomers are sequentially grafted to substrate. It is proposed that Ziegler-Natta catalyst, $TiCl_4$, reacts with hydroxyl groups on zirconia particles surface as shown in following equation. [5]

$$—OH+TiCl_4 \rightarrow —O—TiCl_3 + HCl \qquad (1)$$

Therefore, there is a covalent bond established between the catalyst and the particles, and consequently, the polymerization is initiated from the surface of the particles, which favors their encapsulation. Although the chain transfer termination usually occurs in Ziegler-Natta polymerization systems, an appropriate interaction will be established between the polymer and substrate. Since polymerization reaction starts from the surface and monomers are consecutively added to polymer chains, the diffusional limitations and steric hindrance effects are greatly lower than in the case where polymer chains are simply brought to the surface by the substrate nucleating action. Therefore, appropriate

wetting of solid surface by polymer, and consequently, high interfacial interactions are achieved via polymerization compounding process.

4.2.3 Experiments

Materials

The zirconia powder of 250 nm average particle size was used for all coating experiments. Figure 4.1 shows the SEM image of original particles. Ethylene gas with purity of 99.5%, supplied by Canadian Liquid Air, was used as monomer for polymerization reaction. The Ziegler-Natta catalyst system, consisting of titanium tetrachloride ($TiCl_4$), manufactured by Acros, as catalyst and triethylaluminum ($AlEt_3$) obtained from Sigma-Aldrich, as co-catalyst, was stored and handled in a glove box in order to protect them from moisture and oxygen. Methylaluminoxane (MAO) also procured by Sigma-Aldrich was employed to determine the hydroxyl group density on particles surface.

Quantification of hydroxyl chemical groups on nanoparticles

The polymerization process used in this work necessitates the anchoring of the catalyst to the particles using the OH sites on their outer surface. Accordingly, appropriate amounts of catalyst and co-catalyst needed to be estimated from the OH group density on nanoparticles surface. To carry out this quantification [20], a small amount of nanoparticles, about 0.5 g, is agitated and heated in 5 ml of toluene in a lab test tube where a flow of dry nitrogen and vacuum conditions are first applied to remove oxygen

and humidity from the system. After 1 hr, the lab test tube is cooled to ambient temperature, and subsequently, 1 ml of methylaluminoxane (MAO) is injected in the closed tube through a septum. As a result of the reaction between each mole of MAO and hydroxyl groups of the surface, one mole of methane is released. Consequently, the hydroxyl group density is calculated by determination of methane gas evolved in the process using a pressure monitoring setup. An example of the use of the observed pressure rise to determine the amount of catalyst and co-catalyst employed for a particular polymerization is given in Table 4.1.

Table 4.1. Catalyst and co-catalyst calculated based on OH concentration

Pressure rise	50.7 mmHg/ gr zirconia
OH concentration on the surface of particles	$1.9 * 10^{-4}$ mole/ gr zirconia
$TiCl_4$ (pure catalyst)	0.02 ml/ gr zirconia
$AlEt_3$ (1 Molar solution in Hexane)	0.19 ml/ gr zirconia

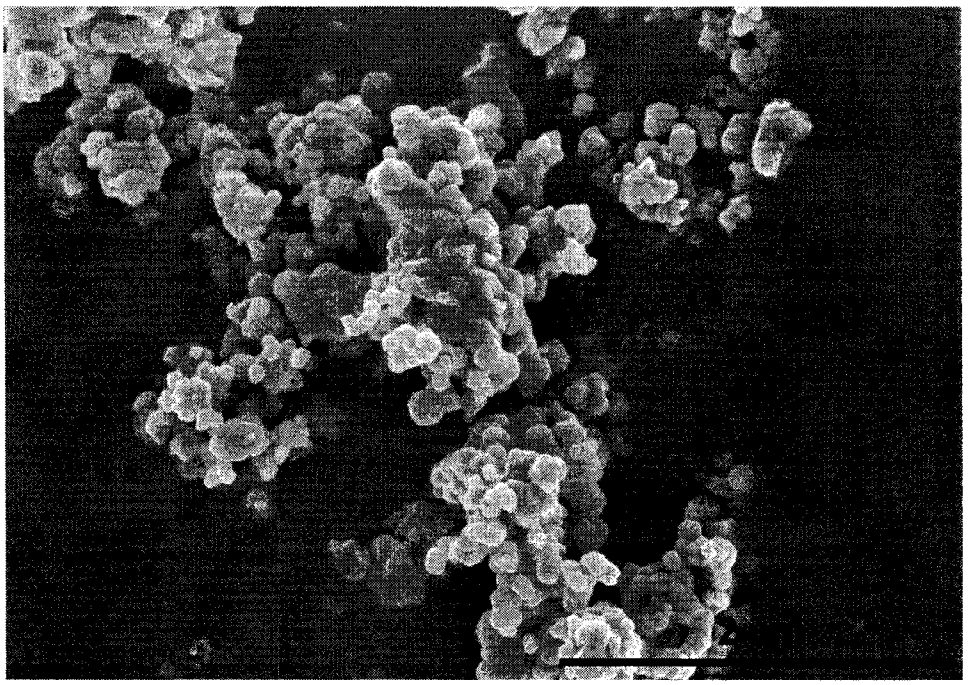

Figure 4.1. SEM image of original zirconia nanoparticles

Synthesis

The polymerization reaction is carried out in a 1 liter pressurized glass vessel BUCHI reactor (BUCHI laboratory autoclave BEP 280) as shown in Figure 4.2. The jacketed reactor is heated to 65 ^{o}C by an external oil bath circulator and mixing is provided by a top mounted magnetic drive impeller. The pressure of reactor is measured by a pressure gauge located on the top of reactor. In a typical polymerization process, the previously oven-dried zirconia powder is dispersed in dried hexane by mechanical agitation at the reaction temperature. The dried nitrogen with a low flow rate is purged to remove oxygen and any trace of water. An ultrasonic processor is mounted on the top of the reactor and periodically activated to facilitate the dispersion of nanoparticles in the

hexane during degassing. After an hour, the desired quantity of catalyst $TiCl_4$ is injected through a septum feeding port, and 15 minutes later, co-catalyst $AlCl_4$ is injected through the same port. The reaction of polymerization starts once nitrogen is replaced by ethylene monomer and continues under a moderate overpressure of 30 kPA for desired time duration before being stopped by an injection of ethanol.

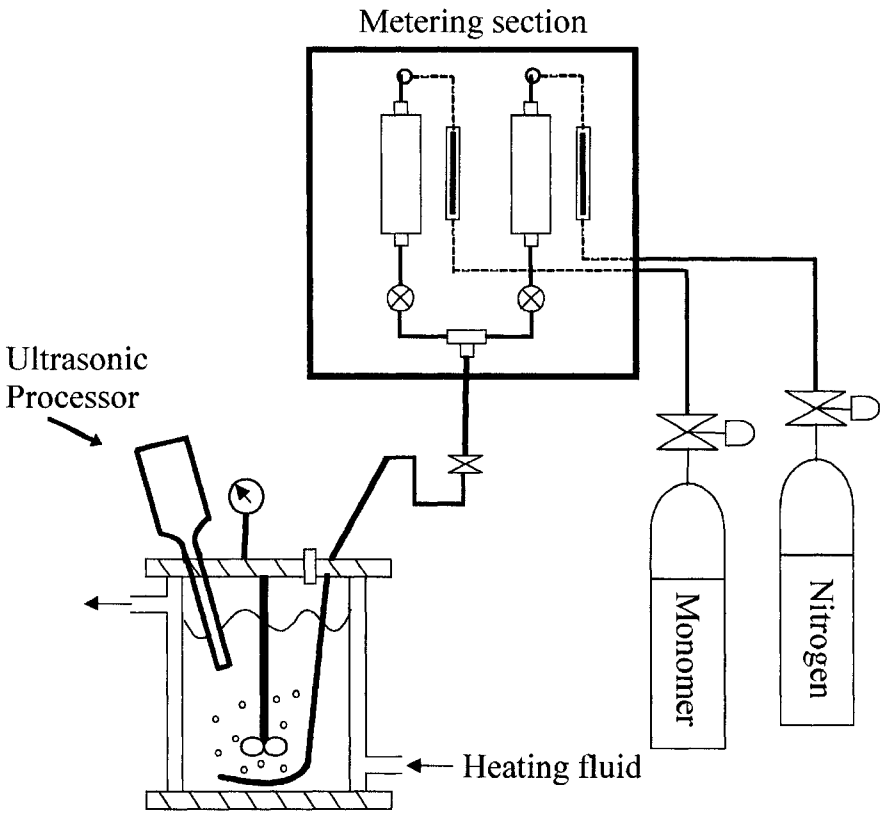

Figure 4.2. Schematic of the reactor setup

Characterization

The amount of polymer on the zirconia particles was determined by thermogravimetry analysis (TGA) using a METTLER TOLEDO apparatus operated on a 25 – 800 °C temperature range at a 10 °C/min heating rate under a flow of argon. The thickness of polymer layer on the surface of nanoparticles was observed using Jeol JEM-2100F Transmission Electron Microscope (TEM). The morphology of coated particles was investigated using Hitachi S-4700 scanning electron microscope (SEM). X-ray photoelectron spectroscopy (XPS) is applied to study the interface of grafted polymer and the original surface of particles.

4.2.4 Results and discussion

A typical thermogravimetry analysis (TGA) of coated zirconia particles is presented in Figure 4.3. One can see that a sharp weight loss appears at 450 to 500 ° C, and since it is known that the pyrolysis of high molecular weight polyethylene (HMWPE) occurs in that region [14], this confirms presence of HMWPE on the surface of nanoparticles.

The characterization of the coated particles was continued by a morphology study using transmission electron microscopy (TEM) and scanning electron microscopy (SEM). TEM observations carried out on original and coated nanoparticles are presented in Figure 4.4. As shown in Figure 4.4-a, the surface of non coated particles possesses a sharp edge and no other phase is distinguished. On the other hand, as shown in Figure 4.4-b for a coated particle, an image contrast is found that corresponds to polyethylene

layer of about 6 nanometer thick uniformly applied around the particle. Although these results confirm that zirconia nanoparticles were individually coated by polyethylene, the coating of particles agglomerate is also possible. Figure 4.5-b shows an agglomerate of nanoparticles which is probably coated by a layer of polyethylene. If so, it demonstrates that the dispersion of original zirconia nanoparticles (Figure 4.5-a) in hexane at the beginning of the polymerization process is a crucial factor that should be considered to avoid the presence of these agglomerates in the final products. However, Figure 5-b might also be the result of agglomeration of individually coated particles.

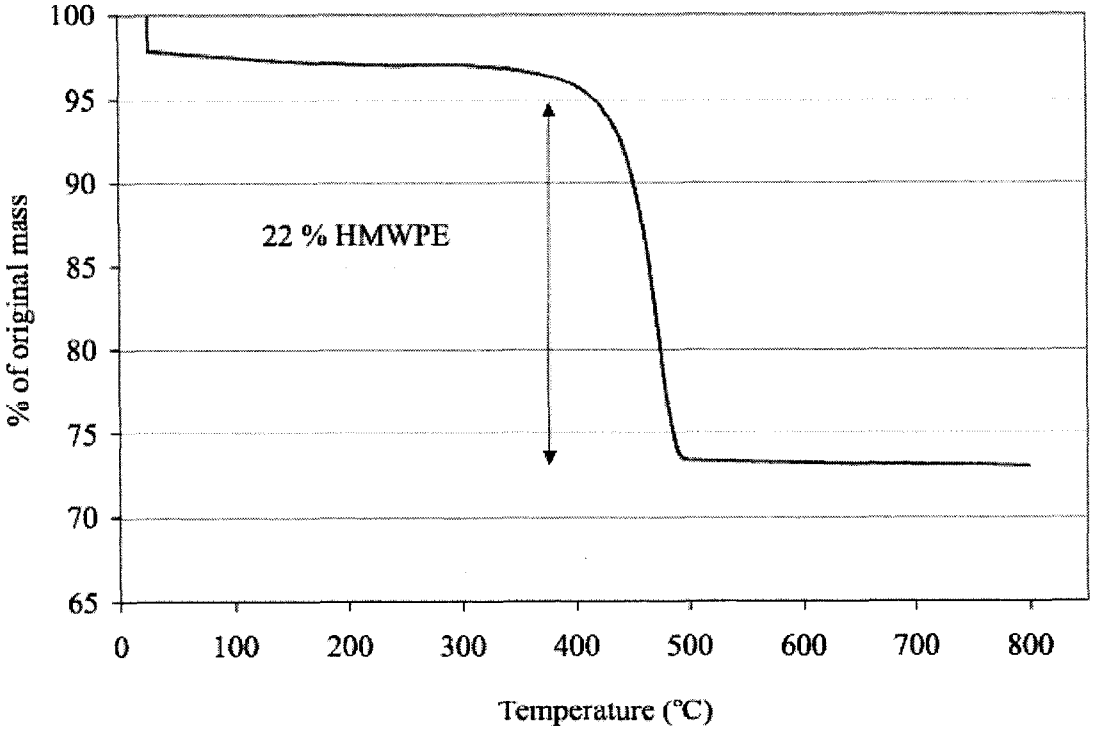

Figure 4.3. TGA graph of coated zirconia nanoparticles

As shown in Figure 4.1, a simple visual observation of SEM image of original zirconia particles reveals a wide distribution of particles sizes, ranging from few ten to few hundred nanometers so that the surface average particle size, reported by the supplier, is 250 nm. Moreover, the particles are in a compact agglomerate state according to the high cohesivity of zirconia powder. However, in the process, agglomerates are broken and particles are dispersed in the solvent by means of stirring and ultrasound processor. On the other side, Figure 4.6 illustrates the coated particles in agglomerate structure as well. While particles had been dispersed in solvent, they retained an agglomerate state after the synthesis. Furthermore, the surface of particles seems to be uniformly coated by polymer after the process, as shown in Figure 4.6.

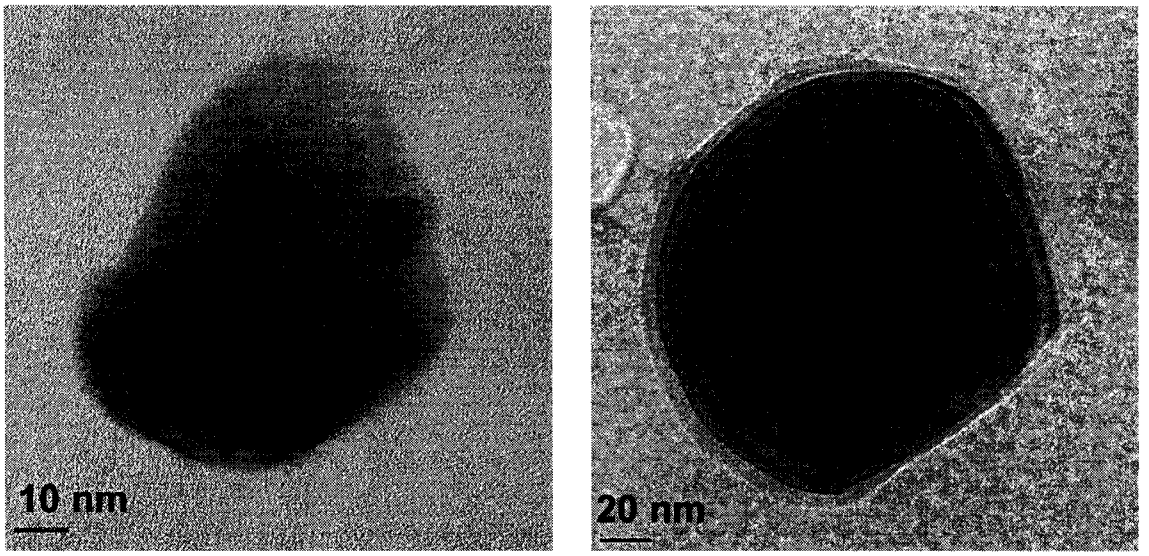

a) b)

Figure 4.4. TEM images of a) original and b) coated zirconia nanoparticles

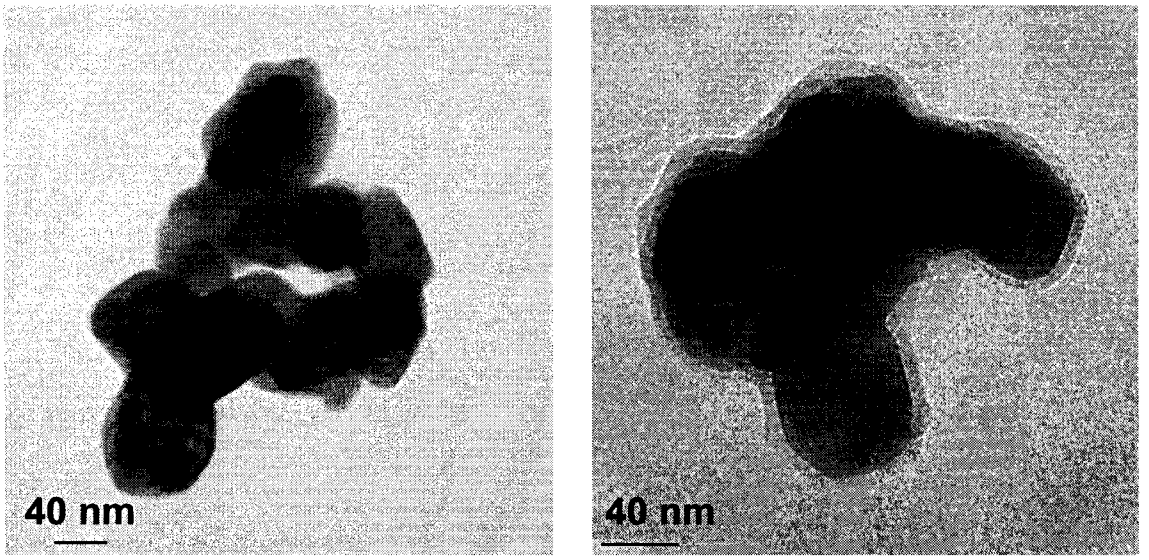

a) b)

Figure 4.5. TEM images of a) original and b) coated zirconia agglomerate

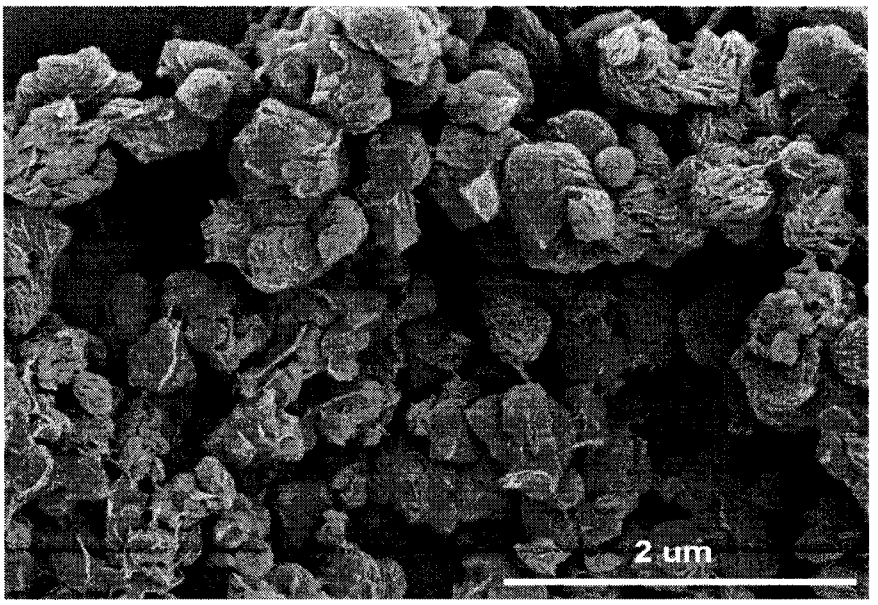

Figure 4.6. SEM image of original zirconia nanoparticles

The XPS analysis reported in Figure 4.7 further confirms the grafting of the catalyst on the surface of particles. As shown in Figure 4.7, the relative intensity of zirconium and oxygen peaks, representing the original surface of particles, is significantly reduced after the polymerization. In addition, the relative intensity of carbon peak, associated to the presence of a hydrocarbon based polymer coating, increased significantly after the polymerization in comparison with original particles. The results mentioned above are summarized in Table 4.2. One can see the weight percentage of zirconium and oxygen elements are considerably lower for coated particles compared to non coated particles. Instead, carbon content augments from 27.45 % for non coated particles to 58.76 % for coated particles. The initial amount of carbon for non coated particles, detected by XPS, is due to the sample contamination by atmospheric carbon (CO2). Furthermore, two different coated particles with respect to amount of polymer on their surface are compared in Figure 4.8. It is evident that for the sample with high amount of polymer (22%), no other high intensity peak is observed except for the carbon peak related to polyethylene. The reason is that XPS experiment is capable to detect only a few nanometers in depth of sample from the free surface. Therefore, if the thickness of polymer layer exceeds that limit, XPS can not detect the interface of substrate and polymer coat. On the other hand, the titanium peak, associated with the Ziegler-Natta catalyst, is detected in the case where the amount of polyethylene is low (4%). These results indicate that the catalyst exists only on the surface of original particles and not in the core of the grafter polymer layer. Therefore, the polymerization reaction can only start from the surface of original particles.

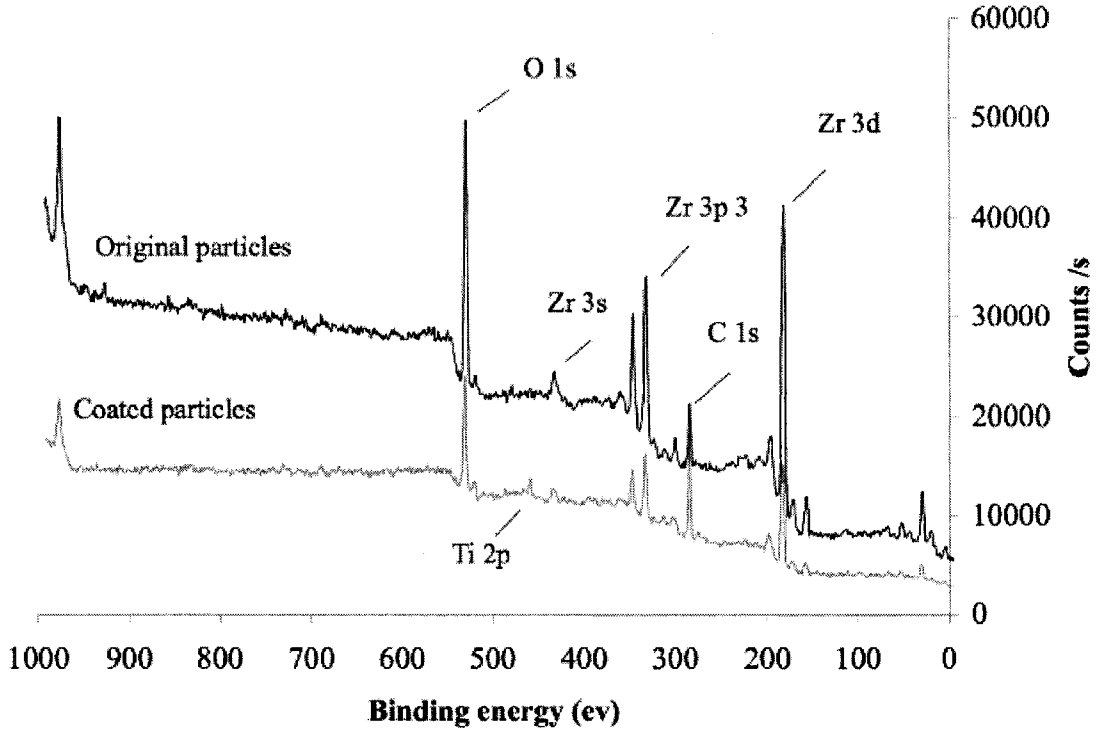

Figure 4.7. XPS graphs of original and coated zirconia nanoparticles

Table 4.2. XPS data for original and coated zirconia nanoparticles

Name	Peak BE	Height cps (original)	Area (p) cps.ev (coated)	Height cps (original)	Area (p) cps.ev (coated)	At. % (original)	At. % (coated)
C 1s	284	5817.20	18175.5	10637.3	32532.3	**27.45**	**58.76**
O 1s	530	25448.2	81156.7	11168.4	38540.2	**51.02**	**28.94**
Zr 3d	183	28648.8	123389.0	9602.14	50822.6	**21.53**	**10.61**
Ti 2p	454	-	-	2.74	6146.33	**-**	**1.64**

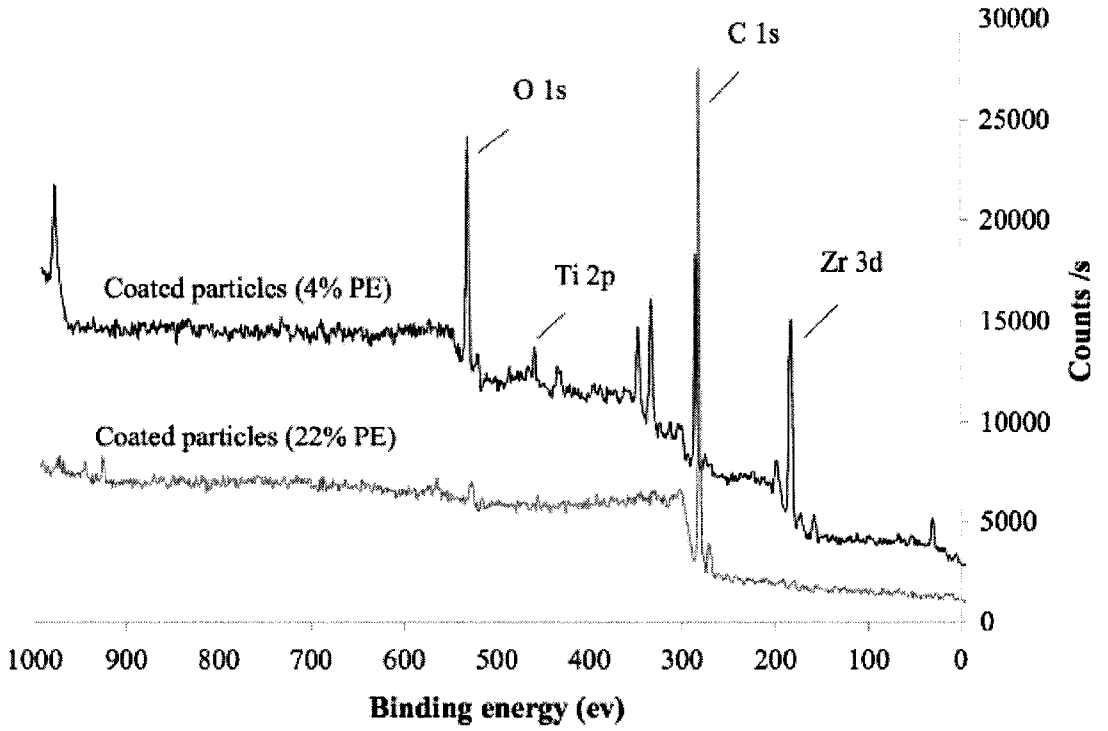

Figure 4.8. XPS graphs of two different coated zirconia nanoparticles

4.2.5 Conclusions

It has been shown that the polymerization compounding technique can be used to encapsulate zirconia nanoparticles by high molecular weight polyethylene using surface-grafted Ziegler-Natta catalysts. XPS results confirmed that the polymerization reaction started only from the original surface of particles, generally leading to a uniform polymer layer applied around nanoparticles. As observed from electron microscopy images, the process is capable of coating individual particles by a polymer film of a few nanometers in thickness. However, it was also revealed that some agglomerates were

encapsulated by the polymer, which is obviously not desirable. To limit the extent of this agglomerates coating phenomenon, the dispersion of nanoparticles in the polymerization solvent is an important factor which must be taken into account. As future work, the effects of process conditions i.e., temperature and pressure will be investigated in order to obtain a better understanding of the reaction kinetics and therefore to achieve a more reliable control of the thickness of the resulting polymer layer.

4.2.6 References

[1] M. Avella, M. E. Errico, G. Gentile, *Macromol. Symp.* **2006,** 234, 170.

[2] W. H. Ruan, X. B. Huang, X. H. Wang, M. Z. Rong, M. Q. Zhang, *Macromol. Rapid Commun.* **2006**, 27, 581.

[3] S. Stolnik, M.C. Davies, L. Illum, S. S. Davis, M. Boustta, M. Vert, *J. Controlled Release* **1994**, 30, 57.

[4] J. L. Zhang, Z. M. Liu, B. X. Han, J. C. Li, Z. H. Li, G. Y. Yang, *J. Nanosci. Nanotechol.* **2005**, 5, 945.

[5] Q. Wang, S. Kaliaguine, A. Ait-Kadi, *J. Appl. Polym. Sci.* **1992**, 44, 1107.

[6] Q. Wang, S. Kaliaguine, A. Ait-Kadi, *J. Appl. Polym. Sci.* **1992**, 45, 1023.

[7] Q. Wang, S. Kaliaguine, A. Ait-Kadi, *J. Appl. Polym. Sci.* **1993**, 48, 121.

[8] H. Salehi-Mobarakeh, A. Ait-Kadi, J. Brisson, *Polym. Eng. Sci.* **1996**, 36, 778.

[9] H. Salehi-Mobarakeh, J. Brisson, A. Ait-Kadi, *J. Mater. Sci.* **1997**, 32, 1297.

[10] H. Salehi-Mobarakeh, J. Brisson, A. Ait-Kadi, *Polym. Compos.* **1998,**19, 264.

[11] M. Rajabian, C. Dubois, *Polym. Compos.* **2006**, 27, 129.

[12] A. Kasseh, A. Ait-Kadi, B. Riedl, J.F. Pierson, *Polymer* **2003**, 44,1367.

[13] Y. Wang, X. Pei, K. Yuan, *Mater. Lett.* **2005**, 59, 52.

[14] C. Roy, C. Dubois, P. Lafleur, P. Brousseau, *Mater. Res. Soc. Symp. Proc.* **2004**, 800.

[15] D. Shi, S.X. Wang, W.L. van Ooij, L.M. Wang, J. Zhao, Z. Yu, *Appl. Phys. Lett.* **2001**, 78, 1243.

[16] X. Ding, J. Zhao, Y. Liu, H. Zhang, Z. Wang, *Mater. Lett.* **2004**, 58, 3126.

[17] W. He, Z. Guo, Y. Pu, L. Yan, W. Si, *Appl. Phys. Lett.* **2004**, 85, 896.

[18] M. Rovira-Bru, F. Giralt, Y. Cohen, *J. Colloid Interface Sci.* **2001**, 235, 70.

[19] C. Dubois, M. Rajabian, D. Rodrigue, *Polym. Eng. Sci.* **2006**, 46, 360.

[20] M. Sato, T.K., Norio Kobayashi, Y. Shima, *J. Catal.* **1967**, 7, 342.

CHAPTER 5
AN EVALUATION OF SOLID HOLD-UP DISTRIBUTION IN A FLUIDIZED BED OF NANOPARTICLES USING RADIOACTIVE DENSITOMETRY AND FIBER OPTICS*

5.1 Presentation of the article

The objective of the current paper is to focus on the fluidization of zirconia and aluminum nanoparticles to investigate their performance in a fluidized bed. Although the fluidization of nanoparticles happens in an agglomerate state, it is very important to understand if the fluidization of these particles would be carried out homogenously in terms of solid and gas phase concentrations within the bed. Otherwise, the polymer encapsulation will not be uniformly applied on the surface of ultrafine particles. Therefore, it must be identified under which operational conditions zirconia and aluminum nanoparticles are capable of being homogenously fluidized, even in an agglomerated state.

* *Accepted to be published in Can. J. Chem. Eng.,* February 2008

5.2 An Evaluation of the Solid Hold-up Distribution in a Fluidized Bed of Nanoparticles Using Radioactive Densitometry and Fiber Optics

Babak Esmaeili, Jamal Chaouki*, Charles Dubois

Département de Génie Chimique, École Polytechnique de Montréal, C.P. 6079, succ. Centre-ville, Montréal, Québec, H3C 3A7, Canada

5.2.1 Summary

An experimental study was conducted to assess the solid hold-up distribution in a fluidized bed of zirconia and aluminum nanoparticles. For this purpose, two different techniques, radioactive densitometry and fiber optic measurement, were used. The results showed that while the fluidization of these nanoparticles occurs in the agglomeration state, it performs homogenously in terms of phase concentration. This matter is important especially when a polymerization reaction should take place uniformly on the surface of nanoparticles, where the monomer is the fluidizing gas. Both techniques presented uniform solid hold-up distribution over the cross section, although the fiber optic method overestimated the overall solid concentration, which was obtained based on bed expansion results. The radioactive densitometry was, however, capable of properly predicting the phase concentration within the bed according to the bed expansion observation. Finally, the effect of bulk density on the fluidization of nanoparticles was discussed by comparing the fluidization of different types of particulate materials.

---

* Corresponding author: J. Chaouki: e-mail: jamal.chaouki@polymtl.ca

5.2.2 Introduction

In the last two decades, fluidization of nanoparticles has been one of the most important research interests in the area of nanoparticle handling and processing [1-29]. The researchers dealt with different aspects of nanoparticle fluidization, for example, the evaluation of agglomerate size via force and energy balance [1-4, 7-8, 12, 18, 26], hydrodynamic modeling of the phenomenon [1, 3, 5-6, 10-11, 16-17, 25, 28], and improving fluidization using external forces, such as a magnetic field [8, 21, 28], centrifuge and rotation [9, 14, 18], vibration [12-13, 16, 28] and ultrasound [17, 22, 24, 26, 29]. However, aside from a small number of studies, no clear objective or application has been presented as a motivation for nanoparticle fluidization. It seems that processing nanoparticles in a fluidized bed has remained merely an academic research topic rather than a method to resolve the problem in industrial applications.

The present work deals with fluidization of two particulate materials, zirconium oxide and aluminum nanoparticles, which are very promising materials in industrial applications. The high mechanical and thermal properties of zirconia lead to its use in applications requiring high temperature, high strength, toughness and aesthetic shade. Accordingly, zirconium oxides have been extensively used in medical and dental applications. To manufacture an artificial denture, zirconia powder on a nanometer scale is densified under high pressure and temperature to obtain a dense ingot, which will be formed to the desired shape via milling by diamond burs. In this process, zirconia powder must be applied on a nanometer scale to avoid anisotropy in the final product, which requires high physical and mechanical properties. The hard processing of dense

sintered zirconia is very time consuming and, also, costly due to wear and tear on the milling instruments. One possible solution is to encapsulate the zirconia nanoparticles beforehand with a thin layer of polymer, which is uniformly applied around the particles, thus eliminating the drawbacks in the milling process. Obviously, after the shaping process, the final hard product will be achieved by thermal degradation of the polymer coat.

On the other hand, ultra fine aluminum powder is being recognized as a good candidate for diverse combustion applications, such as additives in solid rocket propellants and metallic fuel in explosive formulations. The aluminum nanoparticles have been reported to show burning rates 5 to 10 times greater than microsized ones and when used in gas generator fuels, they achieve a more complete combustion. These enhanced properties are due to their large specific surface per unit mass. However, the large specific surface area, which provides these powders with a high reactivity, makes them particularly difficult to maintain in an unoxidized state. Consequently, coating these powders with a polymer would be a solution to protect them from a non-desirable reaction, such as oxidation.

Based on what was mentioned above, encapsulating nanoparticles with a polymer is one way to reduce difficulties in the application of zirconia and aluminum nanoparticles. Accordingly, the encapsulation of different types of nanoparticles by a variety of polymer coatings has been extensively investigated in the literature [30-33]. However, not all methods provide the modified particles with the properties required to obtain high performance compounds. The mechanical properties of encapsulated particles greatly

depend on the interfacial properties of the particle and coating. If the appropriate interaction in the interface of the particle surface and polymer layer is not established, some problems, such as the separation of the coating from the substrate may occur in powder processing. Therefore, particles must be encapsulated in such a way that a proper interaction is provided between the interface of the solid substrate and polymer coating. *Polymerization compounding* is an approach in which the solid becomes involved in the polymerization reaction so that the polymer is forced to grow from the surface of the solid providing good adhesion and interaction between the particles and encapsulating the polymer. Polymerization compounding, also known as graft polymerization, is a well-known approach in the composite and nanocomposite preparation field and, accordingly, there are a number of studies concerning this approach [34-41]. Recently, we successfully applied this technique to encapsulate zirconia nanoparticles with a thin layer of polyethylene in the order of a few nanometres [42]. Nevertheless, nearly all the works dealing with encapsulation of nanoparticles via polymerization compounding have been carried out in the liquid phase where difficulties arise with respect to removing organic solvent and impurities and drying the encapsulated particles.

Consequently, coating the surface of zirconia and aluminum nanoparticles, on the one hand using the polymerization compounding approach to obtain a composite with high interfacial properties and on the other hand, in a gas-solid reactor free of an organic solvent would be the final solution for all of the above cited obstacles. For this purpose, it is believed that a fluidized bed reactor is the appropriate choice, since it possesses the

excellent advantages of high heat and mass transfer rate, temperature homogeneity, and high flowability of particulate materials, which are not all achievable when applying other competing gas-solid reactors. In addition, the process of nanoparticle coating would be flexible enough to extend to the continuous process.

Therefore, prior to performing the polymerization reaction in a fluidized bed reactor to encapsulate zirconia and aluminum nanoparticles, which is the subsequent step of this research, further experimental work is required to study the behavior of these particles in a fluidized bed. Consequently, the objective of the current paper is to focus on the fluidization of zirconia and aluminum nanoparticles to investigate their performance in a fluidized bed. Although the fluidization of nanoparticles happens in an agglomerate state [1-29], it is very important to understand if the fluidization of these particles would be carried out homogenously in terms of solid and gas phase concentrations within the bed. Otherwise, the polymer encapsulation will not be uniformly applied on the surface of ultrafine particles.

Therefore, in this research, it will be identified under which operational conditions zirconia and aluminum nanoparticles are capable of being homogenously fluidized, even in an agglomerated state. In addition, the effect of bulk density, which is a key factor in nanoparticle fluidization [10, 17], will be reviewed by comparing the fluidization of the above mentioned nanoparticles and two nanoparticles with lower bulk density.

5.2.3 Experimental

Materials

Zirconia powder prepared by Sigma-Aldrich and aluminum powder manufactured by

TEKNA were used for all fluidization experiments. In addition, fumed silica, provided by Sigma-Aldrich, and titanium oxide, prepared by Degussa, were employed to investigate the effect of bulk density on the fluidization of nanoparticles. Table 5.1 shows the physical properties of these particulate materials. Before fluidization experiments, the particles were sieved using a 40 mesh sieve with 425 μm openings to remove very large agglomerates generated during storage, packing, and transportation [17]. Air was used as a fluidizing gas in most experiments; however, to see the effect of humidity on fluidization, dry nitrogen was used in some experiments. The humidity content was less than 5 ppm in nitrogen and it was 500 ppm in air. All the results shown in the article correspond to air, unless it is mentioned.

Table 5.1. Physical properties of nanoparticles

	Average diameter (nm)	**Specific surface area (m^2/gr)**	**Solid density (kg/m^3)**	**Bulk density (kg/m^3)**
ZrO_2	250	5.5	5900	1200
Al	120	16.5	2700	350
TiO_2	30	50	4000	120
SiO_2	14	200	2200	35

Experimental setup

A cylindrical column was used as a fluidized bed for fluidization experiments. As demonstrated in figure 5.1, after passing through a rotameter air or nitrogen enters the

wind box. The wind box contains small glass beads, which distributes the gas flow very well before being introduced into the bed. Gas then enters the column homogenously through a porous plate with pores 20 microns in size. The Plexiglas column consists of three transparent parts; bed, freeboard and disengagement zone. The internal diameter and total height of the bed and freeboard are 5 cm and 60 cm, respectively. There are a number of small ports at different heights of the bed and the freeboard provided for the fiber optic probe as well as sampling. The disengagement zone has a diameter about 6 times higher than the bed diameter that provides a significant decrease in gas velocity to permit elutriated particles to return to the bed. After the column, a bag filter is available to remove the entrained nanoparticles in the gas.

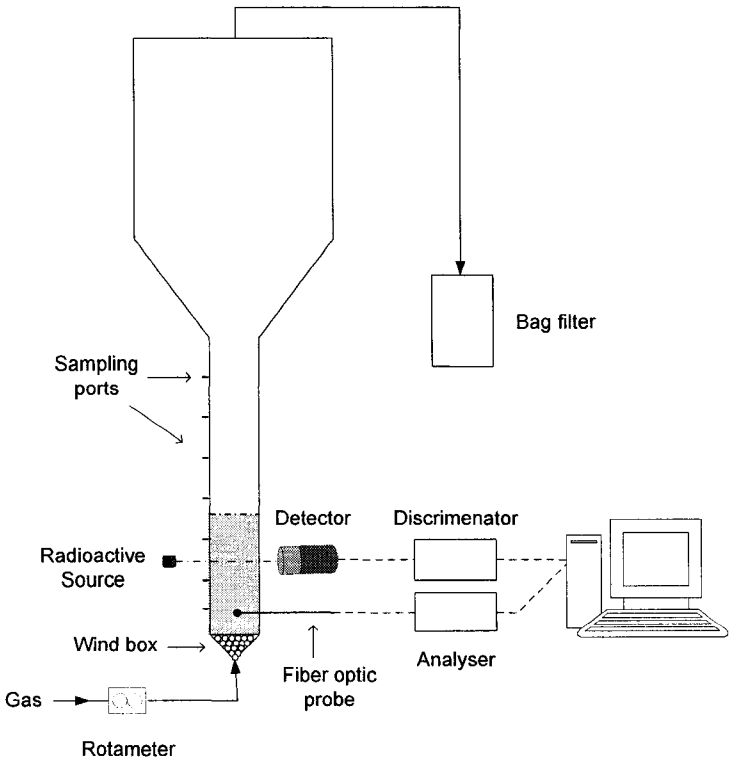

Figure 5.1. Schematic illustration of a fluidized bed and its accessories

Characterization

The conventional method of pressure drop variation as a function of superficial gas velocity was applied to evaluate minimum fluidization velocity. To investigate the solid concentration distribution in the bed, two different techniques, radioactive densitometry and fiber optic measurement, were utilized. The γ- ray densitometry used in this work consists of a radioactive source and a NaI scintillation detector located on opposite sides of the bed. The radioactive source is a Scandium element (Sc 46) with a half-life of 84 days and an intensity of about 10 μCu activated in the SLOWPOKE nuclear reactor at Ecole Polytechnique in Montreal. As shown in Figure 5.2, the source and the detector move along a path to scan the entire cross section of the bed. Therefore, a series of line average hold-ups and, consequently, an average hold-up over the cross section would be determined.

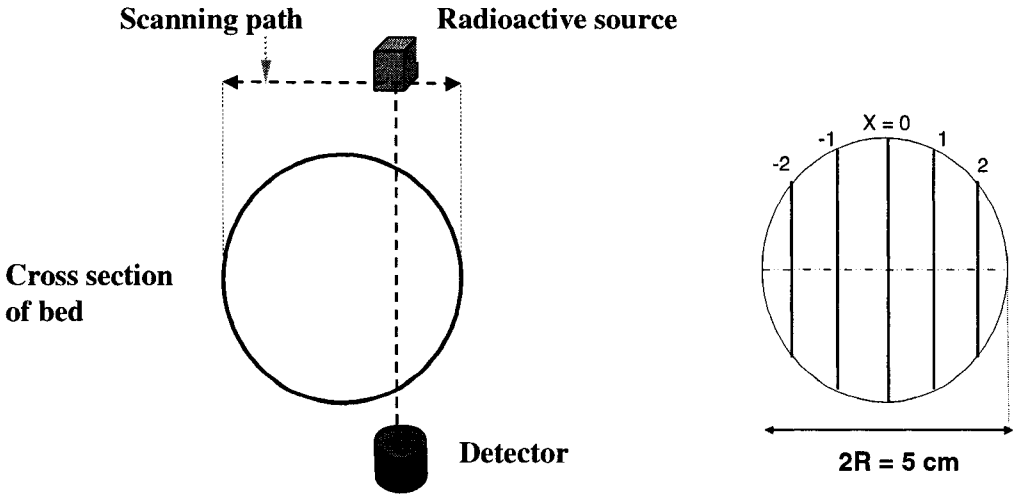

Figure 5.2. γ- ray densitometry and different linear positions for evaluating solid hold-up

For the fiber optic technique, a fiber optic probe consisting of one emitter in the middle and 2 receivers located on opposite sides were used. The sampling frequency was fixed at 1.953 kHz (0.512ms) and the sampling time was 16.77s. The same system of fiber optic measurement was used in earlier works by Mabrouk et al. [43] and Pugsley et al. [44]. Figure 5.3 shows five different positions for evaluating solid concentration by fiber optic. Using these two methods, the solid holdup distribution over the cross section as well as along the bed height were evaluated to identify the fluidization quality of zirconia and aluminum nanoparticles.

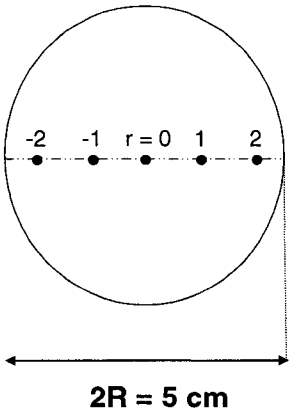

Figure 5.3. Five different positions for evaluating solid hold-up by fiber optic.

5.2.4 Results and Discussions

Typical fluidization characteristics for zirconia and aluminum

At first glance, the fluidization of zirconia and aluminum nanoparticles involves limited bed expansion and bubbles rising up quickly through the bed. It also consisted of the non-uniform distribution of agglomerates in the bed where the small agglomerates appear to be fluidized in the upper part and the larger agglomerates move gradually on

the bottom of the bed. This fluidization behavior for zirconia and aluminum nanoparticles is known as agglomerate bubbling fluidization (ABF) in the literature [10, 17]. Figure 5.4 shows the pressure drop and the bed expansion as a function of gas superficial velocity for zirconia nanoparticles. The pressure drop is normalized by dividing the weight of the particles by the cross section of the bed. As shown in the figure, the minimum fluidization velocity occurs at about 2.3 cm/s, which is much higher than minimum fluidization velocity of individual nanoparticles calculated by available correlations [46]. Therefore, it confirms that fluidization of such particles takes place in the agglomeration state. It was also observed that the bubbling occurs immediately after the minimum fluidization. One can see that the bed of zirconia nanoparticles expands up to 14% by increasing gas velocity. However, an increase in velocity beyond 6.64 cm/s does not lead to an increase in bed expansion. It is the point at which the entire bed of particles seemed to be well mixed. As shown in figure 5.4, the bed expansion occurs after minimum fluidization velocity, which is consistent with the fluidization of Geldart A. This behavior of nanoparticles may be explained as follows: by increasing gas velocity up to the minimum fluidization point, the hydrodynamic force dominates gravity force, causing the fluidization of nanoparticles in agglomerate form. However, the strong interparticle forces, mainly van der Waals, between agglomerates are still dominant so that agglomerates start fluidizing very close together preserving almost the same distance from each other as in the initial static bed. By increasing gas velocity after minimum fluidization, the bed expansion may happen because of two reasons. It can be because the drag force takes over interparticle forces, causing more

spaces between agglomerates and, consequently, higher but limited bed expansion in the bed. On the other hand, the bed expansion may occur due to bubbles.

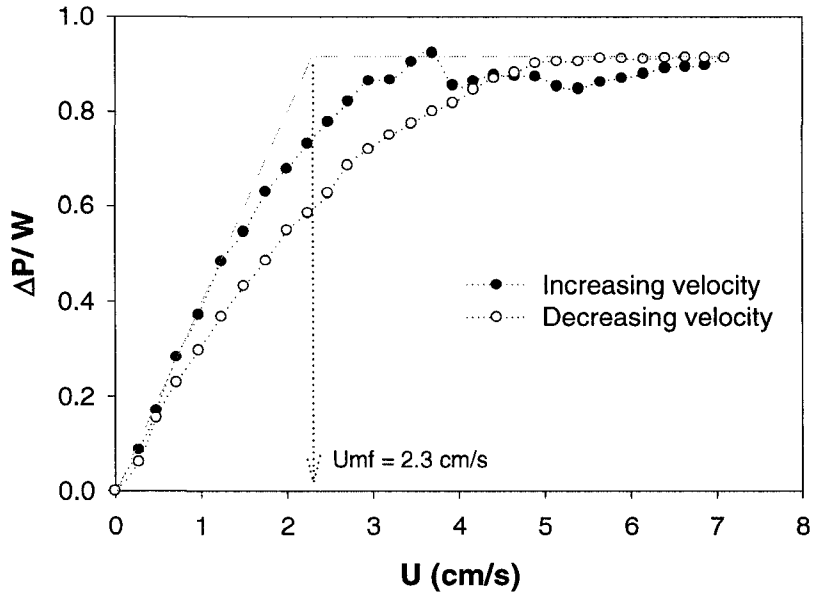

a)

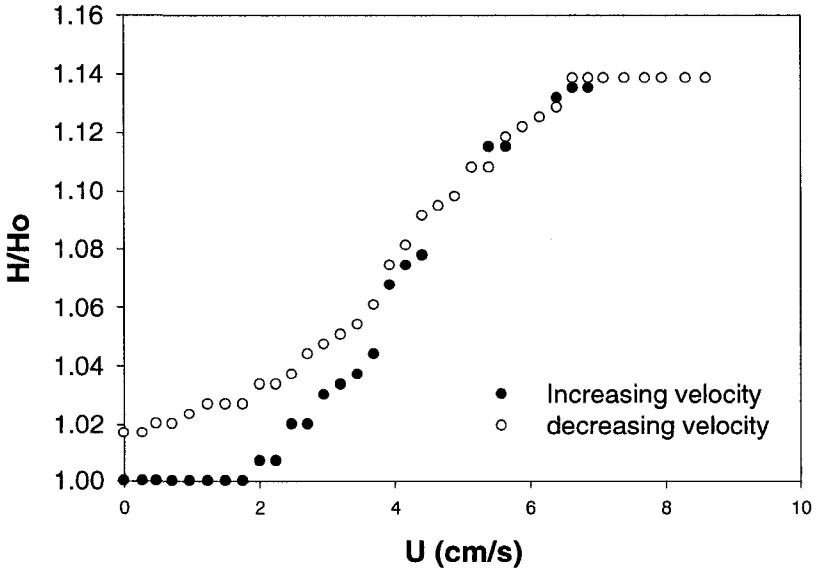

b)

Figure 5.4. a) Normalized pressure drop and b) bed expansion for zirconia nanoparticles

As shown in Figure 5.5, the minimum fluidization velocity of aluminum nanoparticles occurs at a velocity around 0.25 cm/s, which is much less than that of zirconia nanoparticles. It can also be observed that the bed of aluminum particles expanded up to 40%, which is much higher than that of zirconia. In addition, the fluidization of aluminum was fairly smooth compared to zirconia fluidization with a smaller bubble size and excluding very large agglomerates. As mentioned in the literature [10, 17], the bulk density of nanoparticles is an important factor, which influences the fluidization behavior of these materials. Accordingly, the nanoparticles with a bulk density higher than 100 kg/m^3 are expected to show ABF behavior, including large bubbles, low bed expansion and a large distribution of agglomerate size; whereas those with a bulk density lower than 100 kg/m^3 show smooth agglomerate particulate fluidization (APF) without bubbles, quite high bed expansion, and narrow agglomerate size distribution. Both the zirconia and aluminum that are applied in this work possess a bulk density higher than 100 kg/m^3 leading to ABF behavior. The aluminum bulk density is, however, so much lower than the zirconia density that it justifies the higher bed expansion and smoother fluidization behavior of aluminum.

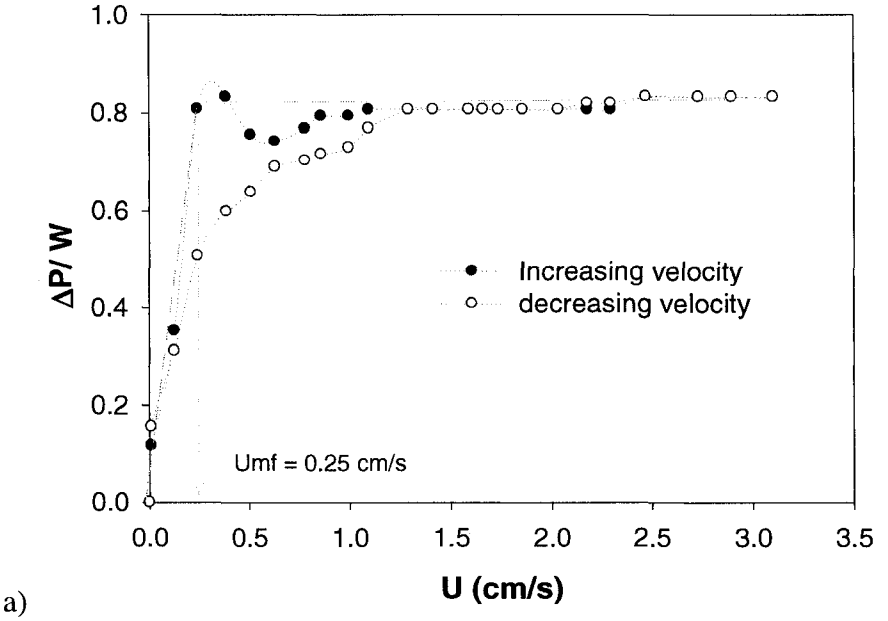

a)

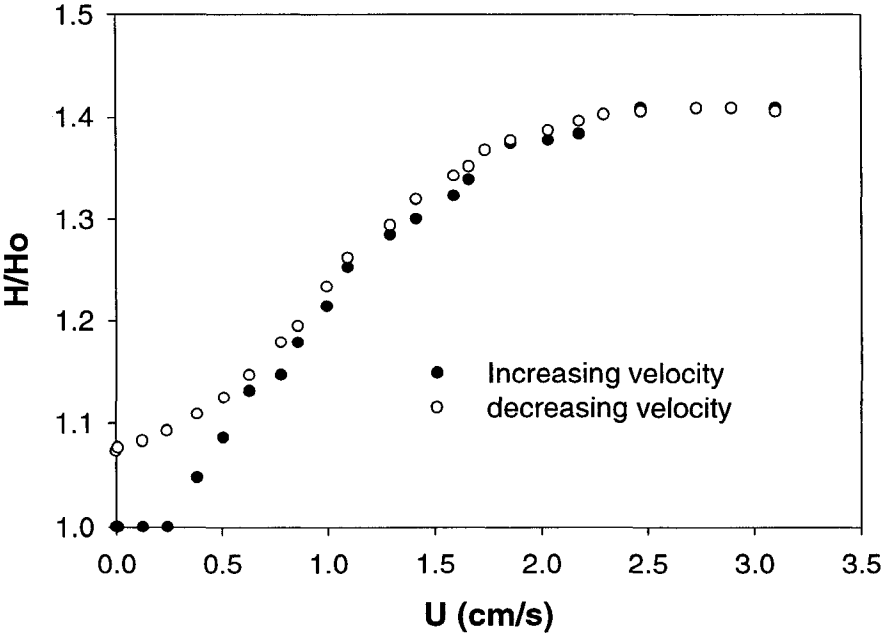

b)

Figure 5.5. a) Normalized pressure drop and b) bed expansion for aluminum nanoparticles

Solid hold-up evaluation by radioactive densitometry for zirconia

To investigate solid concentration distribution within a fluidized bed of zirconia and aluminum, radioactive densitometry and fiber optic measurements were employed. Figure 5.6 shows the results of γ-ray densitometry experiments for zirconia nanoparticles over the cross section 3 cm above the distributor for a wide range of gas velocities. The initial height and porosity of the bed were 11.5 cm and 80%, respectively. A series of line average solid concentrations, as demonstrated in Figure 5.6, in five different linear positions was measured to understand the distribution of phase concentration over the cross section and, also, to calculate the cross section mean hold-up. As illustrated in Figure 5.6, the line average solid hold-up does not decrease less than 15 % by increasing the velocity up to 6.64 cm/s, which is far enough from the minimum fluidization velocity. In addition, it can be observed that solid hold-up is uniform over the bed cross section. The same results are obtained at different heights of the bed, 5 and 10 cm above the distributor, as shown in Figures 5.7 and 5.8.

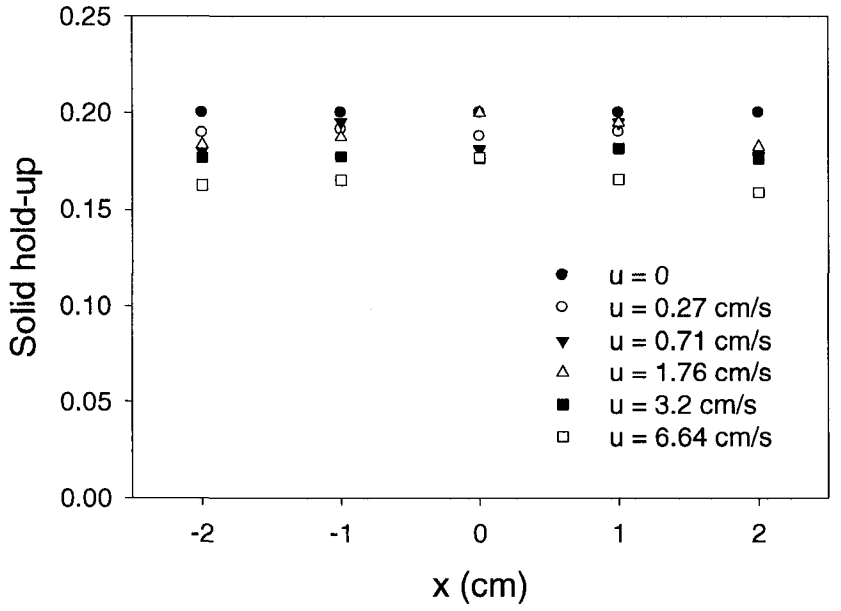

Figure 5.6. Line average solid hold-up at 3 cm above the distributor for zirconia nanoparticles by densitometry

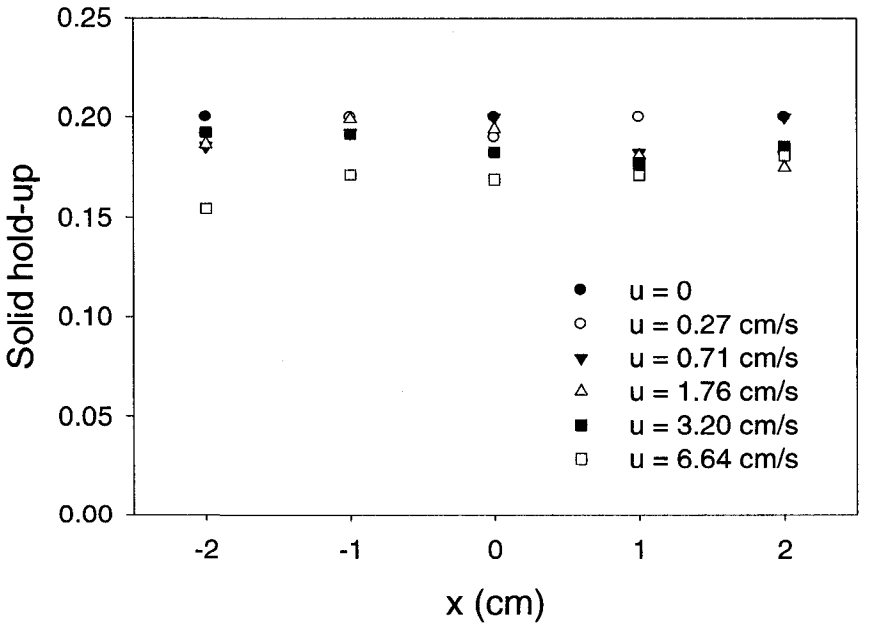

Figure 5.7. Line average solid hold-up at 5 cm above the distributor for zirconia nanoparticles by densitometry

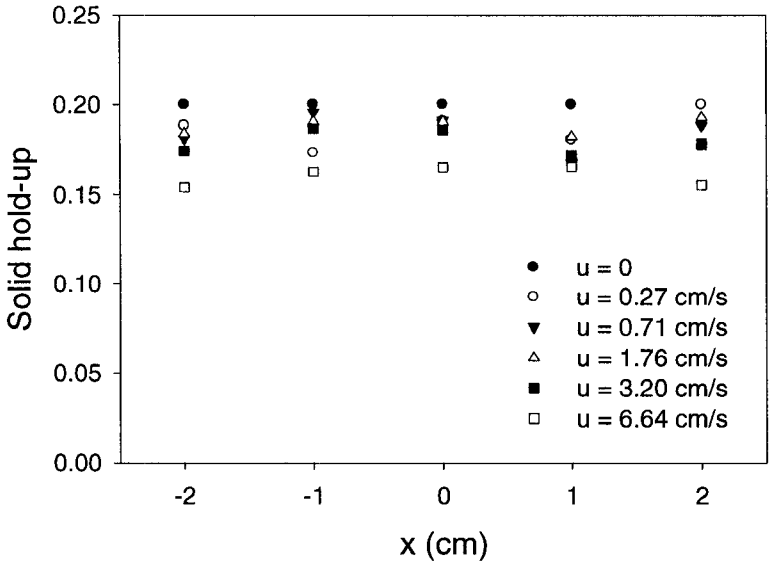

Figure 5.8. Line average solid hold-up at 10 cm above the distributor for zirconia nanoparticles by densitometry

By integrating the line average solid hold-up data over the bed section, the cross section mean hold-up at different heights of the bed are determined as shown in Figure 5.9. It is obvious that the average solid hold-up over the cross section is almost independent of bed height. In addition, the solid hold-up reduction is very low from 20% to 17% by increasing the gas velocity. Therefore, it is concluded that fluidization of zirconia nanoparticles occurs uniformly in terms of solid concentration along the bed height as well as over the bed cross section.

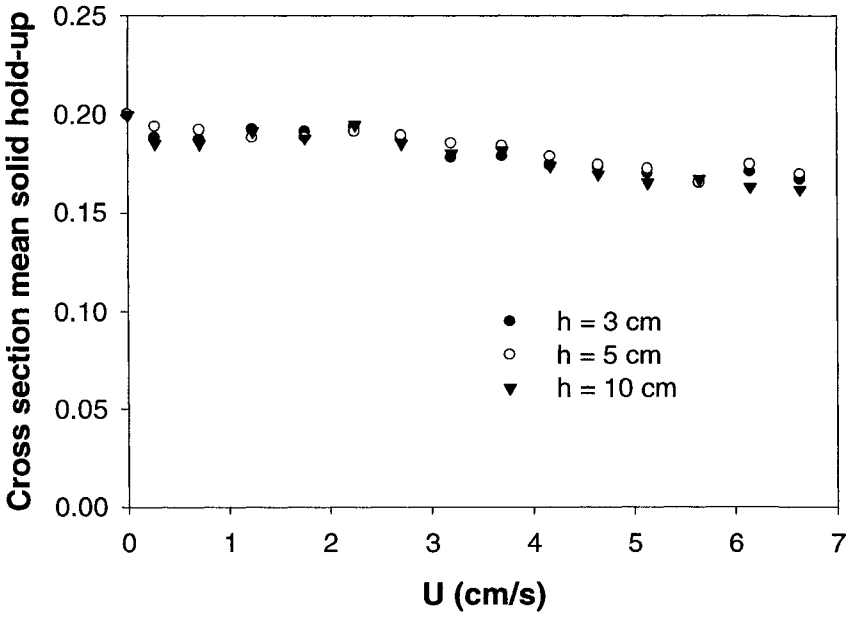

Figure 5.9. Cross section mean solid hold-up for zirconia nanoparticles

The phase concentration data obtained by the radioactive densitometry technique, which was presented above, is in a good agreement with the global measurement obtained by bed expansion information. Based on the bed expansion results, the overall solid hold-up in the bed can be easily calculated as a function of gas velocity. As shown in Figure 5.10, the overall solid hold-up calculated using the densitometry technique is consistent with the data provided by bed expansion results for a wide range of gas velocities.

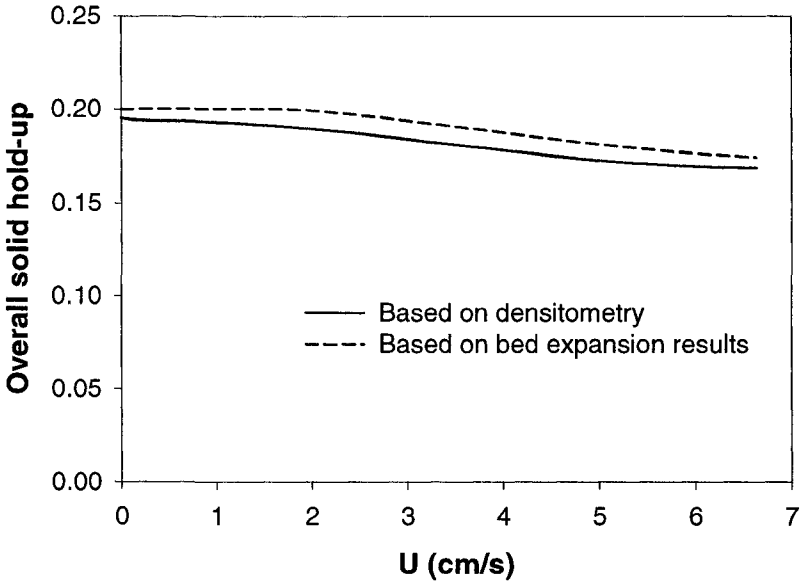

Figure 5.10. The comparison between overall solid-holdup obtained based on densitometry and bed expansion results for zirconia nanoparticles

Solid hold-up evaluation by fiber optic for zirconia

The results of fiber optic experiments will be presented in the following paragraph. Figure 5.11 shows the solid hold-up for zirconia nanoparticles at a height of 3 cm above the distributor for a large range of velocities. The results are considered as local measurement. It can be observed that solid concentration does not change remarkably by increasing gas velocity. In addition, no significant variation in solid hold-up is observed over the cross section. The same results are obtained at different heights of the bed, 5 and 10 cm above the distributor. These results are consistent with the results of radioactive densitometry. However, more variation in phase concentration is observed as a function of velocity by the densitometry technique.

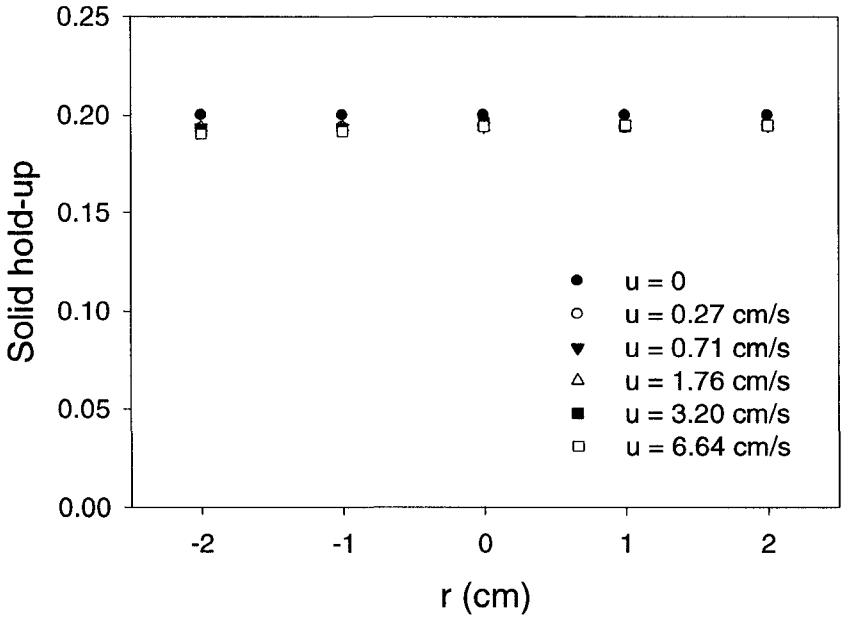

Figure 5.11. Local solid hold-up at 3 cm above the distributor for zirconia nanoparticles by fiber optic

Using the local information provided above, an average solid hold-up over the cross section is obtained at different bed heights as shown in Figure 5.12. One can see that a similar trend for average solid hold-up variation is observed for different heights above the distributor by a change in gas velocity. Moreover, there is no significant change in phase concentration as a function of bed height as would be expected from local information. This information is also in agreement with the densitometry results, which confirms that the phase concentration in the bed of zirconia nanoparticles is independent of bed height.

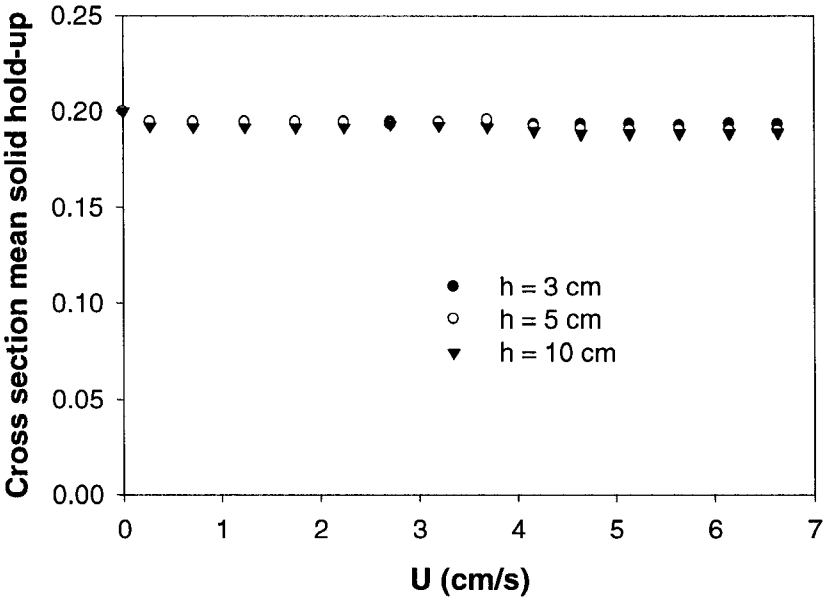

Figure 5.12. Cross section mean solid hold-up for zirconia nanoparticles

However, based on fiber optic results, the overall solid concentration in the bed remains almost constant by increasing the gas velocity, as shown in Figure 5.13, which is not consistent with the radioactive densitometry as well as bed expansion results. Both of these confirm that the overall solid hold-up in the bed decreases from 0.2 to almost 0.17 by increasing the velocity up to 6.64 cm/s, as shown in Figure 5.10. Therefore, to evaluate solid concentration in the bed of nanoparticles, radioactive densitometry appears to be more reliable in comparison with fiber optic measurements.

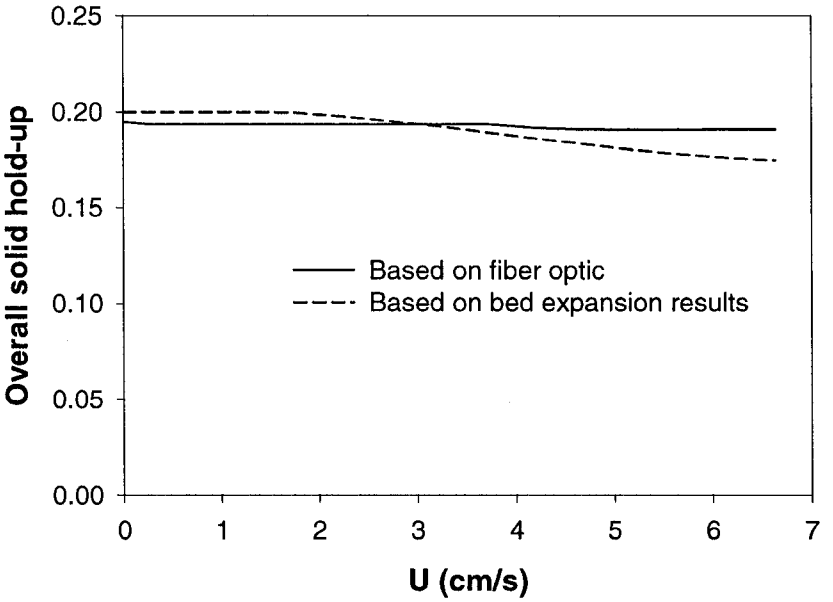

Figure 5.13. The comparison between overall solid-holdup obtained based on fiber optic and bed expansion results for zirconia nanoparticles.

By analyzing the fiber optic data, we did not realize the vigorous bubbling in the bed of zirconia nanoparticles. The following figures correspond to solid concentration as a function of time for zirconia and FCC under the same conditions. The results were taken in the middle of the bed and 5 cm above the distributor. The gas velocity is 7 cm/s, which is far enough from minimum fluidization velocity and it was the highest velocity that we obtained the fiber optic data. At this velocity, FCC particles are in the bubbling regime with large and fast rising bubbles. As results show, the fluctuation of solid hold-up in FCC is significantly more than that of zirconia. These results qualitatively show

that although some bubbles are observed in the fluidized bed of zirconia nanoparticles, the fluidization is in a very gentle mode of bubbling regime.

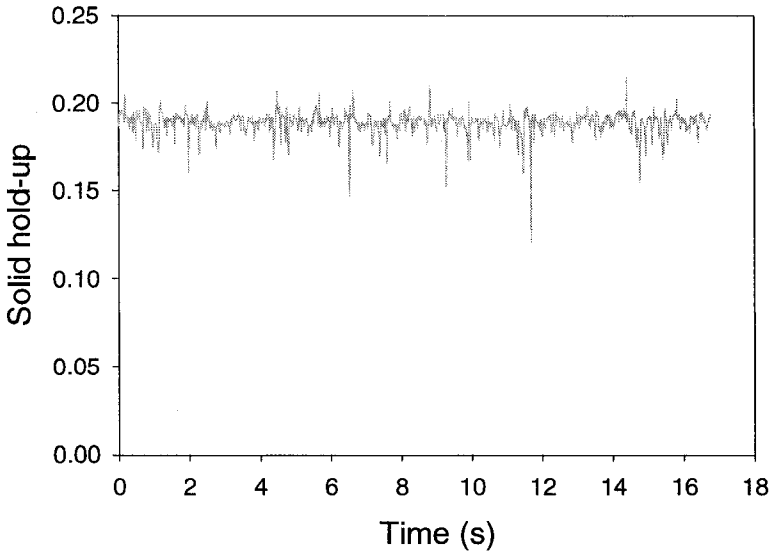

Figure 5.14. Solid hold-up for zirconia fluidization at gas velocity 7 cm/s

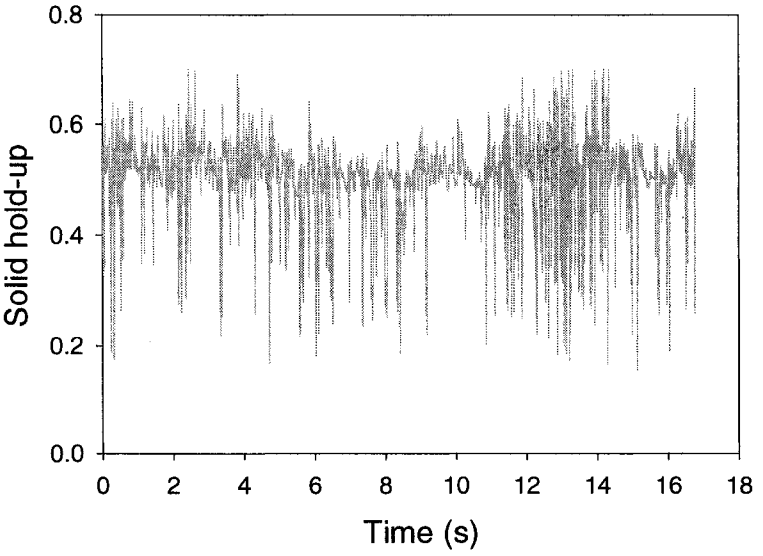

Figure 5.15. Solid hold-up for FCC fluidization at gas velocity 7 cm/s

Solid hold-up evaluation by radioactive densitometry for aluminum

The radioactive densitometry results for aluminum nanoparticles are presented in the following paragraph. The initial height and porosity of the bed were 13 cm and 87%, respectively. As illustrated in Figure 5.16, the cross-section mean hold-up at 3 cm above the distributor significantly decreases by increasing gas velocity. However, the change in solid hold-up for levels 5 and 10 cm above the distributor is not dramatic. In addition, it can be observed that solid hold-up for higher bed levels, 5 and 10 cm, does not change remarkably along the bed height. In bubbling fluidization, it is not usual that the solid concentration in lower positions of bed is less compared to that in higher sections. The reason may be explained as follows. In fluidized bed of nanoparticles showing ABF behavior, there is a wide distribution of agglomerate size along the bed height. As mentioned earlier, we also observed that during fluidization, the larger agglomerates were located in the lower sections of bed, whereas the smaller ones fluidized in higher positions of the bed. The lower solid hold-up at lower position of bed may be due to different bubble sizes in different bed sections. Using available correlations [47], it would be realized that for the same gas velocity and the same particle density, the bubble size is larger for the larger particles. If we suppose that the density of agglomerates does not change by diameter, therefore, it may be concluded that the bubble size in lower positions of bed are larger than that in higher positions leading to lower solid concentration. To completely understand about this matter, further investigations are required.

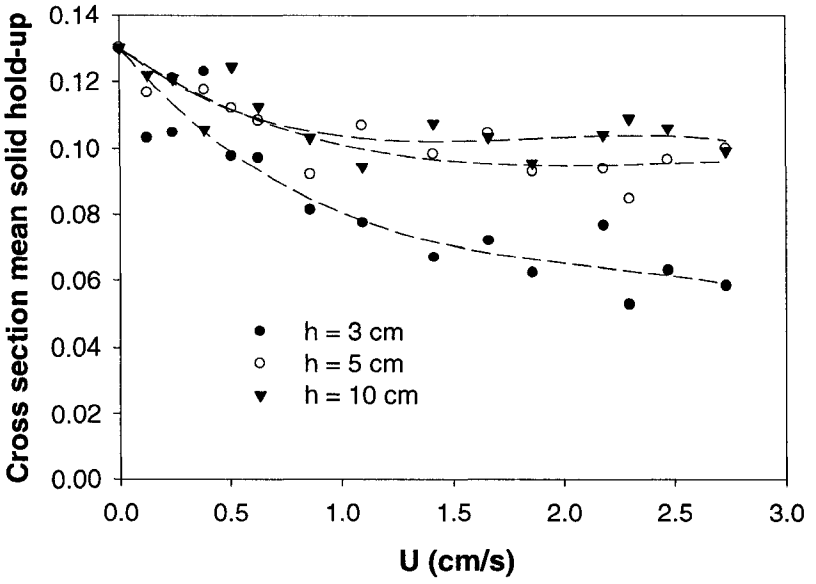

Figure 5.16. Cross section mean solid hold-up for aluminum nanoparticles

The comparison between overall solid hold-up in the bed, provided by integrating the cross section mean hold-up along the bed height, and the one calculated based on bed expansion results is presented in Figure 5.17. Although there are some differences between the graphs for lower velocities, they follow the same trend and become very close for higher velocities. Therefore, based on what was mentioned for zirconia and aluminum nanoparticles, radioactive densitometry is a capable technique to predict the solid hold-up within the bed of these nanoparticles.

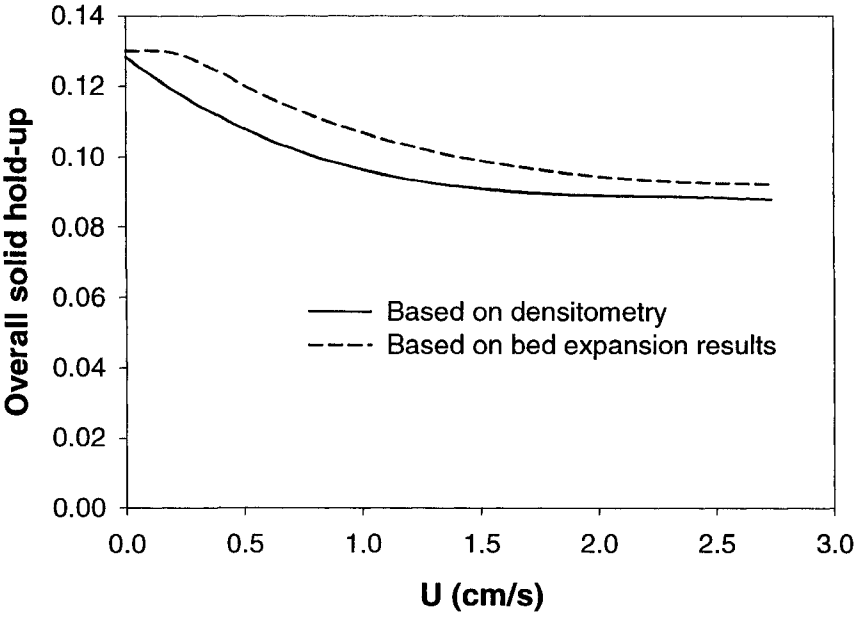

Figure 5.17. The comparison between overall solid-holdup obtained by densitometry and bed expansion results for aluminum nanoparticles

The fiber optic experiments did not perform properly for aluminum nanoparticles, since there was a problem caused by particle cohesion to the tip of the fiber optic probes leading to enormous errors in the results.

Effect of bulk density

As mentioned earlier, the fluidization of zirconia and aluminum nanoparticles shows agglomerate bubbling fluidization (ABF) behavior. According to the literature [10, 17], ABF behavior is predictable for nanoparticles with a bulk density higher than 100 kg/m^3, which is consistent for zirconia and aluminum fluidization results in our work. On the

other hand, nanoparticles with a bulk density lower than 100 kg/m^3 perform *agglomerate particulate fluidization* (APF), including high bed expansion, smooth fluidization and no bubbles. To verify this, we tested the fluidization of fumed silica 14 nm in diameter and 35 kg/m^3 in bulk density. As would be expected, fumed silica nanoparticle fluidization was smooth, with no bubbles, uniform agglomerate distribution in the bed, and high bed expansion. Figure 5.18 shows that the bed expansion of fumed silica nanoparticles reaches 3 and it would increase even more by increasing the velocity. Therefore, the classification of nanoparticles fluidization behavior based on bulk density seems reliable.

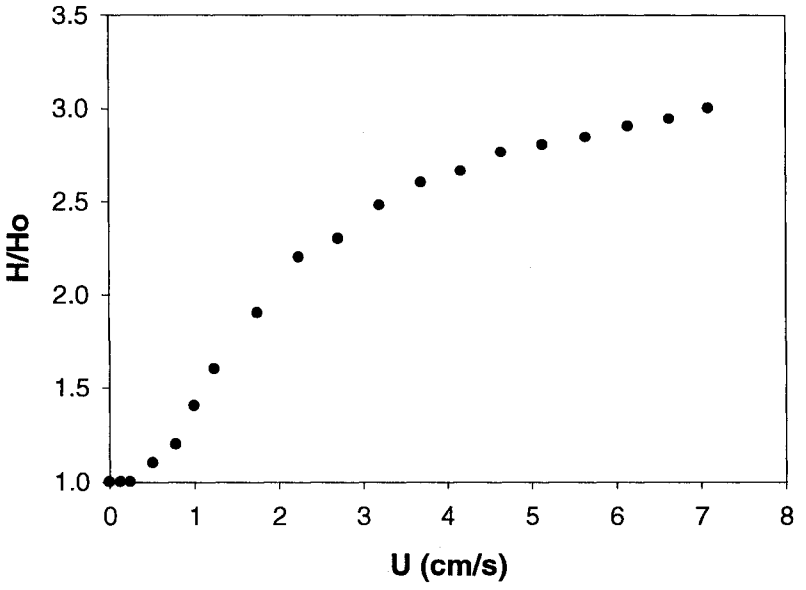

Figure 5.18. Bed expansion for fumed silica nanoparticles

On the other hand, there is a classification for the fluidization of cohesive powders presented by Geldart et al. [48], which is based on the ratio of particle bulk density in

two states; loose and tapped. Accordingly, if that ratio, which is also known as the Hausner ratio, is lower than 1.25, the fine particles appear to be fluidized similar to Geldart group A. This corresponds to our results, since the Hausner ratio for both zirconia and aluminum is less than 1.25, as shown in Table 5.2, and both appear to fluidize, like Geldart group A in terms of bubbles and limited bed expansion. However, Geldart also claimed that when the Hausner ratio is higher than 1.4, the fluidization behavior is similar to Geldart group C, which is not consistent with our results for TiO_2. Titania with the Hausner ratio of 1.48 showed fluidization behavior similar to zirconia and aluminum, including bubbles and low bed expansion up to 1.4, as shown in Figure 5.19. In other words, titania and fumed silica with the same Hausner ratio exhibited completely different fluidization behavior. Therefore, the criterion presented by Geldart to predict the fluidization behavior of fine particles based on the Hausner ratio does not fit for nanoparticle fluidization. However, according to the results of zirconia and aluminum, we believe the fluidization of nanoparticles with the Hausner ratio lower than 1.25 is similar to the fluidization of Group A, as Geldart mentioned.

Table 5.2. Hausner ratio of particles

Particle	**Hausner ratio ($\rho_{b\ tapped}/\ \rho_{b\ loose}$)**
ZrO_2	1.14
Al	1.20
TiO_2	1.48
SiO_2	1.49

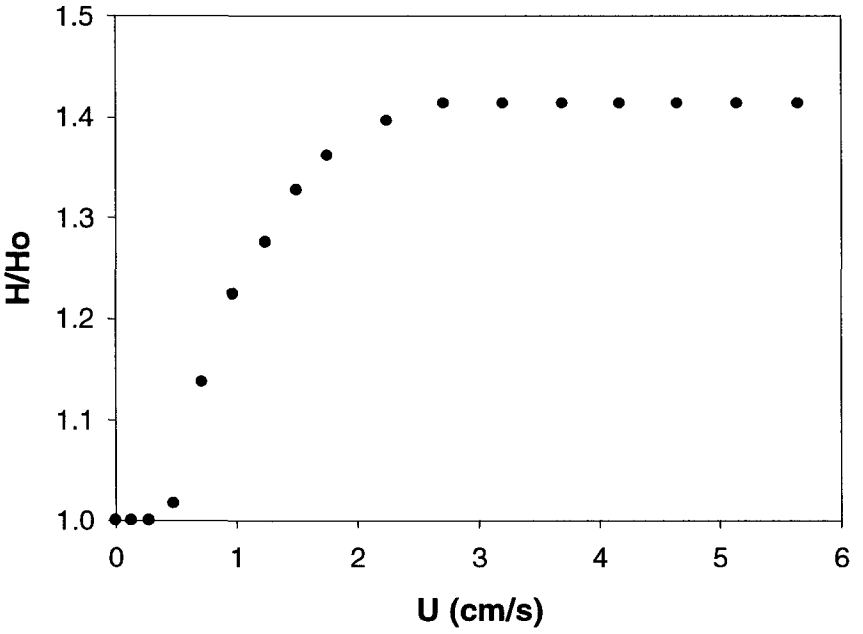

Figure 5.19. Bed expansion for titania nanoparticles.

It seems that bulk density, by itself, is a key factor in explaining fluidization of nanoparticles, as Yao et al. [10] and Zhu et al. [17] believe. Accordingly, the nanoparticles with a bulk density higher than 100 kg/m^3 are expected to present ABF behavior involving bubbles, non-uniform distribution of agglomerate size within the bed and limited bed expansion even at a very high gas velocity. On the contrary, nanoparticles with a relative small diameter (< 20 nm) and bulk density lower than 100 kg/m^3 behave as agglomerate particulate fluidization, which is smooth, without bubbles and with a high bed expansion.

Effect of humidity

The fluidization experiments for zirconia and aluminum nanoparticles were carried out using air with 500 ppm humidity as fluidizing gas. However, when air was used to fluidize fumed silica, the behavior was similar to ABF. On the contrary, fumed silica showed APF in the fluidized bed when nitrogen with humidity content less than 5 ppm was used as fluidizing gas. Since the density of nitrogen is very close to air density, it would be concluded that the difference in fluidization behavior of the fumed silica was due to significant difference in humidity content of fluidizing gases. We also used nitrogen to fluidize titania, which possesses the lowest bulk density among our nanoparticles showing ABF, but the results did not change and the fluidization behavior was ABF. Therefore, it can be concluded the humidity has a great effect on fluidization of nanoparticles having a very low bulk density that show APF. Accordingly, the nanoparticles with the bulk density lower than 100 kg/m^3 can show agglomerate particulate fluidization (APF) if the humidity in the fluidizing gas is very low. Otherwise, those nanoparticles show agglomerate bubbling fluidization (ABF).

5.2.5 Conclusion

It was observed that fluidizations of zirconia and aluminum nanoparticles occur at gas superficial velocities much higher than the minimum fluidization velocities calculated by available correlations for individual nanoparticles. It is a confirmation that fluidization of nanoparticles takes place in the agglomerate state. However, the fluidization of these nanoparticles occurs homogenously in terms of phase concentration

under the experimental conditions in this work. Although the results showed that zirconia nanoparticles exhibit a more homogenous fluidization than aluminum, the bed expansion for aluminum was significantly greater than that of zirconia. Higher bed expansion in the fluidized bed is desired according to the next step of research, which is encapsulation of nanoparticles via polymerization reaction. The higher bed expansion may provide more spaces between the agglomerates as well as particles leading to better contact between the gaseous monomer and particle surface. While both radioactive densitometry and fiber optic measurements provided consistent results in terms of solid hold-up distribution over the cross section, the results obtained by fiber optic measurement overestimated the overall solid concentration for higher velocities compared to the bed expansion observation. However, the results provided by densitometry were in good agreement with the bed expansion results. Therefore, it can be concluded that radioactive densitometry, compared with fiber optic measurement, is a capable technique to predict solid concentration and its distribution over the cross section and along the bed height in a fluidized bed of nanoparticles.

It should be noted that when performing encapsulation in fluidized bed reactor, the agglomerate coating occurs along with individual particle coating, as mentioned in the literature. However, the agglomeration phenomenon seems to be dynamic even if this visual observation must be verified in the future. Therefore, the ratio between the number of coated agglomerates and coated individual particles will depend strongly on the characteristics of the coating reaction and those related to the agglomeration formation- destruction. Moreover, this ratio will depend also on the internal diffusion

within the agglomeration and the intrinsic reaction rate of the coating. One of the best way to quantify this ratio is to carry the reaction and to analyze the encapsulate particle obtained. This work is now underway.

5.2.7 Acknowledgements

The authors wish to acknowledge Prof. Robert Pfeffer for his useful comments and consultations, and Prof. Gregory Kennedy for activating the radioactive source.

5.2.8 Nomenclature

H	Bed height (cm)
H_o	Initial bed height (cm)
ΔP	Pressure drop across the bed (kPa)
r	Local position over the cross section in fiber optic test(cm)
R	Bed Radius (cm)
U	Superficial gas velocity (cm/s)
W	Weight of bed over bed cross section (kPa)
x	Linear position over the cross section in densitometry test(cm)

Greek letters

$\rho_{b\ loose}$	Loose bulk density (cm^3/gr)
$\rho_{b\ tapped}$	Tapped bulk density (cm^3/gr)

5.2.9 References

1- Chaouki J., Chavarie C., Klavana D. and Pajonk G., "Effect of Interparticle Forces on the Hydrodynamic Behaviour of Fluidized Aerogels," Powder Technol. 43, 117-125 (1985).

2- Morooka S., Kusakabe K., Kobata A. and Kato Y., "Fluidization state of ultrafine powders," J. Chem. Eng. Jpn. 21, 41-46 (1988).

3- Iwadate Y. and Horio M., "Prediction of Agglomerate Sizes in Bubbling Fluidized Beds of Group C Powders," Powder Technol. 100, 223-236 (1998).

4- Zhou T. and Li H., "Estimation of Agglomerate size for cohesive particles During Fluidization," Powder Technol. 101, 57-62 (1999).

5- Wang Z., Kwaul M. and Li H., "Fluidization of Fine Particles," Chem. Eng. Sci. 53, 377-395 (1998).

6- Li H., Hong R. and Wang. Z., "Fluidization Ultrafine Powders with Circulating Fluidized bed," Chem. Eng. Sci. 54, 5609-5615 (1999).

7- Zhou T. and Li H., "Force Balance Modeling for Agglomerating Fluidization of Cohesive Particles," Powder Technol. 111, 60-65 (2000).

8- Lu X. and Li H., "Fluidization of $CaCO_3$ and Fe_2O_3 Particle Mixtures in a Transverse Rotating Magnetic Field," Powder Technol. 107, 66-78 (2000).

9- Matsuda S., Hatano H., Kuramoto K. and Tsutsumi A., "Fluidization of Ultrafine Particles with High G," J. Chem. Eng. Jpn. 34, 121-125 (2001).

10- Yao W. Guangsheng G., Fei W. and Jun W., "Fluidization and Agglomerate Structure of SiO_2 Nanoparticles," Powder Technol. 124, 152-159 (2002).

11- Jung J. and Gidaspow D., "Fluidization of Nano-Size Particles," J. Nanoparticles Sci. 4, 483-497 (2002).

12- Mawatari Y., Ikegami T., Tatemoto Y. and Noda K., "Prediction of Agglomerate Size for Fine Particles in Vibro-Fluidized Bed," J. Chem. Eng. Jpn. 36, 277-283 (2003).

13- Mawatari Y., Tatemoto Y. and Noda K., "Prediction of Minimum Fluidization Velocity for Vibrated Fluidized Bed," Powder technol. 131, 66-70 (2003).

14- Watano S., Imada Y., Hamada K., Wakamatsu Y., Tanabe Y., Dave R. N. and Pfeffer R., "Microgranulation of Fine Powders bya Novel Rotating Fluidized Bed Granulator," Powder Technol. 131, 250-255 (2003).

15- Li H. And Tong H., "Multi-Scale Fluidization of Ultrafine Powders in a Fast-Bed-Riser/Conical-Dipleg CFB Lop," Chem. Eng. Sci. 59, 1897-1904 (2004).

16- Nam C. H., Pfeffer R., Dave R. N. and Sundaresan S., "Aerated Vibrofluidization of Silica Nanoparticles," AIChE J. 50, 1776-1785 (2004).

17- Zhu C., Liu G., Yu Q., Pfeffer R., Dave R. N. and Nam C. H., "Sound Assisted Fluidization of Nanoparticle Agglomerate," Powder Technol. 141, 119-123 (2004).

18- Matsuda S. Hatano. H., Muramoto T. And Tsutsumi A., "Modeling for Size Reduction of Agglomerates in Nanoparticles Fluidization," AIChE J. 50, 2763-2771 (2004).

19- Hakim L. F., Portman J. L., Casper M. D. and Weimer A. W., "Aggregation Behavior of Nanoparticles in Fluidized Beds," Powder Technol. 160, 149-160 (2005).

20- Zhu C., Yu Q., Dave R. N. and Pfeffer R., "Gas Fluidization Characteristics of Nanoparticle Agglomerates," AIChE J. 51, 426-438 (2005).

21- Yu Q. Dave R. N., Zhu C., Quevedo J. A. and Pfeffer R., "Enhanced Fluidization of Nanoparticles in an Oscillating Magnetic Field," AIChE J. 51, 1971-1979 (2005).

22- Guo Q., Liu H., Shen W., Yan X. and Jia R., "Influence of Sound Wave Characteristics on Fluidization Behaviors of Ultrafine Particles," Chem. Eng. J. 119, 1-9 (2006).

23- Wang X. S., Palero V., Soria J. And Rhodes M., "Laser-Based Planar Imaging of Nano-Particle Fluidization: Part I-Determination of Aggregation Size and Shape," J., Chem. Eng. Sci. 2006, 61, 5476.

24- Guo Q., Li Y., Wang M., Shen W. and Yang C., "Fluidization Characteristic of SiO_2 Nanoparticles in an Acoustic Fluidized bed," Chem. Eng. Technol. 29, 78-86 (2006).

25- Jiradilok V., Gidaspow D., Kalra J., Damronglerd S. and Nitivattananon S., "Explosive Dissemination and Flow of Nanoparticles," Powder Technol. 164, 33-49 (2006).

26- Guo Q., Yang X., Shen W., and Liu H., "Agglomerate Siza in an Acoustic Fluidized Bed with Sound Assistance," Chem. Eng. Process. 46, 307-313 (2007).

27- Gundogdu O., Jenneson P. M. and Tuzun U., "Nano Particle Fluidisation in Model 2-D and 3-D Beds Using High Speed X-Ray Imaging and Microtomography," J. nanoparticle Res. 9, 215-223 (2007).

28- Quevedo J. A., Flesch J., Pfeffer R. and Dave R., "Evaluation of Assisting Methods on Fluidization of Hydrophilic Nanoagglomerates by Monitoring Moisture in the Gas Phase," Chem. Eng. Sci. 62, 2608-2622 (2007).

29- Liu H., Guo Q. and Chen S., "Sound-Assisted Fluidization of SiO_2 Nanoparticles with Different Surface Properties," Ind. Eng. Chem. Res. 46, 1345-1349 (2007).

30- Avella M., Errico M. E. and Gentile G., "Nylon 6/Calcium Carbonate Nanocomposites: Characterization and Properties," Macromol. Symp. 234, 170-175 (2006).

31- Wang Y., Dave R. N. and Pfeffer R., "Polymer Coating/Encapsulation of Nanoparticles Using a Supercritical Anti-Solvent Process," J. Supercrit. Fluids. 28, 85-99 (2004).

32- Gass J., Poddar P. Almand J., Srinath S. and Srikanth H., "Superparamagnetic Polymer Nanocomposites with Uniform Fe_2O_3 Nanoparticle Dispersion," Adv. Funct. Mater., 16, 71-75 (2006).

33- Zhang J. L., Liu Z. M., Han B. X., Li J. C., Li Z. H. and Yang G. Y.,"Ultrasound-Induced Capping of Polystyrene on TiO_2 Nanoparticles by Precipitation with Compressed CO_2 as Antisolvent," J. Nanosci. Nanotechol. 5, 945-950 (2005).

34- Salehi-Mobarakeh H., Brisson J. and Ait-Kadi A., "Interfacial Polycondesation of nylon-6,6 at the Glass Fibre Surface and its Effect on Fibre-Matrix Adhesion," J. Mater. Sci. 32, 1297-1304 (1997).

35- Salehi-Mobarakeh H., Brisson J. and Ait-Kadi A., "Ionic interphase of glass fiber/polyamide 6,6 composites," Polym. Compos. 19, 264-274 (1998).

36- Kasseh A., Ait-Kadi A., Riedl B. and Pierson J.F., "Organic/inorganic hybrid composites prepared by polymerization compounding and controlled free radical polymerization," Polymer, 44,1367-1375 (2003).

37- Wang Y., Pei X. and Yuan K., "Reverse ATRP Grafting From Silica Surface to Prepare Well-Defined Organic/Inorganic Hybrid Nanocomposite," Mater. Lett. 59, 520-523 (2005).

38- Roy C., Dubois C., Lafleur P. and Brousseau P., "The Dispersion and Polymer Coating of Ultrafine Aluminum Powders by the Ziegler Natta Reaction," in "Mater. Res. Soc. Symp. Proc.," 800, AA.2.5.- AA.2.5.6 (2004).

39- Shi D., Wang S.X., van Ooij W.L., Wang L.M., Zhao J. and Yu Z., "Uniform deposition of ultrathin polymer films on the surfaces of Al_2O_3 nanoparticles by a plasma treatment," Appl. Phys. Lett. 78, 1243-1245 (2001).

40- Rovira-Bru M., Giralt F. and Cohen Y., "Protein Adsorption onto Zirconia Modified with Terminally Grafted Polyvinylpyrolidone," J. Colloid Interface Sci. 235, 70-79 (2001).

41- Dubois C., Rajabian M. and Rodrigue D., "Polymerization Compounding of Polyurethane-Fumed silica Composites," Polym. Eng. Sci. 46, 360-371 (2006).

42- Esmaeili B., Chaouki J. and Dubois C., "Polymerization Compounding on the Surface of Zirconia Nanoparticles," Macromol. Symp. 243, 268-276 (2006).

43- Mabrouk R., Radmanesh R., Chaouki J. and Guy C., "Scale Effects on Fluidized Bed Hydrodynamics Int. J. Chem. Reactor Eng., 3, 1-11 (2005).

44- Pugsley, T., Tanfara, H., Makus, S., Heping, C., Chaouki J. and Winters, C., "Verification of fluidized bed electrical capacitance tomography measurements with a fibre optic probe," Chem. Eng. Sci. 58, 3923-3934 (2003).

45- Geldart G., "Type of Gas fluidization," Powder Technol. 7, 285-292 (19730.

46- Kunii D and Levenspiel O., "Fluidization Engineering," 2nd ed. Butterworth-Heinemann, Newton (1991).

47- Horio M. and Nanoka A, "A Generalized Bubble Diameter Correlation for Gas-Solid Fluidized Beds" AIChE J., 33, 1865-1872 (1987).

48- Geldart D., Harnby, N. and Wong A. C., "Fluidization of Cohesive Particles," Powder Technol. 37, 25-37 (1984).

CHAPTER 6

ENCAPSULATION OF NANOPARTICLES BY POLYMERIZATION COMPOUNDING IN A GAS/SOLID FLUIDIZED BED REACTOR

6.1 Presentation of the article

In the current article, the encapsulation of aluminum and zirconia nanoparticles is investigated in a fluidized bed reactor via the polymerization compounding approach. There is no solvent required in this system, therefore, the process is carried out free of impurities within organic solvents. Moreover, after the encapsulation process, additional steps such as washing, filtering, and drying are not needed, consequently, the coated particles can be used right after encapsulation. The results showed that polymerization compounding is a capable technique to coat nanoparticles in fluidized bed reactor as well as in the slurry phase.

6.2 Encapsulation of Nanoparticles by Polymerization Compounding in a Gas/Solid Fluidized Bed Reactor

Babak Esmaeili, Jamal Chaouki*, Charles Dubois

E-mail: jamal.chaouki@polymtl.ca

Département de Génie Chimique, École Polytechnique de Montréal, C.P. 6079, succ. Centre-ville, Montréal, Québec, H3C 3A7, Canada

6.2.1 Abstract

For the first time, a fluidized bed reactor was employed for encapsulating nanoparticles by the polymerization compounding approach using Ziegler-Natta catalysts. The polymerization reaction was carried out using a solvent-free process in a gas-phase reactor. This direct gas-solid reaction greatly simplified collecting the particles of interest after polymerization since none of the extra steps often found in encapsulation processes, such as filtering and drying, were performed in this work. The grafting of the catalyst to the original surface of particles was confirmed by X-ray photoelectron spectroscopy (XPS). Micrographs obtained by transmission electron microscopy (TEM) confirmed the presence of a thin layer of polymer, in the order of a few nanometers, around the particles. The thickness of this coating was affected by the operating conditions of the process. The characterization of the modified particles with electron microscopy also revealed that zirconia nanoparticles tend to be coated in an agglomerated state, whereas aluminum particles were mostly individually encapsulated by the polymer. In addition, the effects of temperature and pressure were studied on the

encapsulation process and a kinetic analysis was presented based on the available models in the literature.

6.2.2 Introduction

Coating or encapsulating nanoparticles with polymers is desired in many applications in order to improve their chemical stability, reduce their toxicity, and facilitate their storage, transport, and processing. As two particular applications of nanoparticle coating, we specify the encapsulation of zirconia and aluminum nanoparticles. These nanoparticles are very promising materials in industrial applications. Over the last few years, the introduction of zirconium oxide-based ceramics into the field of dentistry has been greatly appreciated. In fact, dentures made from these materials have the required hardness and aesthetic qualities. Their production, however, poses serious cost-effectiveness problems mainly because of their ultra hard mechanical property. One solution to eliminate this difficulty is to coat the nanoparticles with a polymer using polymerization compounding, followed by manufacturing the coping in composite form to make dentures.

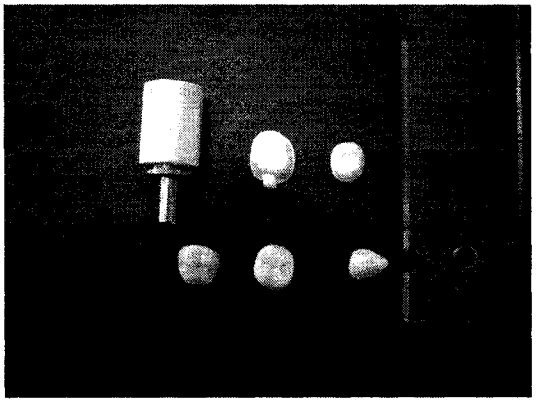

Figure 6.1. From left to right starting from the top: composite ingot, composite coping, densified coping, 3 false teeth ready to be implanted into the mouth.

Manufacturing must take into account the shrinkage that occurs during densification. Finally, the composite denture is densified to sublime the polymer and obtain it in ceramic form. Figure 6.1 shows the compounds corresponding to the different steps mentioned above.

On the other hand, ultra fine aluminum powder is being recognized as a good candidate for diverse combustion applications, such as additives in solid rocket propellants and metallic fuel in explosive formulations. The aluminum nanoparticles have been reported to show burning rates 5 to 10 times greater than microsized ones and when used in gas generator fuels, they achieve a more complete combustion. These enhanced properties are due to their large specific surface per unit mass. However, the large specific surface area, which provides these powders with a high reactivity, makes them particularly difficult to maintain in an unoxidized state. Consequently, coating these powders with a polymer would be a solution to protect them from a non-desirable reaction, such as oxidation. As mentioned earlier, the application of this process is not limited to the applications mentioned for zirconia and aluminum. It can be applied to different types of nanoparticles in order to protect their surface, reduce their toxicity and facilitate their processing.

Polymerization compounding (PC) [1-9] is a technique that provides the modified particles with the properties required to obtain high performance composite materials. In this approach, the particle surface becomes involved in the polymerization reaction so that a very intimate contact between the particle surface and polymer can be established, bringing improved interfacial properties and, consequently, enhanced properties of the

nanocomposite. In the last two decades, PC has been successfully applied to encapsulate nanoparticles with different types of polymers [10-17], and nearly all reported experimental investigations were performed in the liquid phase. The ubiquity of the slurry-based process is easily explained. First, most of the monomers of interest are either readily available in a liquid state at room temperature or very soluble in common organic solvents. Therefore, a liquid phase process is intrinsically compatible with the nature of the reagents. Secondly, the liquid medium provides the appropriate conditions to disperse agglomerates and clusters in finer particles in order to have them individually coated. However, the results showed [14] that this is not completely successful and the coating of agglomerates has always occurred together with the encapsulation of individual particles. Thirdly, the success of the coating process requires that a very small quantity of catalyst or initiator be deposited on a relatively large surface of particles. For example, in the case of ethylene polymerization, a small amount of Ziegler-Natta catalyst, around 1 micro liter, must be placed on a square meter of particle surface to be coated. Therefore, by dissolving that small amount of catalyst in an organic solvent, where particles have already been dispersed, it is easier to achieve a uniform activation of the particle surface prior to the polymerization reaction.

Some drawbacks, however, arise when the process is carried out in liquid phase, as the polymerization reaction must be followed by additional steps to isolate the coated particles. After encapsulation, the reaction slurry must be filtered to separate the coated particles from the solvent. This step is usually accompanied by washing the encapsulated powders to eliminate solvent impurities, catalyst and the non-reacted monomers. Then,

the coated particles must be completely dried in an oven overnight. Subsequently, the dried particles form a hard bulk material, which needs to be grinded to obtain finely coated particles. To accomplish all of the above mentioned additional processes requires more than the polymerization reaction time itself, which usually extends only over a few minutes. Accordingly, the encapsulation process costs for a liquid-solid reaction, particularly when dealing with large amounts of particles, are significant. In addition, under these conditions, it is difficult to ensure a complete removal of the impurities in the solvent, and the bulk material recovered from the process must be grinded to obtain the desired particle sizes.

An evident alternative to eliminate all the aforementioned negative aspects is to perform the nanoparticle encapsulation as a gas-solid reaction, where the gaseous phase contains the monomer of interest. The polymerization of ethylene via Ziegler-Natta catalyst for nanoparticle encapsulation and nanocomposite preparation has been reported by several researchers [6, 9, 10, and 17], using a liquid suspension where the ethylene gas is dissolved. Recently, we also have successfully used this procedure to encapsulate zirconia nanoparticles in hexane [14]. The work reported in this paper was aimed at extending the previously described slurry-based process to a gas phase reaction using a fluidized bed reactor. For this purpose, two different types of nanoparticles, zirconia and aluminum, were considered for encapsulation studies by polyethylene via the Ziegler-Natta polymerization scheme. This simplified process is performed free from solvent impurities (particularly water) and no extra separation steps, such as filtering, washing, drying, and grinding, are required to collect the coated nanoparticles after the

polymerization reaction. To the best of our knowledge, this original work by our group is being accomplished for the first time. It should be mentioned that although this system, in some aspects, is similar to the processes dealing with ethylene homopolymerization using the Ziegler-Natta catalyst, there are some major differences in these two processes. In our case, the polymerization occurs on the surface of nanoparticles, whereas in the homopolymerization of ethylene, the substrate that supports the polymerization catalyst has a characteristic length in the micrometer range. In addition, the amount of catalyst, when performing nanoparticle encapsulation, is limited by the active sites on the surface of nanoparticles. Besides, the pressure in the ethylene homopolymerization process may rise very high, while the pressure used in the nanoparticle encapsulation studies was moderate, and in some instances, close to the ambient pressure.

The major difficulty associated with taking this reaction from a liquid to a gas phase process was to attach the Ziegler-Natta catalyst to the surface of the particle. The approach investigated consisted of evaporating the Ziegler- Natta catalyst before it entered the fluidized bed reactor, and then condensing the resulting vapor on the particle surface in the reactor. Since there is no thermal gradient in the reactor, all particles having the same temperature due to the mixing action of the fluidization process [18], the catalyst vapors uniformly deposit on the particle surface. Therefore, it would be anticipated that the polymerization reaction is uniformly applied on the particles.

6.2.3 Experimental

Materials

Zirconia powder procured from Sigma-Aldrich and aluminum powder manufactured by TEKNA were used for the polymer coatings experiments. Table 6.1 reports some of the physical properties of these particulate materials.

Table 6.1. Physical properties of zirconia and aluminum particles

	Al (TEKNA)	**ZrO_2 (ALDRICH)**
Average diameter (nm)	120	250
Specific surface area (m^2/gr)	16.5	5.5
Solid density (kg/m^3)	2700	5900
Bulk density (kg/m^3)	350	1200

Ethylene gas with a purity of 99.5%, supplied by Canadian Liquid Air, was used as monomer for the polymerization reaction. The Ziegler-Natta catalyst system, consisting of titanium tetrachloride ($TiCl_4$), manufactured by Acros, as the catalyst, and triethylaluminum ($AlEt_3$) obtained from Sigma-Aldrich, as co-catalyst, was stored and handled in a glove box in order to protect them from moisture and oxygen. Methylaluminoxane (MAO) also procured from Sigma-Aldrich was employed to determine the hydroxyl groups density on particles surface.

Quantification of hydroxyl chemical groups on nanoparticles

The polymerization process used in this work necessitates the anchoring of the catalyst to the particles using the OH sites on their outer surface. Accordingly, appropriate amounts of the catalyst and co-catalyst needed to be estimated from the OH group density on the nanoparticles surface. To carry out this quantification [19], a small amount of nanoparticles, about 0.5 g, is agitated and heated in 5 ml of dry toluene in a lab test tube where a flow of dry nitrogen and vacuum conditions are first applied to remove oxygen and humidity from the system. After 1 hr, the lab test tube is cooled to ambient temperature, and, subsequently, 1 ml of methylaluminoxane (MAO) is injected into the closed tube through a septum. As a result of the reaction between each mole of MAO and hydroxyl groups of the surface, one mole of methane is released. Consequently, the hydroxyl group density is calculated by determining the methane gas evolved in the process using a pressure monitoring setup. An example of the use of the observed pressure rise to determine the minimum amount of catalyst and co-catalyst is given in Table 6.2. It should be mentioned that the amount of catalyst and co-catalyst employed in all the reactions were in excess of 100 %.

Table 6.2. Catalyst and co-catalyst calculated based on OH concentration

	Aluminum	**Zirconia**
Pressure rise	142.5 mmHg/ gr	50.7 mmHg/ gr
OH concentration on particles	$5.4 * 10^{-4}$ mole/ gr	$1.9 * 10^{-4}$ mole/ gr
$TiCl_4$ (pure catalyst)	0.06 ml/ gr	0.02 ml/ gr
$AlEt_3$ (1 Molar solution in Hexane)	0.54 ml/ gr	0.19 ml/ gr

Synthesis

Figure 6.2 illustrates the encapsulation process of nanoparticles in a fluidized bed reactor. The reactor itself used for this work was a simple cylinder made of stainless steel, making 2 cm in diameter and 3 cm in height. Gas was introduced into the bed through a porous plate with a 5 μm pore size in order to provide a homogenous fluidization of particles. The reaction proceeds as follow: First, nitrogen gas, passed through an electrical heater, provides sufficient energy to heat the entire system so that the injection point attains a higher temperature than the boiling temperature of the catalyst. A second electrical heater was also located around the fluidized bed to adjust the reactor temperature at the desired reaction temperature. Then, the catalyst, and after a few minutes, the co-catalyst are injected into the system. Since the temperature at the injection point is higher than the boiling temperature of $TiCl_4$ and $AlEt_3$, the catalyst and co-catalyst evaporate and enter the reactor in the gas phase. Subsequently, the catalyst and co-catalyst vapors uniformly condense on nanoparticles in the reactor, where temperature is lower than catalyst and co-catalyst boiling points. After the catalyst

grafting step on the particles, the polymerization reaction was started by switching from nitrogen to ethylene as the fluidizing gas. After the desired reaction time, ethylene flow was stopped and the system was flashed by nitrogen. The gas velocities in the reactor for aluminum and zirconia were 5 and 10 cm/s, respectively, which are much higher than minimum fluidization velocity of these powders [18]. The temperature and the pressure in the reactor were kept constant for a given reaction, and varied within ranges of 65-75 ^{o}C and 140- 280 kPa, respectively, during the series of runs needed for this study.

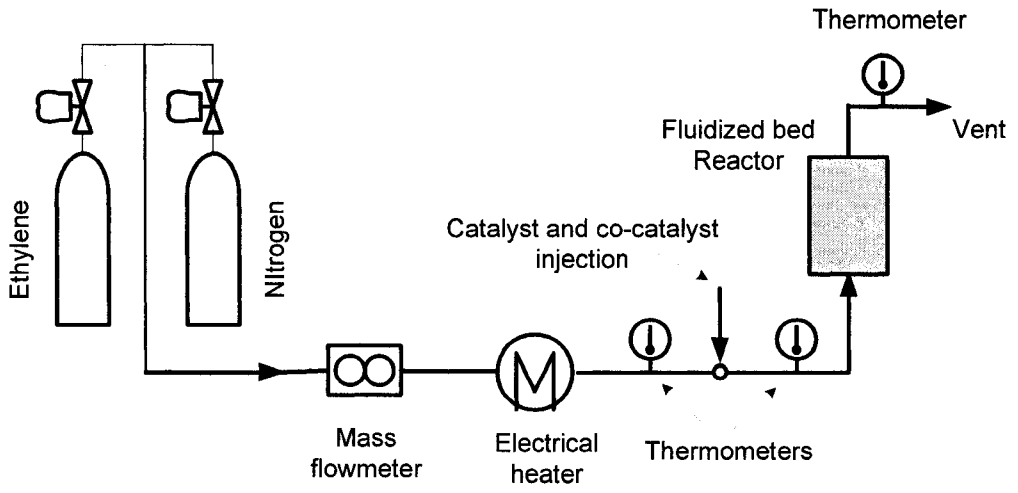

Figure 6.2. Schematic of the encapsulation of nanoparticles in fluidized bed reactor

Characterization

The amount of polymer on the zirconia particles was determined by thermogravimetry analysis (TGA) using a TA instruments 500 apparatus operated in a 25– 800 ^{o}C temperature range at a 10 ^{o}C/min heating rate under a flow of nitrogen. The thickness of the polymer layer on the surface of nanoparticles was observed using Jeol JEM-2100F

Transmission Electron Microscope (TEM). X-ray photoelectron spectroscopy (XPS) was used to study the interface of the grafted polymer and the original surface of particles.

6.2.4 Results and Discussion

A typical thermogravimetry analysis (TGA) of coated zirconia and aluminum nanoparticles is presented in Figures 6.3 and 6.4. One can see that a sharp weight loss appears between 450 to 500 ° C corresponding to the pyrolysis of high molecular weight polyethylene (HMWPE). This confirms the presence of HMWPE on the surface of nanoparticles.

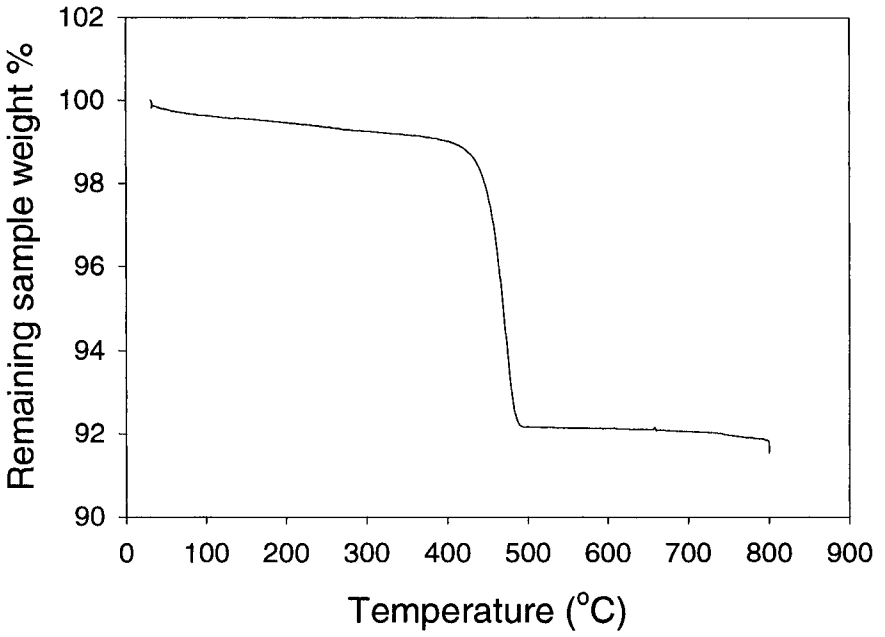

Figure 6.3. TGA graph of zirconia coated nanoparticles
(Reaction conditions T = 65°C, P = 210 kPa)

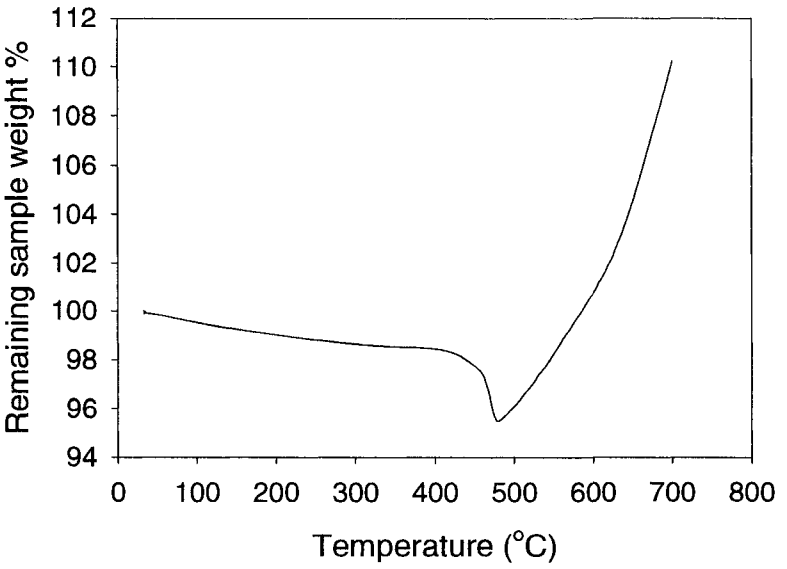

Figure 6.4. TGA graph of aluminum coated nanoparticles
(Reaction conditions: T = 72 °C, P = 140 kPa)

It can be seen that in the TGA graph of aluminum, a weight increase occurs after polyethylene degradation at around 500 °C. It could be because of adsorption of nitrogen on aluminum surface, and also, the oxidation reaction. After polymer degradation, the surface of nanoparticles becomes reactive, and therefore, it can react with the traces of oxygen found in the nitrogen gas leading to a weight increase in the TGA plot.

The characterization of the coated particles was continued by the verification of catalyst grafting on the nanoparticles surface using XPS, as reported in Figure 6.5. It should be noted that in order to show the results of the original and coated particles in the same graph, the spectrum corresponding to coated particles is shifted by 50000 counts/s. However, the original data obtained from the software are reported in Table 6.3. As shown in Figure 6.5, titanium and chlorine picks can be clearly observed at a binding

energy of 458 ev and 199 ev, respectively, corresponding to Ziegler-Natta catalyst in coated aluminum.

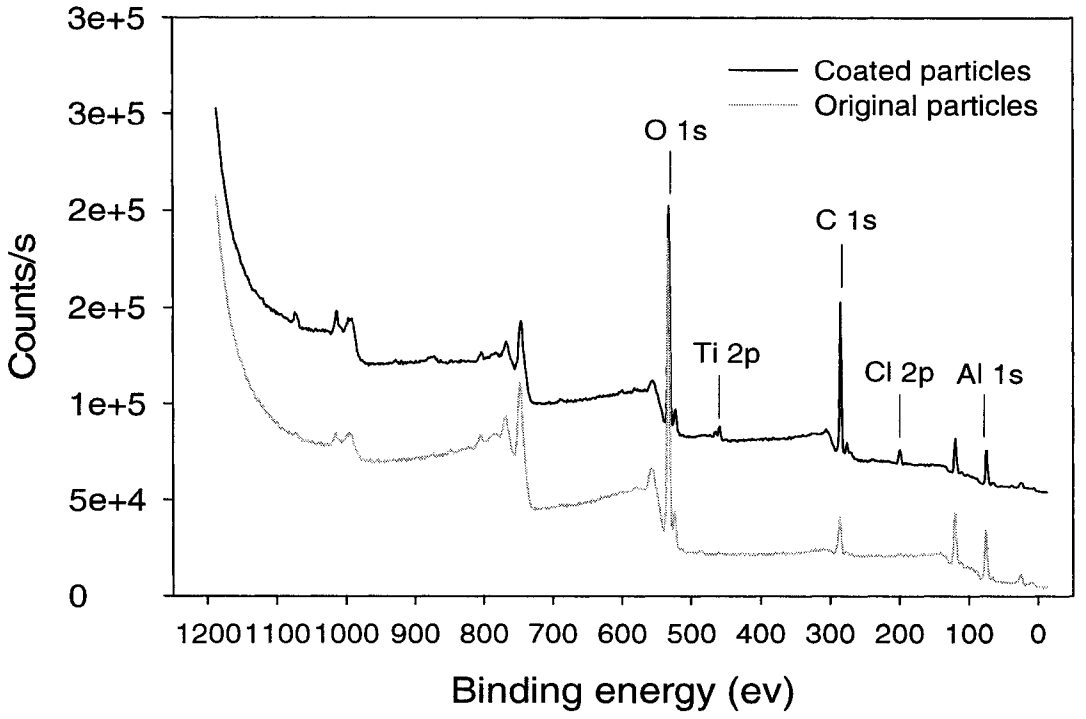

Figure 6.5. XPS graphs of original and coated aluminum nanoparticles

Table 6.3. Elemental ID and quantification for original and coated aluminum nanoparticles

Name	Peak BE	Height cps (original)	Area (p) cps.ev (original)	Height cps (coated)	Area (p) cps.ev (coated)	At. % (original)	At. % (coated)
Al 1s	74	22804.00	110210.15	15132.88	65809.97	**26.59**	**3.46**
O 1s	532	139198.88	657310.45	99992.92	428450.91	**55.82**	**42.82**
C 1s	285	17081.89	90798.42	59493.24	235550.63	**17.59**	**53.72**

In addition, as we previously mentioned [14], by comparing XPS results of the coated particles with different polymer contents, it is confirmed that the catalyst is only found at the polymer-substrate interface, indicating that polymerization reaction can only be initiated only from the original surface of particles. It was proposed that Ziegler-Natta catalyst, $TiCl_4$, reacts with hydroxyl groups on particles surface as shown in following equation [1],

$$—OH + TiCl_4 \rightarrow —O—TiCl_3 + HCl \quad (1)$$

Therefore, there is a covalent bond established between the catalyst and the particles, and as a result, the polymerization starts from the surface of the particles, which favors their encapsulation. Although the chain transfer termination usually occurs in Ziegler-Natta polymerization systems, a favorable interaction is established between the polymer and substrate. Since the polymerization reaction starts from the substrate and monomers are consecutively added to polymer chains, the diffusional limitations and steric hindrance effects are significantly lower than in the case where polymer chains are simply brought to the surface by the substrate nucleating action. Therefore, appropriate wetting of the solid surface by the polymer, and consequently, high interfacial interactions are achieved. As shown in Table 6.3, the relative intensity of aluminum and oxygen peaks, representing the original surface of particles, is significantly reduced after polymerization. In addition, the relative intensity of carbon peak, associated with the presence of a hydrocarbon based polymer coating, increased considerably after the

polymerization in comparison with original particles. It can be seen that the weight percentage of aluminum and oxygen elements was reduced from 26.59 and 55.82 % for non coated particles to 3.46 and 42.82 % for coated particles. In contrast, carbon content increases from 17.59 % for non coated particles to 53.72 % for coated particles. The initial amount of carbon for non coated particles, detected by XPS, is due to the sample contamination by atmospheric carbon (CO2). Similar results were obtained for zirconia nanoparticles.

TEM observations carried out on original and coated aluminum and zirconia nanoparticles are presented in Figures 6.6 and 6.7, respectively. As shown in Figure 6.6-a and 6.7-a, the surface of non-coated particles possesses a sharp edge and no other phase is distinguished. On the other hand, as shown in Figure 6.6-b for a coated aluminum particle, an image contrast is found that corresponds to a polyethylene layer of about 4 nanometers thick uniformly applied around the particles. One can see in Figure 6.7-b that zirconia particle was covered by a polymer layer around 5 nm, however, it is observed that the polymer layer on zirconia particles is not uniform in comparison with that on aluminum. In addition, zirconia particles tend to be coated in a more agglomerated state as observed in Figure 6.8, whereas, aluminum powders were individually encapsulated.

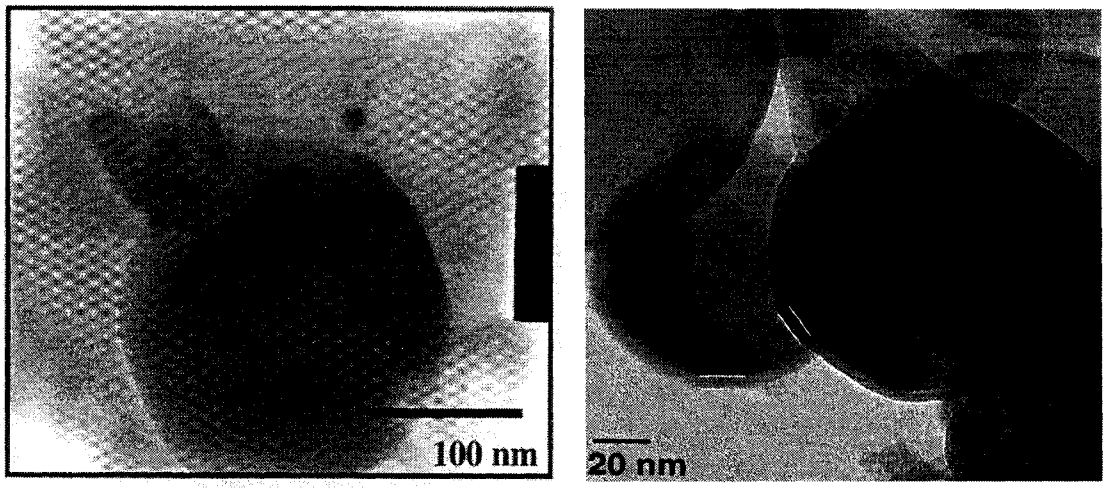

a) b)

Figure 6.6. TEM images of a) original and b) coated aluminum nanoparticles

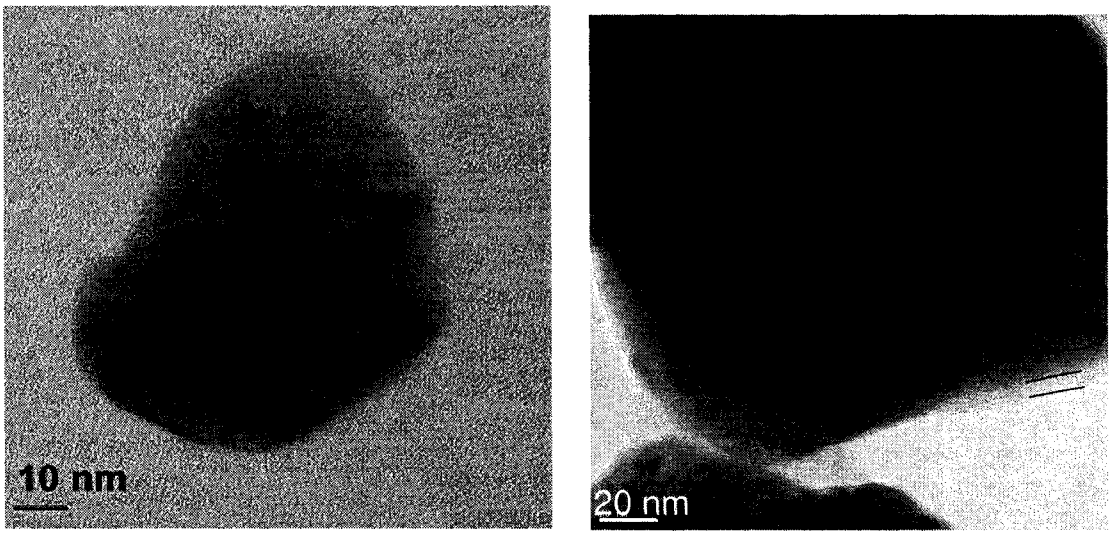

a) b)

Figure 6.7. TEM images of a) original and b) coated zirconia nanoparticles

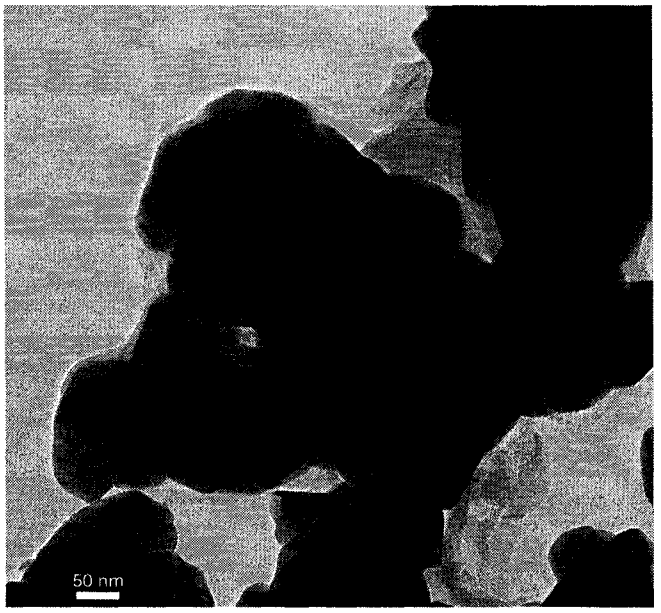

Figure 6.8. TEM image of coated agglomerate of zirconia nanoparticles

These results are consistent with the results obtained in our previous work [18]. It was mentioned that the fluidization of zirconia and aluminum occurs in agglomerate state as shown in Figure 6.9. It was also observed that the minimum fluidization velocities of zirconia and aluminum are 2.3 and 0.25 cm/s, respectively. These values are much higher than minimum fluidization velocity of individual nanoparticles calculated by available correlations [20]. It means that zirconia and aluminum nanoparticles fluidize as clusters of particles. In addition, we observed that the agglomerates in the bed of zirconia are larger compared than those found in the bed of aluminum. Therfore, the agglomerate coating is inevitable when enpsulating nanoparticles, particularly zirconia nanoparticles.

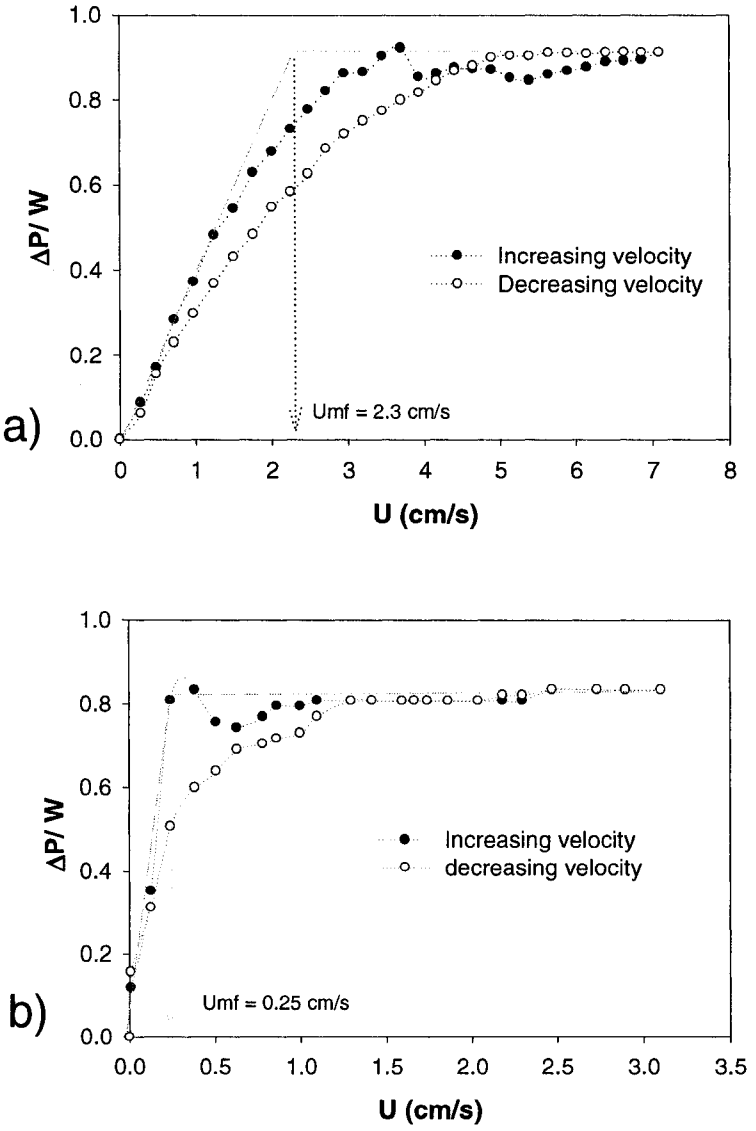

Figure 6.9. Minimum fluidization velocities for a) zirconia and b) aluminum nanoparticles

The effects of polymerization conditions

The encapsulation of zirconia nanoparticles was carried out under different process conditions as listed in Table 6.4. The encapsulation time was around 12 min for all runs except for trial number 4, where the flow of monomer was stopped after 6 min. It can be

seen that the temperature and pressure have considerable effects on the polymerization process. From run No. 1 and 2, it is observed that by increasing the pressure from 140 to 210 kPa, the polymer content increases from 2 to 7%. At 75 °C, the polymer quantity increases from 7.5 to 13% by increasing the pressure from 140 kPa in run 3 to 280 kPa in run 4, where the reaction time was only half of the one used in the low pressure reaction. By comparing run No.1 and No.3, an increase from 2 to 7.5% in polymer content is realized by increasing the temperature from 65 to 75 °C. The corresponding TGA graphs are presented in Figure 6.10.

Table 6.4. Different process conditions for zirconia nanoparticles encapsulation

Operation No.	**Temperature (°C)**	**Pressure (kPa)**	**Polymer content (%)**
1	65	140	2
2	65	210	7
3	75	140	7.5
4	75	280	13

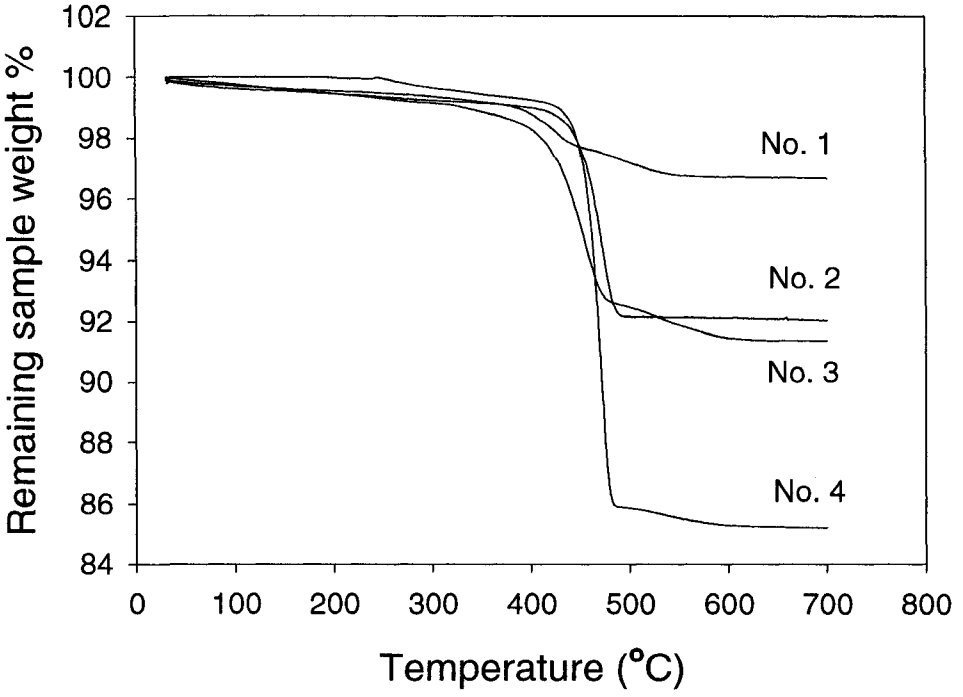

Figure 6.10. TGA graphs of zirconia encapsulation in different operations

Kissin et al. studied the kinetic of ethylene homopolymerization with the heterogeneous Ti-based Ziegler-Natta catalyst [21]. They found that the overall rate of ethylene homopolymerization has the reaction order n with respect to the ethylene concentration, C_E,

$$R_{pol} = k_{eff} C_E^n \tag{2}$$

The order of reaction, n, was evaluated as 1.77 where the polymerization reaction is carried out in the gas phase. The effective rate constant, k_{eff}, is the product of the propagation rate constant, k_p, and the concentration of active centers, C^*. If the propagation rate is assumed to be temperature dependant according to the Arrhenius equation, then the overall polymerization rate can be written as the following equation:

$$R_{pol} = C^{*}k_{p0}\exp(\frac{-E}{RT})C_E^n \quad (3)$$

Where, E is the activation energy for the propagation.

In an investigation on ethylene polymerization kinetic with a heterogeneous metallocene catalyst, Bergstra and Weickert evaluated $C^{*}k_{p0}$ and E as $2.49*10^{10}$ m^3/h.gcat and 74.9 kJ/mol [22]. By applying these values in the reaction rate proposed by Kissin, the amount of polymer was significantly overestimated in comparison with our experimental data. Therefore, we employed the same reaction kinetic and activation energy constant, and by using the experimental results provided in Table 6.4, the $C^{*}k_{p0}$ was modified to $3.3*10^{7}$ m^3/h.gcat. The results are given in Table 6.5.

Table 6.5. Comparison between experimental data and calculated polymer amount using the kinetic in the literature

Operation No.	**Temperature (°C)**	**Pressure (kPa)**	**Polymer quantity (Experimental) (gr)**	**Polymer quantity (Calculated) (gr)**
1	65	140	0.020	0.033
2	65	210	0.070	0.067
3	75	140	0.075	0.067
4	75	280	0.130	0.115

The experimental polymer mass is presented based on 1 gr of zirconia nanoparticles. As shown in the table, the values obtained by the kinetic model using the modified $C^{*}k_{p0}$

are in agreement with the experimental results. Therefore, the model presented by Kissin for ethylene homopolymerization is valid for nanoparticle encapsulation by polyethylene using polymerization compounding. On the other hand, there is a great difference between C^*k_{p0} presented in the work of Bergstra and Weickert and the one modified in this work. There would be two explanations for this difference. First, C^*k_{p0} in the work of Bergstra and Weickert has been obtained for the ethylene polymerization using metallocene catalyst, which is more reactive than Ziegler-Natta catalyst. The second reason is related to the concentration of active centers on the supports. Although in this research, the catalyst injected into the reactor corresponds to the hydroxyl group on nanoparticles, it is expected that a part of the injected catalyst was not deposited on the nanoparticles due to particle agglomeration, as shown in Figure 6.8. Therefore, it seems that the concentrations of active centers available for polymerization reaction are much lower than those in the ethylene homopolymerization process.

A *comparison between nanoparticle encapsulation in slurry and fluidized bed reactors*

The TEM images of coated agglomerates of zirconia produced by the slurry [14] and the gas/solid fluidized bed reactor processes are presented in Figure 6.11. As the images show, the agglomerate in the slurry phase reactor is smaller than those in the fluidized bed reactor. Since in the slurry phase reactor, the particles are dispersed in the solvent by agitation and ultrasound, the large agglomerates are broken into smaller ones and even individual particles, whereas in the fluidized bed reactor used in this work, no external force was applied. The agglomerates in the fluidized bed reactor are, therefore, larger

than those in the slurry phase reactor. If an external force, such as vibration, were applied to the fluidized bed reactor, the agglomerate sizes and the risk of agglomerate coating reactors could be reduced. However, the encapsulation process in the slurry phase must be followed by additional steps, such as filtering, drying, and grinding to isolate the coated particles. Accomplishing all of the above mentioned additional processes requires much more than the polymerization reaction time itself. Accordingly, the encapsulation process cost more for a liquid-solid reaction, particularly when dealing with large amounts of particles. In addition, under these conditions, it is difficult to ensure a complete removal of the impurities in the solvent and the bulk material recovered from the process must be grinded to obtain the desired particle sizes.

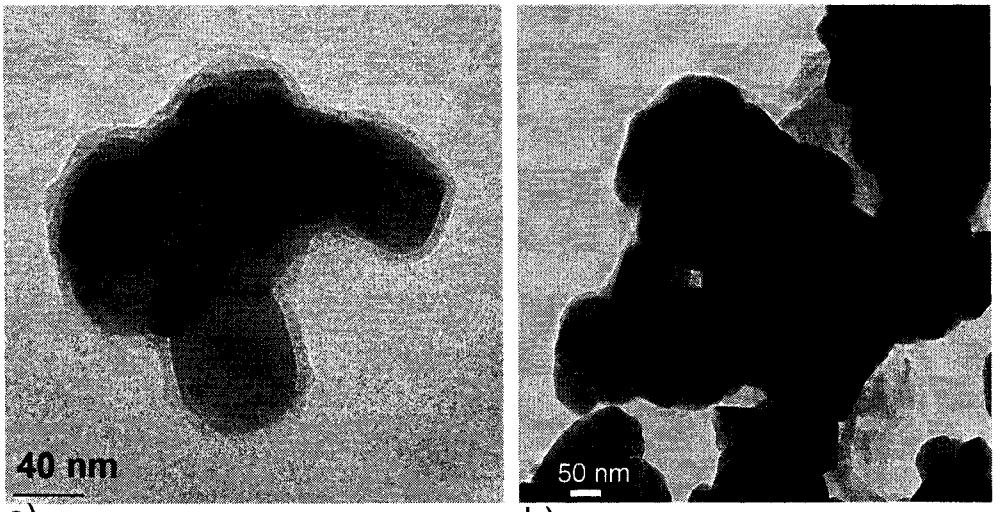

Figure 6.11. Coated agglomerates of zirconia in a) slurry phase and b) in fluidized bed

6.2.5 Conclusions

It was shown that a fluidized bed reactor could be employed for encapsulating nanoparticles via the polymerization compounding approach. In this work, a Ziegler-Natta catalyst was used to polymerize ethylene to encapsulate aluminum and zirconia nanoparticles in the gas phase. Thermogravimetry results showed that particles were coated by a high molecular weight polyethylene. The grafting of polyethylene on the particle surface was further confirmed by XPS results verifying that the polymerization reaction started only from the substrate, which leads to a uniform polymer layer applied around the nanoparticles. As observed from electron microscopy images, the process is capable of coating individual particles with a polymer film a few nanometers in thickness. However, in the case of zirconia, it was also revealed that some agglomerates were encapsulated by the polymer, which is obviously not desirable. It was found that even under the mild process conditions used, the temperature and pressure have a considerable effect on the polymerization reaction and, hence, on polymer content on the coated particles. Therefore, the process of nanoparticle encapsulation can easily be controlled by adjusting the operating conditions. By comparing the encapsulation process in the slurry phase and fluidized bed reactor, it is understood that the size of agglomerates in the fluidized bed reactor are larger than those in the slurry phase, which leads to larger coated agglomerates in the former. On the other hand, there is no solvent employed in the fluidized bed reactor. Therefore, coated particles are easily collected immediately after encapsulation without performing any additional process, such as

filtering or drying, which are required when performing the process in a slurry phase reactor.

6.2.6 References

1- Wang Q., Kaliaguine S., Ait-Kadi A. Catalytic grafting: A new technique for polymer-fiber composites I. Polyethylene-asbestos composites. J. Appl. Polym. Sci.1992; 44, 1107-1119.

2- Wang Q., Kaliaguine S., Ait-Kadi A. Catalytic grafting-A new technique for polymer fiber composites .III. Polyethylene-plasma-treated Kevlar fibers composites. J. Appl. Polym. Sci. 1993; 48, 121-136.

3- Salehi-Mobarakeh H., Brisson J., Ait-Kadi A. Interfacial Polycondesation of nylon-6,6 at the Glass Fibre Surface and its Effect on Fibre-Matrix Adhesion. J. Mater. Sci. 1997; 32, 1297-1304.

4- Salehi-Mobarakeh H., Brisson J., Ait-Kadi A. Ionic interphase of glass fiber/polyamide 6,6 composites. Polym. Compos. 1998; 19, 264-274.

5- Kasseh A., Ait-Kadi A., Riedl B., Pierson J.F. Organic/inorganic hybrid composites prepared by polymerization compounding and controlled free radical polymerization. Polymer. 2003; 44,1367-1375.

6- Shin, S. Y. A., Simon L. C., Soares J. B. P., Scholz G. Polyethylene–clay hybrid nanocomposites: in situ polymerization using bifunctional organic modifiers. Polymer. 2003; 44, 5317-5321.

7- Wang Y., Pei X., Yuan K. Reverse ATRP Grafting From Silica Surface to Prepare Well-Defined Organic/Inorganic Hybrid Nanocomposite. Mater. Lett. 2005; 59, 520-523.

8- Rajabian M., Dubois C. Polymerization compounding of HDPE/Kevlar composites. I. Morphology and mechanical properties. Polym. Compos. 2006; 27, 129-137.

9- He F. A., Zhang L. M., Jiang H. L., Chen L. S., Wu Q., Wang H. H. A new strategy to prepare polyethylene nanocomposites by using a late-transition-metal catalyst supported on $AlEt_3$-activated organoclay. Composites Science and technology. 2007; 67, 1727-1733.

10- Roy C., Dubois C., Lafleur P., Brousseau P. The Dispersion and Polymer Coating of Ultrafine Aluminum Powders by the Ziegler Natta Reaction. Mater. Res. Soc. Symp. Proc. 2004; 800, AA.2.5.- AA.2.5.6.

11- Shi D., Wang S.X., van Ooij W.L., Wang L.M., Zhao J., Yu Z. Uniform deposition of ultrathin polymer films on the surfaces of Al_2O_3 nanoparticles by a plasma treatment. Appl. Phys. Lett. 2001; 78, 1243-1245.

12- Rovira-Bru M., Giralt F., Cohen Y. Protein Adsorption onto Zirconia Modified with Terminally Grafted Polyvinylpyrolidone. J. Colloid Interface Sci. 2001; 235, 70-79.

13- Dubois C., Rajabian M., Rodrigue D. Polymerization Compounding of Polyurethane-Fumed silica Composites. Polym. Eng. Sci. 2006; 46, 360-371.

14- Esmaeili B., Chaouki J., Dubois C. Polymerization Compounding on the Surface of Zirconia Nanoparticles. Macromol. Symp. 2006; 243, 268-276.

15- Che J., Wang X., Xiao Y., Wu X., Zhou L., Yuan W. Effect of Inorganic–Organic Composite Coating on the Dispersion of Silicon Carbide Nanoparticles in Non-Aqueous Medium. Nanotechnology. 2007; 18 1-6,

16- Garcia I., Tercjak A., Zafeiropoulos N. E., Stamm M., Mondragon I. Generation of Core/Shell Iron Oxide Magnetic Nanoparticles with Polystyrene Brushes by Atom Transfer Radical Polymerization. J. Polym. Sci., Part A: Polym. Chem. 2007; 45, 4744-4570.

17- Zhang X., Simon L.C. In situ polymerization of hybrid polyethylene-alumina nanocomposites. Macromol. Mater. Eng. 2005; 290, 573-583.

18- Esmaeili B., Chaouki J., Dubois C. An Evaluation of the Solid Hold-up distribution in a Fluidized Bed of Nanoparticles Using Radioactive Densitometry and Fiber Optics. Accepted to be published in Canadian Journal of Chemical engineering.

19- Sato M., Norio Kobayashi T.K., Shima Y. Hydroxyl groups on silica, alumina, and silica-alumina catalysts. J. Catal. 1967; 7, 342- 351.

20- Kunii D., Levenspiel O., Fluidization Engineering, Boston:Butterworth-Heinemann. 1991.

21- Kissin Y. V., Mink R. I., Nowlin T. E. Ethylene polymerization reactions with Ziegler-Natta catalysts. I. Ethylene polymerization kinetics and kinetic mechanism. J. Polym. Sci. 1999; 37, 4255-4272.

22- Bergstra M. F., Weickert G. Ethylene polymerization kinetics with a heterogeneous metallocene catalyst- Comparison of gas and slurry phases. Macromol. Mater. Eng. 2005; 290, 610-620.

CHAPTER 7
GENERAL DISCUSSION

The main objective in this research was to encapsulate zirconia and aluminum nanoparticles, on the one hand using the polymerization compounding approach in order to provide improved interfacial properties and, on the other hand, using solvent-free process in a fluidized bed reactor. In the first part of this work, we investigated the feasibility of coating zirconia nanoparticles by polymerization compounding using a simple Ziegler-Natta catalyst. We carried out this investigation in a slurry phase. The thermogravimetry analysis results confirmed the presence of high molecular weight polyethylene on the surface of zirconia nanoparticles, since the degradation of high molecular weight polyethylene appears at the temperature range of 450-500 °C. However, we did not further analyze the encapsulated particles to determine the mass molecular weight of polyethylene coat. To evaluate polyethylene molecular weight, it would have been required to extract the polyethylene from the particles and then analyze the polymer by GPC (Gel Permeation Chromatography).

The electron microscopy results demonstrated a thin polymer coat uniformly applied around zirconia nanoparticles. Although the results confirmed that nanoparticles were individually coated by polyethylene, some images showed that coating of particles agglomerate also occurred. This phenomenon was also observed when performing the encapsulation in the fluidized bed reactor. The TEM images of coated agglomerates of zirconia produced by the slurry and the gas/solid fluidized bed reactor processes are

presented in Figure 7.1. As images show, the agglomerate in the slurry phase reactor is smaller than those in the fluidized bed reactor. Since in the slurry phase reactor, the particles are dispersed in the solvent by agitation and ultrasound, the large agglomerates are broken to the smaller ones and even to the individual particles, whereas in the fluidized bed reactor used in this work, no external force was applied. Therefore, the agglomerates in the fluidized bed reactor are larger than those in the slurry phase reactor. If an external force such as vibration would be applied to the fluidized bed reactor, the agglomerate sizes and the risk of agglomerate coating could be reduced.

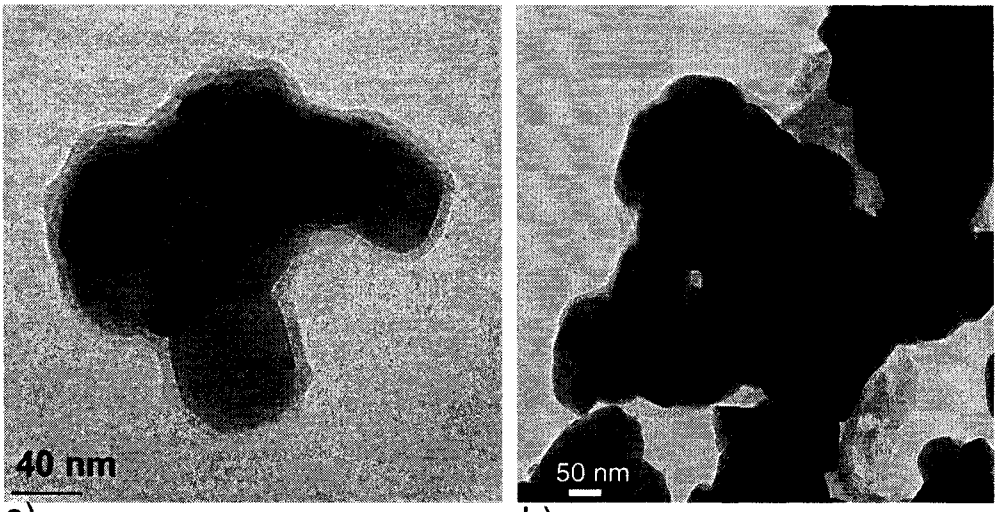

Figure 7.1. The coated agglomerates of zirconia in a) slurry phase and b) fluidized bed reactors

Prior to performing nanoparticle encapsulation in a fluidized bed reactor, it was necessary to investigate their fluidization behavior. At first glance, the fluidization of zirconia and aluminum nanoparticles involved limited bed expansion and bubbles rising

up quickly through the bed. It also consisted of the non-uniform distribution of agglomerates in the bed where the larger agglomerates were located in the lower sections of bed and the smaller ones fluidized in higher positions of the bed. The bed expansion in the fluidized bed of zirconia was very limited in comparison with the one observed in the bed of aluminum. In addition, the agglomerate size distribution for zirconia was wider than that for aluminum. These differences are due to the large difference in bulk density of zirconia and aluminum nanoparticles.

The radioactive densitometry and fiber optic results showed that the solid concentration was uniform over the cross section of the zirconia and aluminum fluidized bed over a wide range of gas velocities at different levels of the bed. In the case of zirconia, it was found that the average solid hold-up over the cross section was almost independent of bed height and the solid hold-up reduction was very low. However, the average solid hold-up in the fluidized bed of aluminum decreased along the bed height. In bubbling fluidization, it is not usual that the solid concentration in lower positions of bed is less compared to that in higher sections. As mentioned earlier, in fluidized bed of nanoparticles showing ABF behavior, there is a wide distribution of agglomerate size along the bed height. The lower solid hold-up at lower position of bed may be due to different bubble sizes in different bed sections. Using available correlations in the literature, it was realized that for the same gas velocity and the same particle density, the bubble size is larger for the larger particles. If it is supposed that the density of agglomerates does not change with diameter, therefore, it may be concluded that the bubble size in lower positions of bed are larger than that in higher positions leading to

lower solid concentration. However, more investigations are required to completely understand about this matter.

The overall solid concentration obtained by the radioactive densitometry technique was in good agreement with the global measurement obtained by the bed expansion data. On the contrary, the overall solid hold-up calculated by the fiber optic method was overestimated for higher gas velocities.

To study the effect of bulk density on the fluidization of nanoparticles, we also tested the fluidization of fumed silica and titania with very low bulk density. It was understood that bulk density is a key factor in the fluidization of nanoparticles, as had been mentioned in the literature. Accordingly, nanoparticles with a bulk density lower than 100 kg/m^3, such as fumed silica in our study, perform agglomerate particulate fluidization, including high bed expansion, smooth fluidization, uniform agglomerate distribution in the bed, and no bubbles. On the other hand, nanoparticles with a bulk density higher than 100 kg/m^3, such as zirconia, aluminum and titania in our case, show agglomerate bubbling fluidization, including bubbles, limited bed expansion, and non-uniform agglomerate distribution within the bed.

The effect of humidity was also verified on the fluidization of nanoparticles. The results showed that humidity has a major effect on the fluidization of nanoparticles showing agglomerate particulate fluidization. Thus, by increasing the humidity content in the fluidizing gas, the agglomerate particulate fluidization may shift to agglomerate bubbling fluidization.

In the last part, the polymerization compounding method was applied to encapsulate zirconia and aluminum nanoparticles in a fluidized bed reactor. The main challenge in this part was to install the catalyst on the surface of nanoparticles, since a very small amount of catalyst must be fixed on a relatively large surface of particles (about 1 $\mu l/m^2$). When performing the encapsulation process in the slurry phase, there is no obstacle to do so, because the particles are dispersed in an organic solvent where the catalyst is injected and dissolved. Therefore, the particles dispersed in the solvent are uniformly exposed to the catalysts dissolved in it. On the other hand, when encapsulating particles in the gas phase reactor, such as a fluidized bed, there is no liquid media where the catalyst can be dissolved. The procedure we develop to anchor the catalyst on nanoparticles called for evaporating the Ziegler- Natta catalyst before it enters the fluidized bed reactor, followed by subliming the catalyst vapor on the particle surface in the reactor. Since there was no thermal gradient in the reactor, all particles were at the same temperature and homogenously fluidized in the reactor, which means the catalyst vapors could uniformly condense on the particle surface.

As showed by the results, the nanoparticles were coated by a high molecular weight polyethylene. In addition, the presence of the catalyst in the interface of the particles and polymer coat, proved by XPS, confirms that the polymerization reaction was initiated from the substrate. It was also confirmed that the encapsulation occurred uniformly within the reactor, since the polymer content determined by TGA was similar for different tested samples in the same batch. The results showed that both temperature and pressure have a considerable effect on the reaction of polymerization.

CONCLUSIONS AND RECOMMANDATIONS

In this dissertation, polyolefin encapsulation of nanoparticles in a fluidized bed reactor by a Ziegler-Natta polymerization was investigated and the following conclusions can be drawn from the work:

1- When conducted in a solvent/particles suspension, polymerization compounding approach to nanoparticles encapsulation resulted in improved interfacial properties between the original surface and the polymer layer, and uniformed coatings were observed.

2- Even if the slurry phase reactor was equipped with a mechanical stirrer and an ultrasound processor to enhance the dispersion of the particles, only a fraction of the particles in the reactor are individually coated. Clusters of particles and agglomerates were also coated. It was found that the coalescence of individually coated particles (after the end of the polymerization reaction) in larger agglomerates, also happens.

3- The fluidization of zirconia and aluminum nanoparticles takes place in the agglomerate state, however, the fluidization of these nanoparticles occurs homogenously in terms of phase concentration.

4- Aluminum nanoparticles show higher bed expansion and smoother fluidization compared to zirconia nanoparticles, which is due to the lower bulk density of aluminum.

5- Both radioactive densitometry and fiber optic provide consistent results in terms of solid hold-up distribution over the cross section. However, the results obtained by fiber optic measurement overestimate the overall solid concentration for higher velocities compared to the bed expansion observations.

6- The bulk density is a key factor to determine fluidization behavior of nanoparticles.

7- Polymerization compounding is a capable technique to encapsulate nanoparticles in the gas-phase following the grafting of the polymerization catalyst on the substrate in a fluidized bed reactor.

8- By performing encapsulation in a fluidized bed reactor, no additional steps after the polymerization reaction, such as filtering and drying, is required to isolate the treated particles. They can be immediately collected and used as found in the reactor.

9- Aluminum nanoparticles were individually and uniformly coated by polymer in a fluidized bed reactor, whereas, zirconia nanoparticles tend to be coated in agglomerate form.

10- The polymer content on the encapsulated particles can be controlled by the operating conditions of the process, such as temperature and pressure.

To further develop and optimize the use of fluidized bed reactors for nanoparticles encapsulation using an in-situ polymerization technique, the following recommendations are made:

1- It was observed that the fluidization of zirconia and aluminum nanoparticles involves bubbling. Since we did not focus on this aspect of fluidization, there is no detail about bubble characteristics reported in this work. Therefore, it is proposed to investigate bubbling characteristics in the fluidized bed of these nanoparticles in order to have a better understanding about nanoparticle fluidization.

2- It is recommended to apply some external force, such as vibration, in nanoparticles encapsulation in a fluidized bed reactor in order to reduce the risk of agglomerate coating in the process.

3- The fluidized bed reactor used in this research was small, therefore, it is recommended to investigate the nanoparticles encapsulation process in a fluidized bed reactor with larger dimensions.

REFERENCES

Avella M., Errico M. E., Gentile G., (2006), 'Nylon 6/Calcium Carbonate Nanocomposites: Characterization and Properties', *Macromlecular Symposia*, 234, 170-175.

Bergstra M. F., Weickert G., (2005), 'Ethylene polymerization kinetics with a heterogeneous metallocene catalyst - Comparison of gas and slurry phases' *Macromolecular Materials and Engineering*, 290, 610-620.

Chaouki J., Chavarie C., Klvana D., Pajonk G., (1985), 'Effect of interparticle forces on the hydrodynamic behaviour of fluidized aerogels', *Powder Technology*, 43, 117-125.

Che J., Wang X., Xiao Y., Wu X., Zhou L., Yuan W., (2007), 'Effect of Inorganic–Organic Composite Coating on the Dispersion of Silicon Carbide Nanoparticles in Non-Aqueous Medium', *Nanotechnology*, 18.

Deiva Vanketash R., Chaouki J., Klvana D., (1996), 'Fluidization of cryogels in a conical column', *Powder Technology*, 89, 179-186.

Ding X., Zhao J., Liu Y., Zhang H., Wang Z., (2004), 'Silica nanoparticles encapsulated by polystyrene via surface grafting and in situ emulsion polymerization', *Materials Letter*, 58, 3126-3130.

Dubois C., Rajabian M., Rodrigue D., (2006), 'Polymerization compounding of polyurethane-fumed silica composites', *Polymer Engineering Science*, 46, 360-371.

Esmaeili B., Chaouki J., Dubois C., (2006),'Polymerization Compounding on the Surface of Zirconia Nanoparticles', *Macromolecular Symposia*, 243, 268-276.

Esmaeili B., Chaouki J., Dubois C., 'An Evaluation of the Solid Hold-up Distribution in a Fluidized Bed of Nanoparticles Using Radioactive Densitometry and Fiber Optics', Accepted to be published in *Canadian Journal of Chemical engineering*.

Garcia I., Tercjak A., Zafeiropoulos N. E., Stamm M., Mondragon I., (2007), 'Generation of Core/Shell Iron Oxide Magnetic Nanoparticles with Polystyrene Brushes by Atom Transfer Radical Polymerization', *Journal of Polymer Science, Part A: Polymer Chemistry*, 45, 4744- 4570.

Gass J., Poddar P. Almand J., Srinath S., Srikanth H., (2006), 'Superparamagnetic Polymer Nanocomposites with Uniform Fe_2O_3 Nanoparticle Dispersion', *Advanced Functional Materials*, 16, 71-75.

Geldart D. (1973),'Types of gas fluidization', *Powder Technology*, 7, 285-292.

Guo Q., Yang X., Shen W., Liu H., (2007), 'Agglomerate size in an acoustic fluidized bed with sound Assistance', *Chemical Engineering and Processing*, 46, 307-313.

He W., Guo Z., Pu Y., Yan L., Si W., (2004), 'Polymer coating on the surface of zirconia nanoparticles by inductively coupled plasma polymerization', *Applied Physics Letter*, 85, 896-898.

He F. A., Zhang L. M., Jiang H. L., Chen L. S., Wu Q., and Wang H. H., (2007) ,'A new strategy to prepare polyethylene nanocomposites by using a late-transition-metal catalyst supported on $AlEt_3$-activated organoclay', *Composites Science and technology*, 67, 1727-1733.

Herrera C.A. , Levy E.K., (2001), 'Bubbling characteristics of sound-assisted fluidized beds', *Powder Technology*, 119, 229-240.

Kasseh A., Ait-Kadi A., Riedl B., Pierson J.F., (2003), 'Organic/inorganic hybrid composites prepared by polymerization compounding and controlled free radical

polymerization', *Polymer*, 44,1367-1375.

Kissin Y. V., Mink R. I., Nowlin T. E., (1999), 'Ethylene polymerization reactions with Ziegler-Natta catalysts. I. Ethylene polymerization kinetics and kinetic mechanism' Journal of Polymer Science, 37, 4255-4272.

Kunii D., Levenspiel O., (1991), *Fluidization Engineering*, 2nd Ed., Boston:Butterworth-Heinemann, P 491.

Li H., Hong R., Wang Z., (1999), 'Fluidizing ultrafine powders with circulating fluidized bed', *Chemical Engineering Science*, 54, 5609-5615.

Li H., Tong H., (2004), 'Multi-scale fluidization of ultrafine powders in a fast-bed-riser/conical-dipleg CFB loop', *Chemical Engineering Science*, 59, 1897-1904.

Liu H., Guo Q., Chen S., (2007), 'Sound-Assisted Fluidization of SiO_2 Nanoparticles with Different Surface Properties', *Industrial and Engineering Chemistry Research*, 46, 1345-1349.

Mabrouk R., Radmanesh R., Chaouki J. and Guy C., 'Scale Effects on Fluidized Bed Hydrodynamics', *International Journal of Chemical Reactor Engineering*, 3, 1-11 (2005).

Matsuda S., Hatano H., Muramoto T., Tsutsumi A., (2001),'Fluidization of ultrafine particles with high G', *Journal of Chemical Engineering of Japan*, 34. 121-125.

Morooka S. , Kusakabe K., Kobata A., Kato Y., (1988), 'Fluidization state of ultrafine powders', *Journal of Chemical Engineering of Japan*, 21, 41-46

Nam C. H., Pfeffer R., Dave R. N., Sundaresan S., (2004), 'Aerated vibrofluidization of silica nanoparticle', *AIChE Journal*, 50, 1776-1785.

Noda K., Mawatari Y., Uchida S., (1998), 'Flow patterns of fine particles in a vibrated fluidized bed under atmospheric or reduced pressure', *Powder Technology*, 99, 11-14.

Pugsley, T., Tanfara, H., Makus, S., Heping, C., Chaouki J., Winters, C., 'Verification of fluidized bed electrical capacitance tomography measurements with a fibre optic probe', *Chemical Engineering Science*, 58, 3923-3934 (2003).

Quevedo J. A., Flisch J., Pfeffer. R. , Dave R, (2007), 'Evaluation of Assisting Methods on Fluidization of Hydrophilic Nanoagglomerates by Montioring Moisture in th Gas Phase', *Chemical Engineering Science*, 62, 2608-2622.

Rajabian M., Dubois C., (2006), 'Polymerization compounding of HDPE/Kevlar composites. I. Morphology and mechanical properties', *Polymer Composite*, 27, 129-137.

Richardson J. F., Zaki W. N., (1954), 'Sedimentation and fluidisation: Part 1.', *Transactions of the Institution of Chemical Engineering*, 32, 35-53.

Rovira-Bru M., Giralt F., Cohen Y., (2001), 'Protein Adsorption onto Zirconia Modified with Terminally Grafted Polyvinylpyrrolidone', *Journal of Colloid Interface Science*, 235, 70-79.

Roy C., Dubois C., Lafleur P., Brousseau P., (2004), 'The dispersion and polymer coating of ultrafine aluminum powders by the Ziegler-Natta reaction', *Material Research Society Symposium Proceeding*, 800, A.A2.5.1.

Russo P., Chiron R., Massimilla L., Russo S., (1995), 'The influence of the frequency of acoustic waves on sound-assisted fluidization of beds of fine particles', *Powder Technology*, 82, 219-230.

Salehi-Mobarakeh H., Ait-Kadi A., Brisson J. (1996), 'Improvement of mechanical properties of composites through polyamide grafting onto kevlar fibers', *Polymer*

Engineering Science, 36, 778-785.

Salehi-Mobarakeh H., Ait-Kadi A., Brisson J. (1997), 'Interfacial polycondensation of nylon-6,6 at the glass fibre surface and its effect on fibre–matrix adhesion', *Journal of Material Science*, 32, 1297-1304.

Salehi-Mobarakeh H., Ait-Kadi A., Brisson J. (1998), 'Ionic interphase of glass fiber/polyamide 6,6 composites', *Polymer Composite*, 19, 264-274.

Sato M., Norio Kobayashi T.K. and Shima Y., (1967), 'Hydroxyl groups on silica, alumina, and silica-alumina catalysts', *Journal of Catalysis*, 7, 342- 351.

Shi D., Wang S.X., van Ooij W.L., Wang L.M., Zhao J., Yu Z., (2001),'Uniform deposition of ultrathin polymer films on the surfaces of Al_2O_3 nanoparticles by a plasma treatment', *Applied Physic Letter*, 78, 1243-1245.

Shin, S. Y. A., Simon L. C., Soares J. B. P. and Scholz G., (2003), 'Polyethylene–clay hybrid nanocomposites: in situ polymerization using bifunctional organic modifiers', *Polymer*, 44, 5317-5321.

Wang Q., Kaliaguine S., Ait-Kadi A., (1992), 'Catalytic grafting: A new technique for polymer-fiber composites I. Polyethylene-asbestos composites', *Journal of Applied Polymer Science*, 44, 1107-1119.

Wang Q., Ait-Kadi A., Kaliaguine S., (1992), 'Catalytic grafting: A new technique for polymer/fiber composites. II. Plasma treated UHMPE', fibers/polyethylene composites', *Journal of Applied Polymer Science*, 45, 1023-1033.

Wang Q., Kaliaguine S., Ait-Kadi A., (1993), 'Catalytic grafting: A new technique for polymer-fiber composites. III. Polyethylene-plasma-treated Kevlar™ fibers composites: Analysis of the fiber surface', *Journal of Applied Polymer Science*, 48, 121-136.

Wang Y., Dave R. N., Pfeffer R., (2004), 'Polymer Coating/Encapsulation of Nanoparticles Using a Supercritical Anti-Solvent Process', *Journal of Supercritical Fluids*, 28, 85-99.

Wang Y., Pei X., Yuan K., (2005), 'Reverse ATRP grafting from silica surface to prepare well-defined organic/inorganic hybrid nanocomposite', *Materials Letter*, 59, 520-523.

Wang Z., Kwauk M. , Li H., (1998), 'Fluidization of fine particles', *Chemical Engineering Science*, 53, 377-395.

Wank J.R., George S.M., Weimer A.W., (2001), 'Vibro-fluidization of fine boron nitride powder at low pressure', *Powder Technology*, 121, 195-204.

Watano S., Imada Y., Hamada K., Wakamastu Y., Tanabe Y., Dave R.N., Pfeffer R., (2003), 'Microgranulation of fine powders by a novel rotating fluidized bed granulator', *Powder Technology*, 131, 250-255.

Yao W. , Guangsheng G., Fei W., Jun W., (2002), 'Fluidization and agglomerate structure of SiO_2 nanoparticles', *Powder Technology*, 124, 152-159.

Zhang J. L., Liu Z. M., Han B. X., Li J. C., Li Z. H., Yang G. Y., (2005), 'Ultrasound-Induced Capping of Polystyrene on TiO_2 Nanoparticles by Precipitation with Compressed CO_2 as Antisolvent', *Journal of Nanoscience and Nanotechology*, 5, 945-950.

Zhu C., Liu G., Yu Q., Pfeffer R., Dave R. N., Nam C. H., (2004), 'Sound assisted fluidization of nanoparticle agglomerates', *Powder Technology*, 141, 119-123.

Zhu C., Yu Q., Dave R. N., Pfeffer R., (2005), 'Gas fluidization characteristics of nanoparticle agglomerates', *AIChE Journal*, 51, 426-439.